UNIVERSIDADE DE SÃO PAULO
INSTITUTO DE QUÍMICA
Programa de Pós-Graduação em Ciências Biológicas (Bioquímica)

AMANDA RIBEIRO MARTINS DA SILVA

Proteomics: a tool to investigate the composition and function of HDL in hyperlipidemia

Versão original da Tese defendida

São Paulo

Data do Depósito na SPG:

06/06/2022

AMANDA RIBEIRO MARTINS DA SILVA

Proteômica: uma ferramenta para a investigação da composição e função da HDL em hiperlipidemia

Tese apresentada ao Instituto de Química da Universidade de São Paulo para obtenção do Título de Doutora em Ciências (Bioquímica)

Orientadora: Profa. Dra. Graziella Eliza Ronsein

São Paulo

2022

Ficha Catalográfica elaborada eletronicamente pelo autor, utilizando o programa desenvolvido pela Seção Técnica de Informática do ICMC/USP e adaptado para a Divisão de Biblioteca e Documentação do Conjunto das Químicas da USP

Bibliotecária responsável pela orientação de catalogação da publicação:
Marlene Aparecida Vieira - CRB - 8/5562

S586p

Silva, Amanda Ribeiro Martins
Proteômica: uma ferramenta para a investigação da composição e função da HDL em hiperlipidemia / Amanda Ribeiro Martins Silva. - São Paulo, 2022.
86 p.

Tese (doutorado) - Instituto de Química da Universidade de São Paulo. Departamento de Bioquímica.
Orientador: Ronsein, Graziella Eliza

1. HDL. 2. Lipoproteínas. 3. Proteômica. 4. Ômega-3. I. T. II. Ronsein, Graziella Eliza, orientador.

Ao meu amado Vitor e
à minha doce Clarice,
com toda minha força e amor

AGRADECIMENTOS

E mais um ciclo da viva chega ao seu final. De importância imensurável, desafiador, repleto de alegrias, perturbações, e sem dúvidas o mais transformador que já vivenciei. No início a tônica era a ânsia de aprender, crescer profissionalmente, conquistar, trabalhar e trabalhar por horas a fio, em busca de resultados, de reconhecimento. Junto, você esteve, Grazi. Agradeço-te enormemente por todas as oportunidades que me apresentou, por confiar no meu trabalho, e principalmente, por me permitir escrever com você. Sua escrita é vibrante, seu raciocínio é inteligentíssimo, e é encantador ver sua paixão pela ciência. Obrigada, Profa. Graziella, muito obrigada por me apresentar o universo da HDL.

Nesse caminhar também tive a sorte de conviver com seres humanos que valem muito a pena. Fernanda (Fê), muito obrigada pela amizade e pelo acolhimento no início dessa jornada. Izaura, muito obrigada pelo auxílio diário. Agda, muito obrigada por organizar nossa vida de uma maneira tão gentil. Márcia, muito obrigada pela boa música do dia-a-dia. E Mariana (Mari), muito obrigada pela delicadeza, carinho e sua encantadora didática no explicar.

E os amigos foram se somando. Muito obrigada meus queridos e queridas por terem deixado a vida mais prazerosa de se viver. Muito obrigada Bias ou Beas (Bianca e Beatriz), Laurinha, Litieli e Marcela. Peter, obrigada pelos almoços, Carol, obrigada pela amizade, e Rai, muito obrigada por tanta filosofia, parte do que sou hoje é retrato das nossas conversas. Agradeço à Rebeca, à Stella e à Rafa pelo frescor da juventude que traziam em nossas reuniões de grupo. Hellen, muito obrigada pelo seu brilhantismo. Gaby, muito obrigada por me apresentar as novidades da nova geração. E em especial, muito obrigada Douglas e Lorenna. Doug, foi um prazer estar ao seu lado nesses 5 anos. Muito obrigada por sua inteligência, muito obrigada pela generosidade, muito obrigada por me ensinar tanto. Você é admirável. E Lory...ah, minha querida...sou uma privilegiada em poder partilhar a vida contigo. Muito obrigada por tanto, obrigada por ser minha família.

Agradeço também aos colaboradores desse processo: ao Prof. Paolo Di Mascio e à Profa. Marisa Passarelli, Monique, Beatriz e Marcos da FMUSP. Agradeço também ao Prof. Giuseppe Palmisano e Lívia do ICB-USP. Agradeço à Coordenação de Aperfeiçoamento de Pessoal de Nível Superior (CAPES) e à Fundação de Amparo à Pesquisa do Estado de São Paulo (FAPESP, processo nº 2017/07725-1) pelo financiamento concedido.

E entre o início e quase fim dessa jornada, fomos surpreendidos por uma pandemia sem precedentes. A vida mudou, outros planos passaram a fazer parte de mim. Adotamos Lis e Flora, e o desejo de cuidar se aflorou. Me tornei mãe. A vida ficou insana, completamente desajustada, mas também ficou doce, o coração ficou acalentado. Minha menina Clarice trouxe luz nesse caminhar. Obrigada minha Clarice

por ser quem és. E muito obrigada meu amado Vitor, por estar aqui comigo e conosco nessa luta, nas novas descobertas, obrigada por nos trazer tanta paz e arte.

Essa tese não foi escrita só por mim. Meu companheiro e muitas mulheres foram fundamentais por cada palavra escrita aqui. Mãe, serei eternamente grata pelo seu acolhimento e paciência em nos ajudar a passar por essa etapa. Muito obrigada Mônica por trazer leveza e deixar os dias muito mais saborosos. Muito obrigada Dona Chica, por nos receber quase que diariamente com tanta alegria. Muito obrigada Cris, por fazer minha menina sorrir. Muito obrigada Ri, pela diversão e afeto conosco. Muito obrigada pai pelo cuidado, alegria e bom humor. Muito obrigada Adilson pelo imenso carinho. Agradeço também os familiares, aos meus avós Ivone e Zezo, à Pá, a Isa e ao Marcos pelo amor desmedido e olhar sincero.

O fim desse doutorado representa um ato de resistência para mim. Ser mulher, profissional altamente produtiva, e mãe são “títulos” humanamente impossíveis de se equilibrar. A conta não fecha nunca, o que chega mesmo é a exaustão. Nossa luta por espaço e liberdade é constante. Ainda temos muito a fazer. O meu profundo desejo e o meu principal objetivo como responsável pela formação de uma nova cidadã é que a vida futura seja mais acolhedora, mais sensível, que seja simplesmente humana.

Maria, Maria, é um dom, uma certa magia
Uma força que nos alerta
Uma mulher que merece viver e amar
Como outra qualquer do planeta

Maria, Maria, é o som, é a cor, é o suor
É a dose mais forte e lenta
De uma gente que ri quando deve chorar
E não vive, apenas aguenta

Mas é preciso ter força, é preciso ter raça
É preciso ter gana sempre
Quem traz no corpo a marca, Maria, Maria
Mistura a dor e a alegria

Mas é preciso ter manha, é preciso ter graça
É preciso ter sonho sempre
Quem traz na pele essa marca possui
A estranha mania de ter fé na vida

(Fernando Blant e Milton Nascimento)

RESUMO

Silva, A.R.M. **Proteômica: uma ferramenta para a investigação da composição e função da HDL em hiperlipidemia**. 2022. 86p. Tese – Programa de Pós-Graduação em Ciências Biológicas (Bioquímica). Instituto de Química, Universidade de São Paulo, São Paulo.

A inversa relação entre HDL-C (do inglês, *high-density lipoprotein cholesterol*) e doenças cardiovasculares é bem estabelecida. No entanto, é consenso que o conteúdo de colesterol presente na HDL não captura sua complexidade, e outras métricas precisam ser exploradas. A HDL é uma partícula heterogênea, enriquecida em proteínas, com funções que vão além do metabolismo de lipídeos. Dessa forma, seu conteúdo proteico parece ser mais atrativo para exprimir seu comportamento frente às patologias. Muitas das proteínas com função importante estão em baixa abundância (<1% do total de proteínas), o que torna a detecção desafiadora. Métodos quantitativos de proteômica permitem detectar proteínas com alta precisão e robustez em matrizes complexas. No entanto, a proteômica quantitativa ainda é pouco explorada no contexto da HDL. Nesse sentido, no segundo capítulo dessa tese, a performance analítica de dois métodos quantitativos foi criteriosamente investigada, os quais alcançaram adequada linearidade e alta precisão usando peptídeos marcados em um *pool* de HDL, além de comparável habilidade em diferenciar as proteínas das subclasses da HDL de indivíduos saudáveis. Outro gargalo que aguarda por solução em proteômica é a falta de padronização no processamento e análise de dados após a aquisição por espectrometria de massas. Além disso, é crescente o interesse das propriedades cardioprotetivas do ômega-3, porém pouco se conhece sobre seus efeitos no proteoma da HDL. Então, no terceiro capítulo dessa tese, comparamos cinco estratégias de quantificação de proteínas utilizando os softwares Skyline e MaxDIA com o intuito de comparar o proteoma da HDL de camundongos submetidos a uma dieta hiperlipídica suplementados ou não com ômega-3. MaxDIA com quantificação *label-free* (MaxLFQ) apresentou alta precisão para mostrar que o ômega-3 remodela o proteoma da HDL para um perfil menos inflamatório. Portanto, os dois estudos apresentados nessa tesa começam a abrir novos caminhos para o entendimento mais profundo e confiável da HDL tanto por meio da quantificação das proteínas por espectrometria de massas quanto após à aquisição dos dados.

Palavras-chave: HDL, proteômica quantitativa, ômega-3, dieta rica em gordura saturada, hiperlipidemia.

ABSTRACT

Silva, A.R.M. **Proteomics: a tool to investigate of composition and function of HDL in hyperlipidemia**. 2022. 86p. PhD Thesis – Graduate Program in Biochemistry. Instituto de Química, Universidade de São Paulo, São Paulo.

The inverse relationship between HDL-C (high-density lipoprotein cholesterol) and cardiovascular disease is well established. However, it is consensus that the cholesterol content present in HDL does not capture its complexity, and other metrics need to be explored. HDL is a heterogeneous, protein-enriched particle with functions going beyond lipid metabolism. In this way, its protein content seems to be attractive to investigate its behavior in the face of pathologies. Many of the proteins with important function in HDL are in low abundance (<1% of total proteins), which makes their detection challenging. Quantitative proteomics allows detecting proteins with high precision and robustness in complex matrix. However, quantitative proteomics is still poorly explored in the context of HDL. In this sense, in the second chapter of this thesis, the analytical performance of two quantitative methodologies was carefully investigated. These methods achieved adequate linearity and high precision using labeled peptides in a pool HDL, in addition to comparable ability to differentiate proteins from HDL subclasses of healthy subjects. Another bottleneck that waits for a solution in proteomics is the lack of standardization in data processing and analysis after mass spectrometry acquisition. In addition, interest in the cardioprotective properties of omega-3 is growing, but little is known about its effects on the HDL proteome. Thus, in the third chapter of this thesis, we compared five protein quantification strategies using Skyline and MaxDIA software platforms in order to investigate the HDL proteome from mice submitted to a high-fat diet supplemented or not with omega-3. MaxDIA with label-free quantification (MaxLFQ) achieved high precision to show that polyunsaturated fatty acids remodel the HDL proteome to a less inflammatory profile. Therefore, the two studies presented in this thesis begin to open new paths for a deeper and more reliable understanding of HDL, both at the level of protein quantification by mass spectrometry and after data acquisition.

Keywords: HDL, quantitative proteomics, omega-3, high-fat diet, hyperlipidemia.

SUMMARY

CHAPTER 1 - Introduction

1.1. Lipoproteins

Lipoproteins are complex particles responsible for the transport of cholesterol and triglycerides in blood circulation due to the insolubility of lipids in water[1]. As shown in **Figure 1**, these molecules are composed of a central hydrophobic core of cholesterol esters and triglycerides surrounded by a monolayer of phospholipids, free cholesterol, and apolipoproteins, which are essential for lipoproteins metabolism[1]. Such apolipoproteins may play a structural role, participate in binding lipoproteins to their receptors, guide the formation of new lipoproteins, in addition to activating or inhibiting enzymes involved in lipoproteins metabolism[2]. The functions of some of the main apolipoproteins are described in **Table 1**.

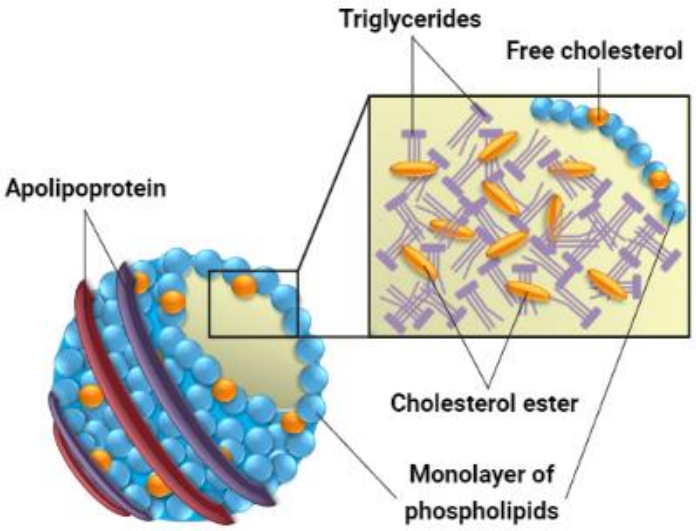

Figure 1. Lipoprotein structure (image modified[1] and created with BioRender.com).

Table 1. Biological functions of some of the main apolipoproteins that make up plasma lipoproteins[3].

Apolipoprotein	Gene name	Function
Apolipoprotein A-I	APOA1	Structural protein for HDL; Participates in reverse cholesterol transport; Activates LCAT (lecithin cholesterol acyltransferase)
Apolipoprotein A-II	APOA2	Structural protein for HDL; Activates hepatic lipase
Apolipoprotein A-IV	APOA4	Activates LCAT; Required for efficient activation of lipoprotein lipase by APOC2
Apolipoprotein B-48	APOB-48	Structural protein for chylomicrons
Apolipoprotein B-100	APOB-100	Structural protein for VLDL, IDL and LDL; Ligand for LDL receptor
Apolipoprotein C-I	APOC1	Inhibits lipoprotein binding to LDL receptor; Inhibits CETP (cholesteryl ester transfer protein);
Apolipoprotein C-II	APOC2	Activates lipoprotein lipase
Apolipoprotein C-III	APOC3	Inhibits lipoprotein lipase; Inhibits uptake of triglycerides-rich lipoproteins
Apolipoprotein E	APOE	Ligand for LDL receptor
Apolipoprotein(a)	LPA	Inhibits plasminogen activation

Based on density, size, and composition of lipids and apolipoproteins, chylomicrons, chylomicron remnants, very low-density lipoprotein (VLDL), intermediate density lipoprotein (IDL), low-density lipoprotein (LDL), lipoprotein (a) (Lp (a)) and high-density lipoprotein (HDL) integrate the 7 classes of plasma lipoproteins (**Table 2**)[2].

Table 2. Lipoproteins classes based on density, size, and composition of lipids and apolipoproteins[2].

Lipoprotein	Density (g/mL)	Size (nm)	Major Lipids	Major Apolipoproteins
Chylomicrons	<0.930	75-1200	Triglycerides	APOB-48, APOCs, APOE, APOA1, APOA2, APOA4
Chylomicrons remnants	0.930-1.006	30-80	Triglycerides Cholesterol	APOB-48, APOE
VLDL	0.930-1.006	30-80	Triglycerides	APOB-100, APOE, APOCs
IDL	1.006-1.019	25-35	Triglycerides Cholesterol	APOB-100, APOE, APOCs
LDL	1.019-1.063	18-25	Cholesterol	APOB-100
HDL	1.063-1.210	5-12	Cholesterol Phospholipids	APOA1, APOA2, APOA4 APOCs, APOE
Lp (a)	1.055-1.085	~30	Cholesterol	APOB-100, APO(a)

Chylomicrons are large triglyceride-enriched particles made by intestine, which transport dietary lipids to peripheral tissues and liver (**Figure 2**)[4]. These particles contain mainly apolipoproteins A-I, A-II and A-IV (APOA1, APOA2 and APOA4, respectively), in addition to apolipoproteins C-II, C-III (APOC2 and APOC3, respectively), and E (APOE). Apolipoprotein B-48 (APOB-48) is the major structural protein of this lipoprotein, and one APOB-48 molecule is found in each chylomicron particle[2]. In extrahepatic tissues, their triglycerides are hydrolyzed by lipoprotein lipase (LPL), providing fatty acids. Cholesterol-enriched and smaller particles are the result of LPL action. These particles are called chylomicron remnants, and they are cleared from circulation by the liver. When triglycerides and cholesterol (endogenous and exogenous) levels exceed the requirements of hepatocytes, VLDL synthesis occurs[4]. Very low-density lipoprotein is a triglycerides-enriched particle composed manly by apolipoproteins C-I, C-II, C-III (APOC1, APOC2 and APOC3, respectively), and E (APOE). Different of the chylomicrons, apolipoprotein B-100 (APOB-100) is the core structural protein, and one APOB-100 molecule surrounds each VLDL particle[2]. In the circulation, VLDL triglycerides are also removed by LPL, resulting in a cholesterol-enriched particle, now called IDL. A part of the IDL returns to the liver, and the other part goes through a new cycle of triglycerides removal, originating the LDL particle, the lipoprotein with the highest cholesterol levels in the circulation. Indeed, LDL is the main cholesterol transporter, since tissues (except the liver and intestine) take up exogenous cholesterol from the endocytosis of this lipoprotein[4]. APOB-100 is the predominant apolipoprotein in LDL, and there is one molecule per lipoprotein particle[2]. While Lp (a) is composed of an LDL-like particle in which APOB-100 is covalently attached by a single disulfide bond to apolipoprotein(a)[5].

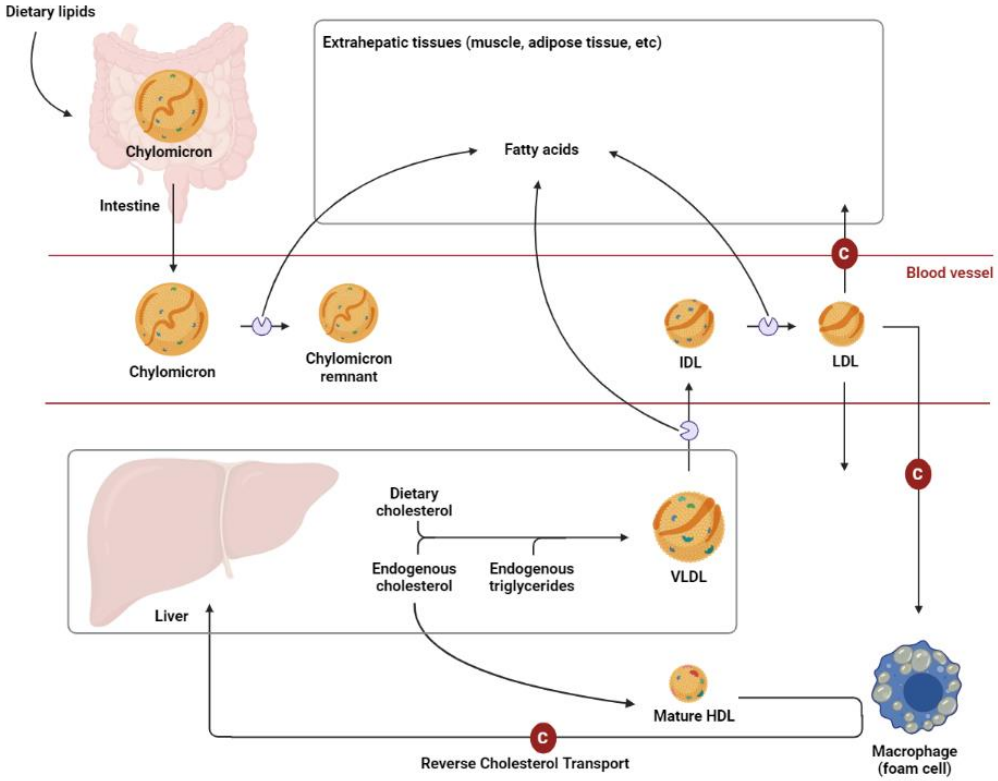

Figure 2. Lipids transport to tissues by plasma lipoproteins. The circles cut in blue represent lipoprotein lipase and red circles represent cholesterol. Scheme adapted[1; 4] and created with BioRender.com.

High-density lipoprotein acts in the opposite direction to LDL. HDL is responsible for mobilizing cholesterol from tissues and from macrophages, as shown in **Figure 2**. Initially, APOA1, the core structural protein of HDL, is synthesized and secreted by liver and intestine. This lipid-poor molecule interacts with the cholesterol-phospholipid transporter ABCA1 (ATP Binding Cassette A1) present in many cell types – hepatocytes, enterocytes and macrophages – to exchange lipids generating a nascent discoidal HDL particle, also known as pre-β-HDL. The enzyme lecithin cholesterol acyltransferase (LCAT) present on lipoprotein esterifies the cholesterol uptaked, forming the cholesterol ester-containing core of the spherical HDL particle. Thus, mature HDL may be absorbed by the liver, and

cholesterol be excreted as bile salts. In addition, HDL may transfer cholesterol to APOB-containing lipoproteins (usually in exchange for triglycerides) by cholesteryl ester transfer protein (CETP)[6]. Therefore, APOB-containing lipoproteins provide lipids (fatty acids and cholesterol) to the tissues, while HDL mediates the reverse cholesterol transport from tissues to liver, only organ capable of eliminating the excess of cholesterol (**Figure 2**).

1.2. HDL

In 1929, at the Pasteur Institute in Paris, the physician Michel Machebouef reported the first isolation, using salt precipitation technique, of a lipoprotein particle from horse serum, which later became known as HDL[7]. Lipid composition of this lipoprotein was rapidly determined – phospholipids (~25%), cholesterol (~4%), triglycerides (~3%), and cholesterol esters (~12%). However, it took nearly 40 years to have its protein composition properly investigated, largely because it was believed that HDL particles were homogeneous, just like LDL (made up mostly of APOB-100)[8]. From the identification of the first HDL protein[9; 10; 11], now known to be APOA1[12], other proteins and enzymes were being identified and associated to this lipoprotein. Apolipoprotein A2 was the second protein determined followed by APOCs, APOE, apolipoprotein D (APOD), apolipoprotein F (APOF), serum amyloid A (SAA), apolipoprotein A-IV (APOA4), paraoxonase 1 (PON1), clusterin (CLU), LCAT, CETP, and phospholipid transfer protein (PLTP), among others, which makes HDL the most protein diverse lipoprotein[8].

In parallel, several HDL subspecies also have been identified based on density, size, apolipoprotein composition, and electrophoretic mobility. Defined historically by its

density, HDL (d=1.063-1.21 g/mL) is smaller and denser than others lipoproteins classes precisely because of high proportion of protein to lipids (50:50, w/w)[13]. Density ultracentrifugation (UC) is the gold standard technique for its isolation from plasma, and two distinct subclasses may be obtained: HDL2 (d=1.063 to 1.125 g/mL), larger and more buoyant, and HDL3 (d=1.125 to 1.21 g/mL), smaller and denser[14; 15]. These subclasses can be further fractionated by size on non-denaturing gradient gel electrophoresis, distinguishing 5 new particles: HDL2a, b (from HDL2) and HDL3a, b, c (from HDL3)[16]. Aloupovic defined three major classes of HDL from apolipoprotein content: particles containing APOA1 (LpA-I), those containing APOA1 and APOA2 (LpA-I/LpA-II), and those containing only APOA2 (LpA-II)[17]. Finally, HDL have electrophoretic mobility, with migrating predominantly alpha, but beta electrophoretic mobility also can be found[18].

Interestingly, the different ways of defining HDL generate distinct particles both at a structural and functional level. For example, HDL defined by density does not fit the classification based upon the presence or not of APOA1 and APOA2[19]. Thus, it is evident the heterogeneity and complexity of this lipoprotein. Several HDL subspecies can be obtained depending on isolation method, and its protein enrichment may explain its functional diversity.

1.3. Lipoproteins and Cardiovascular Disease

Over the last century, population's lifestyle modifications have caused dramatic rise in prevalence of metabolic syndromes[20]. Known by association of risk factor such as obesity, dyslipidemia, hypertension, and smoking, metabolic syndromes are closely related to the development of cardiovascular diseases (CVD), the number one cause of morbidity and

mortality worldwide[21]. The World Health Organization (WHO) estimated that around 17.9 million people died of CVD in 2019, representing 32% of all global deaths[22]. A critical data contributes to the worsening of this scenario: studies predict that by 2030, 1.12 billion people will be obese[23]. Excess lipids in the body triggers several adverse effects on plasma lipoproteins, and dyslipidemia is the comorbidity most commonly associated with obesity[24]. Dislipidemic states are characterized by high triglycerides levels, predominance of small dense LDL, and low HDL-C levels[25].

Small dense LDL particles have a lower affinity for the LDL receptor, making them more pro-atherogenic than large LDL from healthy subjects[25]. LDL receptor is regulated by cholesterol concentration in cell – the greater the amount of this lipid, fewer receptors are expressed. In this sense, the low affinity of the receptors for small LDL, together with the presence of few receptors, result in a prolonged period of time for LDL in the circulation. This scenario favors the transfer of cholesterol to peripheral tissues, including cells characteristics of atherosclerosis, macrophage foam cells[2; 25]. Lipoproteins from subjects with metabolic syndromes may undergo chemicals changes with significant modification in their functions. Henriksen *et al*.[26] were the first to observe that LDL modification favored its capture when incubated with endothelial cells in culture. Oxidized lipoprotein is rapidly recognized and captured by macrophages, which may be transformed into foam cells, promoting the formation of plaques in the arterial wall.

Faced with the causal relationship between LDL, popularly called “bad cholesterol”, and CVD, there is a worldwide search for more efficient treatments to reduce its blood levels. In this sense, a monoclonal antibody that inhibits proprotein convertase subtilisin-kexin type 9 (PCSK9), which directs LDL receptor for lysosomal degradation, is most

recently developed therapy against atherosclerosis[27]. Patients treated with statin, the drug usually used for this purpose, together with the antibody, decreased 15% the risk of a cardiovascular event when compared to individuals treated with statin alone. However, the combined therapy (antibody + statin) and very low LDL-C levels obtained after treatment were not able to prevent heart attack or death of almost 20% of patients during the 2 years of the research. In the other words, the residual risk, not explained by LDL-C levels, remains high.

In contrast to the atherogenic effects of LDL, HDL lives up to its popular denomination, “good cholesterol”. The relationship between high cholesterol levels in HDL (HDL-C) and decreased CVD risk is historically established. The most widely recognized atheroprotective effect of HDL is its ability to transport excess cholesterol from peripheral tissues to the liver during reverse cholesterol transport, thereby reducing the development of atherosclerotic plaques[28]. In addition, HDL has been associated with anti-inflammatory, vasoprotective and antioxidant properties[29]. It appears that removal of excess cholesterol from foamy macrophages reduces cytokine expression and stimulates nitric oxide production, fundamental molecule for vasodilation. HDL seems also protects LDL against oxidation due its protein composition[30].

Multiple genetic studies[31; 32; 33] and recent failures in clinical trials of drugs that elevate plasma HDL-C content[34; 35; 36] have raised questions about the causal association of HDL-C levels with CVD risk. Therapies with niacin[37; 38] and three inhibitors (torcetrapib[39], dalcetrapib[35] and evacetrapib[40]) of CETP significantly increased HDL-C levels in the blood. Despite promoting the elevation of cholesterol in HDL, torcetrapib and dalcetrapib were not able to improve reverse cholesterol transport through ABCA1 receptor. In

contrast, evacetrapib treatment increased cholesterol uptake from foam cells by HDL via ABCA1 pathway. However, its use has not shown clinical benefits.

This apparent paradox – increased HDL-C levels without benefit in cardiovascular outcomes – might be related to the clinical parameter currently used to evaluate HDL levels in plasma, its cholesterol content. As described earlier, HDL are heterogeneous particles varying in size, density, protein and lipid composition. Thus, several studies have shown that HDL-C does not capture HDL diverse functions[41], and therefore other metrics need to be explored. Evidence has attributed the functions plurality of the lipoprotein to its heterogeneous structure and composition[42]. Being a protein-enriched particle, its protein content seems to be a more attractive source to investigate its functions and behaviors in face of different pathologies. Indeed, HDL protein content has been remodeled in response to chronic inflammatory diseases, such as type 2 diabetes[43], kidney disease[44], psoriasis[45], and rheumatoid arthritis[46], thus compromising its functionality. This damage can directly contribute to coronary injury. An important review[30] reported that the loss of HDL ability to mobilize cholesterol from peripheral tissues in inflammatory scenario seems to be related with the replacement of APOA1 for inflammatory proteins, such as SAA1 and SAA2, which can be increased 1000 times in plasma during inflammation[47].

1.4. Lipoproteins and Diet

The complex relationship between lipoproteins and CVD may also be influenced by diet[48]. The first observation in this sense was made in1908[49], when rabbits treated with high cholesterol concentration developed plaques of containing lipids on the arterial wall. In 1957, Keys *et al*.[50] reported that high consumption of saturated fat by Western

populations triggered high plasma cholesterol levels with consequent progression of coronary events. Since then, government guidelines have recommended changes in the population's dietary pattern by reducing the consumption of these fats, replacing them by vegetable oils and whole grains[51]. Since in 2010 alone, 250,900 deaths were estimated worldwide as result of excessive intake of saturated fatty acids[52].

Numerous studies[53; 54; 55] have corroborated the cardioprotective effects of diets rich in monounsaturated fatty acids (MUFA), in polyunsaturated fatty acids (PUFA), as well as diets based on good quality carbohydrates (e.g. cereal, excluding refined starches and sugars, which are positively associated with disease). Indeed, when replacing 5% of energy intake from saturated fat with the equivalent in PUFA, MUFA or whole grains, there was a decrease of 25%, 15% and 9%, respectively, in the development of heart disease in humans[56]. Recently, a randomized controlled trial[48] described the beneficial role of the Mediterranean diet in improving HDL function, particularly when olive oil-enriched. Rich in polyunsaturated fatty acids, the diet contributed to the ability of HDL to carry out the reverse cholesterol transport, in addition to favoring antioxidant, anti-inflammatory and vasoprotective properties of the lipoprotein.

Among the PUFAs, omega-3 fatty acids, especially eicosapentaenoic acid (EPA; 20:5n-3) and docosahexaenoic acid (DHA; 22:6n-3) present in fish, stand out for benefits promoted to the reduction of atherosclerotic plaques[57], being superior to the effects of polyunsaturated fatty acids of the omega-6 class[58]. A clinical trial[59] reported that after approximately 42 days of supplementation with fish oil, patients with carotid atherosclerosis showed stabilization of their plaques, due to the decrease in the number of macrophages present. However, the same beneficial effect was not observed in

patients who received sunflower oil (omega-6). Such stability may explain the inverse association between omega-3 consumption and the occurrence of cardiovascular events.

The greatest known effect of fish oil is to reduce plasma triglyceride levels, which may also beneficially contribute to various cardiac disorders[60]. This is due to the decrease in its synthesis in the liver and to the limited secretion of triglycerides-enriched lipoprotein, VLDL[61]. Several meta-analyses[62] support this evidence in individuals with hyperlipidemia, however, the consumption of EPA and DHA did not influence total cholesterol, LDL-C and HDL-C levels. Although omega-3 supplementation shows favorable results, its mechanisms of action is not yet clear. In addition, there are some controversies to its employment[63]. The epidemiological study ORIGIN[64] found that the daily intake of 1 g of omega-3 did not prevent the occurrence of vascular events in patients who suffered myocardial infarction, even though it reduced triglyceride levels. In the same way, a French clinical trial[65] does not support the routine use of fatty acids as prophylactic measure for cardiovascular diseases, at least in people with a history of the pathology.

Due to the inconsistency of the results obtained to date, further studies should be carried out to deepen the understanding of the influence of omega-3-enriched diets on coronary events. Clinical trials require recruitment of a large number of subjects that must be followed for a long time. Besides, they present difficulties in the control and adherence of the patients, in addition to a high cost[66]. In this way, animal models represent a promising alternative to examine the direct effect of diet on atherosclerosis. LDL receptor knockout mice ($LDLr^{-/-}$) are among the most commonly used models for the investigation of the disease[67; 68]. The absence of the receptor impairs the uptake of LDL by tissues, resulting in its accumulation in plasma. Therefore, on a regular chow diet, animals develop

moderate hypercholesterolemia, as found in humans, but with mild vascular injury[69]. On diets containing high levels of fat (21%) and cholesterol (0.15%), mice develop severe hyperlipidemia and atherosclerosis, in addition to becoming obese and insulin resistant[70].

Interestingly, it has been shown that a saturated fatty acids-enriched diet promoted remodeling of HDL proteins to an inflammatory profile even in mice without genetic modification[71]. Increased levels of SAA family were found in HDL from mice fed with saturated fat when compared to HDL from mice submitted to low-fat diet or monounsaturated fatty acids-enriched diet. In addition, mice fed high-fat diet showed deficiency in hepatic cholesterol excretion.

1.5. HDL Proteomics

Depending on the detection method, over 90 proteins have been identified as resident in HDL, although the two most abundant, APOA1 and APOA2, make up 90% of its protein mass. Therefore, many of the proteins that can express HDL functionality are in low abundance (<1% total protein)[8], making detection challenging. Technological advances mainly in peptide separation, mass spectrometry and bioinformatics have allowed the high-throughput characterization of proteins and proteomes in multiplex biological samples, and consequently, the deeper investigation of the HDL proteome[72].

Two approaches are available for proteomics analysis: bottom-up, considered standard for routine proteomics, which identify peptides, and top-down, which analyze the intact protein[73]. The well-established bottom-up workflow starts with proteins isolation from a biological matrix, followed by enzymatic digestion to peptides by a sequence-specific protease. Trypsin is the enzyme most widely used, and it cleaves the peptide

bonds at the carboxyl side of arginine and lysine[74]. Peptides are then separated by reverse-phase chromatography, gently ionized by an ion source, and directed to a gas phase into the mass spectrometer. Finally, extensive data analysis is required (**Figure 3**)[75].

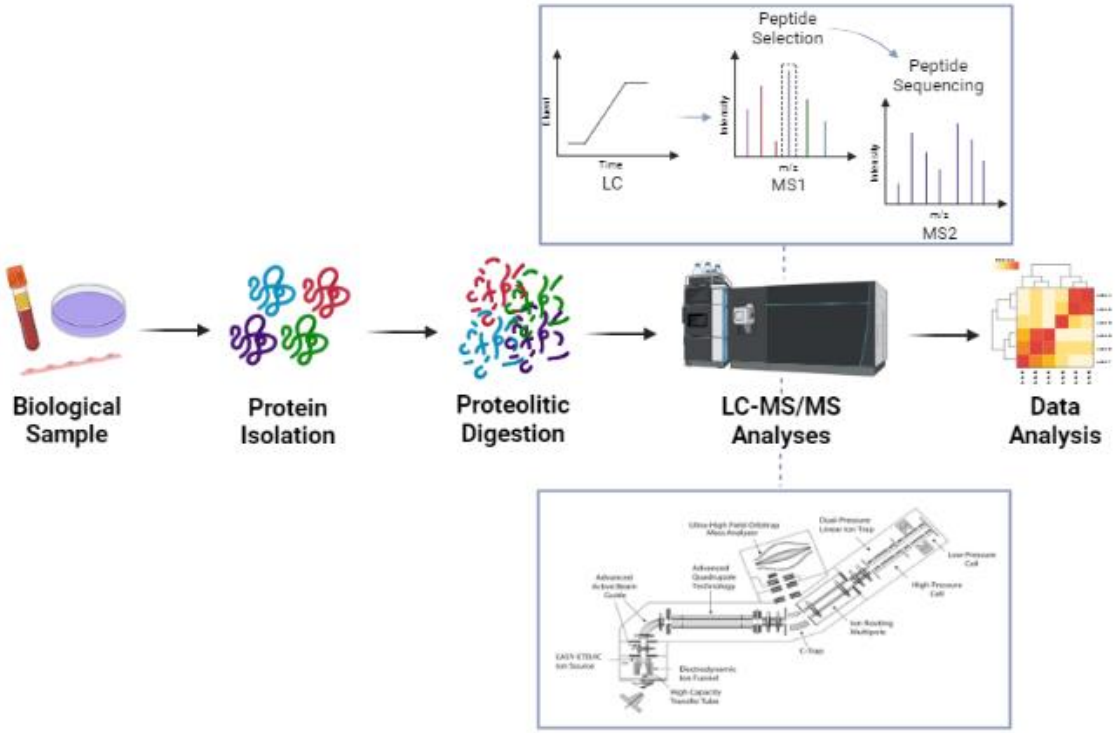

Figure 3. Proteomics workflow following bottom-up approach and data-dependent acquisition mode (image created with BioRender.com, and mass spectrometer Orbitrap Fusion Lumos scheme from Thermo Scientific™).

The heart of the mass spectrometer is the mass analyzer. As the name implies, these instruments separate the formed ions according to its *m/z* ratio. Different types of mass spectrometers can be found commercially, such as quadrupoles, ion-traps, time-of-flight (TOF), Fourier-transform ion cyclotron resonance (FT-ICR), and orbitrap. The analyzers can be used “alone” and independently, or coupled together, giving rise to equipment classified as hybrid, which make use of the inherent advantages of each analyzer. A

diagram summary of the hybrid mass spectrometer Orbitrap Fusion Lumos used for data acquisition in this thesis is shown in **Figure 3**.

The basic principle in mass spectrometry-based proteomics consists of initially determining the *m/z* of ionized peptides (known as precursor ions) that co-elute at a specific point in the gradient elution. These ions are analyzed generating a mass spectrum, called MS1 (full scan). Next, precursor ions are fragmented in a collision cell, and the resulting product ions from each precursor ion are detected by the mass analyzer, and another mass spectrum is recorded, called, MS/MS spectrum or MS2 (**Figure 3**). The identity of the peptide is obtained in MS2. Its fragmentation profile is determined in this spectrum, resulting in its specific amino acid sequence[75].

Shotgun proteomics using data dependent acquisition (DDA) is the most common untargeted methodology used to solve the proteome in complex peptides mixtures. As a discovery-driven technique that does not focus on proteins of interest, it offers a hypothesis-free and systems-wide analysis. In that way, shotgun proteomics allows us to have amplified knowledge of sample without any prior question[76]. In this acquisition mode, a MS1 scan is acquired, followed by successive MS2 spectra of the most abundant precursor ions detected in MS1, as shown in **Figure 3**. MS2 scans are performed stochastically and on as many precursor ions as possible, to achieve identification of large number of peptides and thereby proteins[77]. Protein identification is then accomplished by matching the experimental MS2 to theoretical MS2 derived from *in silico* digestion of proteins in protein databases. Several vendor-free computational proteomic platforms are available, including MaxQuant, a database search widely used for this purpose[78].

1.6. Quantitative Proteomics

The vast majority of studies explore the HDL proteome using shotgun proteomics[79]. The methodology is important for small studies, and to create a peptide library, aiding further development of more quantitative methods. However, the stochastic nature of the untargeted approach, together with the high rate of missing values generated, impairs the precise quantification of the molecules of lesser abundance[80]. In this sense, through targeted proteomics, high sensitivity, accuracy and reproducibility have been achieved to quantify concurrently multiple peptides present in a complex biological sample with a wide linear range[81].

There are three main targeted strategies for quantitative proteomics. Selected reaction monitoring (SRM, also called multiple reaction monitoring (MRM)) is the standard approach in quantitative MS-based proteomics. An SRM experiment is generally performed in a triple quadrupole (QqQ) mass spectrometer. Typically, the Q1 is set to filter a particular ion (precursor ion), which is fragmented in the collision cell, generating product ions. The Q3 is subsequently used to filter a specific product ion which is then detected[81]. Therefore, this acquisition mode requires previous knowledge of the peptides present in the sample to select the representative precursor ions (at least two or three) for each protein. Likewise, three to five fragments (product ions) per precursor are selected and monitored individually[82].

An alternative methodology for quantitative proteomics is parallel reaction monitoring (PRM), that can be performed on quadrupole-orbitrap (Q-orbitrap) or quadrupole-time of flight (Q-TOF) mass spectrometers. Parallel reaction monitoring is a hypothesis-driven experiment like SRM, where precursor ions are also selected before starting the analysis.

However, different from SRM, all product ions are detected. This is a great advantage over SRM, since the subset of product ions can be selected post factum to improve signal and eliminate possible noise contamination. In addition, product ions are obtained with high resolution, improving thus the selectivity[83].

Finally, data independent acquisition (DIA) is the most recently developed methodology for quantitative proteomics. Like PRM methodology, DIA is performed on hybrid mass spectrometers, typically employing a quadrupole as the first mass analyzer, and a TOF or orbitrap as second mass analyzer. In DIA, typically a MS1 is recorded, followed by a series of MS2 scans with wide precursor isolation windows covering the *m/z* range of the MS1 scan. Repeated cycling of consecutive precursor isolation window over a defined mass range happens, obtaining information on all detectable fragments, as well as the precursor ions. In fact, the term DIA refers to the fact that MS2 spectra are acquired without obtaining specific precursor ion mass from MS1 scan[84]. Isolation windows of 10 to 25 *m/z* are usually employed in DIA experiments, different from PRM or SRM experiments that use isolation windows of 1 or 2 *m/z*. This emerging strategy has some important advantages over shotgun, SRM and PRM. First, it does not require previous knowledge of the proteins and peptides present in the sample. In addition, because full MS2 spectra are recorded across a wide range of *m/z*, it is possible re-examine the data after acquisition, allowing the selection of new peptides and proteins[85]. A schematic representation of the three quantitative proteomics methodologies described above can be seen in **Figure 4**.

In terms of data analysis, no standardized pipeline has been developed, and there is still little discussion about the best ways to analyze data from quantitative methodologies.

Technological advances are widely reported, but the details of data processing as well as comparative studies of the strategies used for protein quantification are still scarce[86].

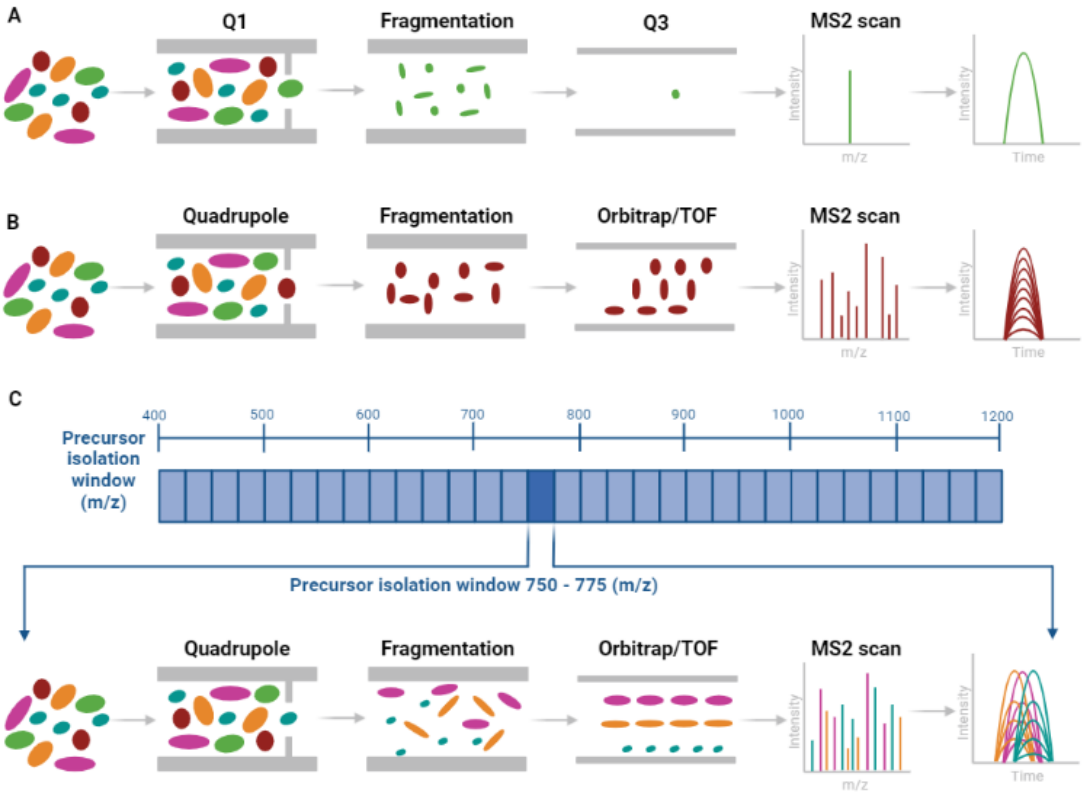

Figure 4. Principles of MS/MS techniques in quantitative proteomics. (**A**) SRM: one precursor ion is selected in the first quadrupole (Q1), fragmented in the second quadrupole (Q2) and one product ion is filtered in the third quadrupole (Q3) to be then detected. (**B**) PRM: one precursor ion is filtered in quadrupole, fragmented, and all product ions are detected in Orbitrap or TOF mass analyzers. (**C**) DIA: All precursor ions within of the chosen isolation window are fragmented, and all product ions are detected in Orbitrap or TOF mass analyzers. Image created with BioRender.com.

1.7. Overview of work described in this thesis

Despite of the rapid development in mass spectrometry-based proteomics over the last 20 years, a small percentage of proteins classified as biomarkers are approved by US Food and Drug Administration (FDA) when quantified by MS/MS. The majority continue to be measured by immunoaffinity assays. Thus, efforts need to be made to ensure

accurate and robust methodologies for protein quantification[81]. The same is true in the HDL context. It is consensus that HDL cholesterol content does not explain cardiovascular risk. Therefore, given the heterogeneity of this lipoprotein and its function plurality, it is urgent to develop reliable methodologies that will allow its proteome quantification. In this way, in Chapter 2 this thesis, we investigated the analytical performances of DIA and PRM methodologies using labeled peptides in pooled digested HDL as a biological matrix. Next, we compared the quantification capabilities of the two methodologies for 24 proteins found in HDL2 and HDL3 from 19 apparently healthy subjects.

Another bottleneck that waits for a solution in proteomics is the lack of standardization for data processing and analysis after mass spectrometry acquisition. Therefore, the third chapter of this thesis addresses the performance of different quantification strategies using Skyline and MaxDIA software platforms to compare HDL proteome from mice submitted to a high-fat diet supplemented or not with omega-3. It also shows the consequences of a high-fat diet on HDL proteome of mice.

1.8. References

1 NELSON, D. L.; COX, M. M. **Princípios de Bioquímica de Lehninger**. 6. ed. Tradução: Ana Beatriz Gorini da Veiga, *et al*. Porto Alegre: Artmed, 2014. 1298 p. ISBN 978-85-8271-072-2.

2 FEINGOLD, K. R. **Introduction to Lipids and Lipoproteins**. In: FEINGOLD, K. R.; ANAWALT, B.*, et al*. (Ed.). Endotext. South Dartmouth (MA): MDText.com, Inc., 2000. 39 p.

3 UniProt: a worldwide hub of protein knowledge. **Nucleic Acids Research**, v. 47, p. D506-D515, 2019. DOI 10.1093/nar/gky1049. Disponível em: https://academic.oup.com/nar/article-pdf/47/D1/D506/27437297/gky1049.pdf.

4 MARZZOCO, A.; TORRES, B. B. **Bioquímica Básica**. 2. ed. Rio de Janeiro: Editora Guanabara Koogan S.A., 1999. 360 p. ISBN 85-277-0462-5.

5 TSIMIKAS, S. A Test in Context: Lipoprotein(a): Diagnosis, Prognosis, Controversies, and Emerging Therapies. **Journal of the American College of Cardiology**, v. 69, n. 6, 692-711, 2017. DOI 10.1016/j.jacc.2016.11.042. Disponível em: https://www.sciencedirect.com/science/article/pii/S0735109716372540?via%3Dihub

6 BEN-AICHA, S.; BADIMON, L.; VILAHUR, G. Advances in HDL: Much More than Lipid Transporters. **International Journal of Molecular Sciences**, v. 21, n. 3, 732-774, 2020. DOI 10.3390/ijms21030732. Disponível em: https://www.ncbi.nlm.nih.gov/pmc/articles/PMC7037660/.

7 MACHEBOEUF, M. Recherches sur les phosphoaminolipides du sérum sanguin. Nature des phospholipides liés aux albumines du sérum de Cheval à l'état de cenapses acido-précipitables. **Bull. Soc. Chim. Biol.**, v. 11, p. 485-503, 1929. Disponível em: https://scholar.google.com/scholar_lookup?journal=Bull.+Soc.+Chim.+Biol.+(Paris)&title=Recherches+sur+les+phosphoaminolipides+du+s%C3%A9rum+sanguin.+Nature+des+phospholipides+li%C3%A9s+aux+albumines+du+s%C3%A9rum+de+Cheval+%C3%A0+l%E2%80%99%C3%A9tat+de+cenapses+acidopr%C3%A9cipitables&author=M.+Macheboeuf&volume=11&publication_year=1929&pages=485-503&

8 SHAH, A. S. *et al*. Proteomic diversity of high density lipoproteins: our emerging understanding of its importance in lipid transport and beyond. **Journal of Lipid Research**, v. 54, n. 10, p. 2575-2585, 2013. DOI 10.1194/jlr.R035725. Disponível em: https://www.ncbi.nlm.nih.gov/pmc/articles/PMC3770071/.

9 SHORE, B.; SHORE, V. Heterogeneity in protein subunits of human serum high-density lipoproteins. **Biochemistry**, v. 7, n. 8, p. 2773-2777, 1968. DOI 10.1021/bi00848a011. Disponível em: https://pubmed.ncbi.nlm.nih.gov/5666751/.

10 SCANU, A. *et al*. Fractionation of human serum high density lipoprotein in urea solutions. Evidence for polypeptide heterogeneity. **Biochemistry**, v. 8, n. 8, p. 3309-3316, 1969. DOI 10.1021/bi00836a027. Disponível em: https://pubmed.ncbi.nlm.nih.gov/4980192/.

11 RUDMAN, D.; GARCIA, L. A.; HOWARD, C. H. A new method for isolating the nonidentical protein subunits of human plasma alpha-lipoprotein. **The Journal of Clinical Investigation**, v. 49, n. 2, p. 365-372, 1970. DOI 10.1172/JCI106245. Disponível em: https://www.ncbi.nlm.nih.gov/pubmed/5411787.

12 GUSTAFSON, A.; ALAUPOVIC, P.; FURMAN, R. H. Studies of the composition and structure of serum lipoproteins. Separation and characterization of phospholipid-protein residues obtained by partial delipidization of very low density lipoproteins of human serum. **Biochemistry**, v. 5, n. 2, p. 632-640, 1966. DOI 10.1021/bi00866a033. Disponível em: https://www.ncbi.nlm.nih.gov/pubmed/4957397.

13 HAVEL, R. J.; EDER, H. A.; BRAGDON, J. H. The distribution and chemical composition of ultracentrifugally separated lipoproteins in human serum. **The Journal of Clinical Investigation**,

v. 34, n. 9, p. 1345-1353, 1955. DOI 10.1172/JCI103182. Disponível em: http://dx.doi.org/10.1172/jci103182 .

14 SCANU, A. Studies on the conformation of human serum high-density lipoproteins HDL2 and HDL3. **Proceedings of the National Academy of Science of the United States of America**, v. 54, n. 6, p. 1699-1705, 1965. DOI 10.1073/pnas.54.6.1699. Disponível em: https://www.ncbi.nlm.nih.gov/pmc/articles/PMC300537/.

15 SCHAEFER, E. J. *et al*. The composition and metabolism of high density lipoprotein subfractions. **Lipids**, v. 14, n. 5, p. 511-522, 1979. DOI 10.1007/BF02533471. Disponível em: https://pubmed.ncbi.nlm.nih.gov/222991/.

16 BLANCHE, P. J. *et al*. Characterization of human high-density lipoproteins by gradient gel electrophoresis. **Biochimica et Biophysica Acta**, v. 665, n. 3, p. 408-419, 1981. DOI 10.1016/0005-2760(81)90253-8. Disponível em: https://www.ncbi.nlm.nih.gov/pubmed/7295744.

17 ALAUPOVIC, P. The concept of apolipoprotein-defined lipoprotein families and its clinical significance. **Current Atherosclerosis Reports**, v. 5, n. 6, p. 459-467, 2003. DOI 10.1007/s11883-003-0036-8. Disponível em: https://www.ncbi.nlm.nih.gov/pubmed/14525679.

18 LEWIS, L. A.; PAGE, I. H. Electrophoretic and ultracentrifugal analysis of serum lipoproteins of normal, nephrotic and hypertensive persons. **Circulation**, v. 7, n. 5, p. 707-717, 1953. DOI 10.1161/01.cir.7.5.707. Disponível em: https://www.ncbi.nlm.nih.gov/pubmed/13042925.

19 ASZTALOS, B. F.; TANI, M.; SCHAEFER, E. J. Metabolic and functional relevance of HDL subspecies. **Current Opinion in Lipidology**, v. 22, n. 3, p. 176-185, 2011. DOI 10.1097/MOL.0b013e3283468061. Disponível em: https://www.ncbi.nlm.nih.gov/pubmed/21537175.

20 HAFFNER, S.; TAEGTMEYER, H. Epidemic obesity and the metabolic syndrome. **Circulation**, v. 108, n. 13, p. 1541-1545, 2003. DOI 10.1161/01.cir.0000088845.17586.ec. Disponível em: https://www.ahajournals.org/doi/10.1161/01.CIR.0000088845.17586.EC.

21 GO, A. S. *et al*. Heart Disease and Stroke Statistics—2013 Update. **Circulation**, v. 127, n. 1, p. e6-e245, 2013. DOI 10.1161/CIR.0b013e31828124ad. Disponível em: https://www.ahajournals.org/doi/10.1161/CIR.0b013e31828124ad.

22 World Health Organization. Cardiovascular Diseases (CVDs). 2021. Disponível em: https://www.who.int/news-room/fact-sheets/detail/cardiovascular-diseases-(cvds)#:~:text=Cardiovascular%20diseases%20(CVDs)%20are%20the,to%20heart%20attack%20and%20stroke. >. Acesso em: 31 maio 2022.

[23] KELLY, T. *et al*. Global burden of obesity in 2005 and projections to 2030. **International Journal of Obesity**, v. 32, n. 9, p. 1431-1437, 2008. DOI 10.1038/ijo.2008.102. Disponível em: https://www.nature.com/articles/ijo2008102.

[24] BAYS, H. E. *et al*. Obesity, adiposity, and dyslipidemia: a consensus statement from the National Lipid Association. **Journal of Clinical Lipidology**, v. 7, n. 4, p. 304-383, 2013. DOI 10.1016/j.jacl.2013.04.001. Disponível em: https://www.lipidjournal.com/article/S1933-2874(13)00160-8/fulltext.

[25] WU, L.; PARHOFER, K. G. Diabetic dyslipidemia. **Metabolism**, v. 63, n. 12, p. 1469-1479, 2014. DOI 10.1016/j.metabol.2014.08.010. Disponível em: https://www.metabolismjournal.com/article/S0026-0495(14)00258-3/fulltext.

[26] CHISTIAKOV, D. A. *et al*. How do macrophages sense modified low-density lipoproteins? **International Journal of Cardiology**, v. 230, n. 1, p. 232-240, 2017. DOI 10.1016/j.ijcard.2016.12.164. Disponível em: http://www.sciencedirect.com/science/article/pii/S016752731634815X.

[27] SABATINE, M. S. *et al*. Evolocumab and Clinical Outcomes in Patients with Cardiovascular Disease. The **New England Journal of Medicine**, v. 376, n. 18, p. 1713-1722, 2017. DOI 10.1056/NEJMoa1615664. Disponível em: https://www.nejm.org/doi/10.1056/NEJMoa1615664.

[28] LEWIS, G. F.; RADER, D. J. New insights into the regulation of HDL metabolism and reverse cholesterol transport. **Circulation Research**, v. 96, n. 12, p. 1221-1232, 2005. DOI 10.1161/01.RES.0000170946.56981.5c. Disponível em: https://www.ahajournals.org/doi/10.1161/01.RES.0000170946.56981.5c.

[29] VAISAR, T. *et al*. Shotgun proteomics implicates protease inhibition and complement activation in the antiinflammatory properties of HDL. **The Journal of Clinical Investigation**, v. 117, n. 3, p. 746-756, 2007. DOI 10.1172/JCI26206. Disponível em: https://www.jci.org/articles/view/26206/pdf.

[30] BIRNER-GRUENBERGER, R. *et al*. Understanding high-density lipoprotein function in disease: Recent advances in proteomics unravel the complexity of its composition and biology. **Progress in Lipid Research**, v. 56, p. 36-46, 2014. DOI 10.1016/j.plipres.2014.07.003. Disponível em: http://www.sciencedirect.com/science/article/pii/S0163782714000411.

[31] HOLMES, M. V. *et al*. Mendelian randomization of blood lipids for coronary heart disease. **European Heart Journal**, v. 36, n. 9, p. 539-550, 2015. DOI 10.1093/eurheartj/eht571. Disponível em: https://www.ncbi.nlm.nih.gov/pubmed/24474739.

[32] WILLER, C. J. *et al*. Discovery and refinement of loci associated with lipid levels. **Nature Genetics**, v. 45, n. 11, p. 1274-1283, 2013. DOI 10.1038/ng.2797. Disponível em: < https://www.ncbi.nlm.nih.gov/pubmed/24097068 >.

[33] VOIGHT, B. F. *et al*. Plasma HDL cholesterol and risk of myocardial infarction: a mendelian randomisation study. **The Lancet**, v. 380, n. 9841, p. 572-580, 2012. DOI 10.1016/S0140-6736(12)60312-2. Disponível em: < https://www.ncbi.nlm.nih.gov/pubmed/22607825 >.

[34] RADER, D. J.; TALL, A. R. The not-so-simple HDL story: Is it time to revise the HDL cholesterol hypothesis? **Nature Medicine**, v. 18, n. 9, p. 1344-1346, 2012. DOI 10.1038/nm.2937. Disponível em: https://www.ncbi.nlm.nih.gov/pubmed/22961164.

[35] SCHWARTZ, G. G. *et al*. Effects of dalcetrapib in patients with a recent acute coronary syndrome. **The New England Journal of Medicine**, v. 367, n. 22, p. 2089-2099, 2012. DOI 10.1056/NEJMoa1206797. Disponível em: https://www.nejm.org/doi/full/10.1056/NEJMoa1206797.

[36] BODEN, W. E. *et al*. Niacin in patients with low HDL cholesterol levels receiving intensive statin therapy. **The New England Journal of Medicine**, v. 365, n. 24, p. 2255-2267, 2011. DOI 10.1056/NEJMoa1107579. Disponível em: https://www.ncbi.nlm.nih.gov/pubmed/22085343.

[37] ROSEIN, G. E. *et al*. Niacin Therapy Increases High-Density Lipoprotein Particles and Total Cholesterol Efflux Capacity But Not ABCA1-Specific Cholesterol Efflux in Statin-Treated Subjects. **Arteriosclerosis, Thrombosis, and Vascular Biology**, v. 36, n. 2, p. 404-411, 2016. DOI 10.1161/ATVBAHA.115.306268. Disponível em: https://www.ncbi.nlm.nih.gov/pubmed/26681752.

[38] YVAN-CHARVET, L. *et al*. Cholesterol efflux potential and antiinflammatory properties of high-density lipoprotein after treatment with niacin or anacetrapib. **Arteriosclerosis, Thrombosis, and Vascular Biology**, v. 30, n. 7, p. 1430-1438, 2010. DOI 10.1161/ATVBAHA.110.207142. Disponível em: https://www.ncbi.nlm.nih.gov/pubmed/20448206.

[39] BARTER, P. J. *et al*. Effects of torcetrapib in patients at high risk for coronary events. The **New England Journal of Medicine**, v. 357, n. 21, p. 2109-2122, 2007. DOI 10.1056/NEJMoa0706628. Disponível em: https://www.nejm.org/doi/full/10.1056/NEJMoa0706628.

[40] CHEN, Y. *et al*. Evacetrapib reduces preβ-1 HDL in patients with atherosclerotic cardiovascular disease or diabetes. **Atherosclerosis**, v. 285, p. 147-152, 2019. DOI 10.1016/j.atherosclerosis.2019.04.211. Disponível em: https://www.ncbi.nlm.nih.gov/pubmed/31054484 >.

[41] ROSENSON, R. S. *et al*. Dysfunctional HDL and atherosclerotic cardiovascular disease. **Nature Reviews Cardiology**, v. 13, n. 1, p. 48-60, 2016. DOI 10.1038/nrcardio.2015.124. Disponível em: https://www.ncbi.nlm.nih.gov/pubmed/26323267.

[42] SWERTFEGER, D. K. *et al*. Mapping Atheroprotective Functions and Related Proteins/Lipoproteins in Size Fractionated Human Plasma. **Molecular & Cellular Proteomics**, v. 16, n. 4, p. 680-693, 2017. DOI 10.1074/mcp.M116.066290. Disponível em: https://www.mcponline.org/article/S1535-9476(20)32412-9/fulltext.

[43] GORDON, S. M. *et al*. The effects of type 2 diabetes on lipoprotein composition and arterial stiffness in male youth. **Diabetes**, v. 62, n. 8, p. 2958-2967, 2013. DOI 10.2337/db12-1753. Disponível em: https://diabetesjournals.org/diabetes/article/62/8/2958/34108/The-Effects-of-Type-2-Diabetes-on-Lipoprotein.

[44] SANTANA, M. F. M. *et al*. Enrichment of apolipoprotein A-IV and apolipoprotein D in the HDL proteome is associated with HDL functions in diabetic kidney disease without dialysis. **Lipids in Health and Disease**, v. 19, n. 1, p. 1-14, 2020. DOI 10.1186/s12944-020-01381-w. Disponível em: https://lipidworld.biomedcentral.com/articles/10.1186/s12944-020-01381-w.

[45] HOLZER, M. *et al*. Psoriasis alters HDL composition and cholesterol efflux capacity[S]. In: (Ed.). **Journal of Lipid Research**, v.53, n. 8, p.1618-1624, 2012. DOI 10.1194/jlr.M027367. Disponível em: https://www.ncbi.nlm.nih.gov/pmc/articles/PMC3540842/.

[46] WATANABE, J. *et al*. Proteomic profiling following immunoaffinity capture of high-density lipoprotein: association of acute-phase proteins and complement factors with proinflammatory high-density lipoprotein in rheumatoid arthritis. **Arthritis Rheumatism**, v. 64, n. 6, p. 1828-1837, 2012. DOI 10.1002/art.34363. Disponível em: https://www.ncbi.nlm.nih.gov/pmc/articles/PMC3330163/.

[47] PRUFER, N.; KLEUSER, B.; GIET, M. The role of serum amyloid A and sphingosine-1-phosphate on high-density lipoprotein functionality. **Biological Chemistry,** v. 396, n. 6-7, p. 573-583, 2015. DOI 10.1515/hsz-2014-0192. Disponível em: < https://www.ncbi.nlm.nih.gov/pubmed/25252751 >.

[48] RADER, D. J. Mediterranean Approach to Improving High-Density Lipoprotein Function. **Circulation**, v. 135, n. 7, p. 644-647, 2017. DOI 10.1161/CIRCULATIONAHA.117.026278. Disponível em: https://www.ncbi.nlm.nih.gov/pubmed/28193798.

[49] IGNATOWSKI, A. C. Influence of animal food on the organsim of rabbits. **Izvest Imper Voennomed Akad St Petersburg**, v. 16, p. 154-173, 1908. Disponível em: https://scholar.google.com/scholar_lookup?journal=S.+Peterb.+Izviest.+Imp.+Voyenno-Med.+Akad.&title=Influence+of+animal+food+on+the+organism+of+rabbits&author=AC+Ignatowski&volume=16&publication_year=1908&pages=154-173&.

[50] KEYS, A.; ARAVANIS, C.; BLACKBURN, H. **Seven Countries: A Multi variate Analysis of Death and Coronary Heart Disease**. Cambridge, MA, and London, England: Harvard University Press Cambridge. 1980. p. 381.

[51] RAMSDEN, C. E.; DOMENICHIELLO, A. F. PURE study challenges the definition of a healthy diet: but key questions remain. **The Lancet**, v. 390, n. 10107, p. 2018-2019, 2017. DOI 10.1016/S0140-6736(17)32241-9. Disponível em: http://www.sciencedirect.com/science/article/pii/S0140673617322419.

[52] WANG, Q. *et al*. Impact of Nonoptimal Intakes of Saturated, Polyunsaturated, and Trans Fat on Global Burdens of Coronary Heart Disease. **Journal of the American Heart Association**, v. 5, n.

1, p. e002891, 2016. DOI 10.1161/JAHA.115.002891. Disponível em: < http://jaha.ahajournals.org/content/5/1/e002891 >.

53 HOOPER, L. *et al*. Reduction in saturated fat intake for cardiovascular disease. **Cochrane Database of Systematic Reviews**, n. 6, p. 1-153, 2015. DOI 10.1002/14651858.CD011737. Disponível em: https://www.cochranelibrary.com/cdsr/doi/10.1002/14651858.CD011737/full.

54 WANG, D. D. *et al*. Association of Specific Dietary Fats With Total and Cause-Specific Mortality. **JAMA Internal Medicine**, v. 176, n. 8, p. 1134-1145, 2016. DOI 10.1001/jamainternmed.2016.2417 ISSN 2168-6106. Disponível em: https://jamanetwork.com/journals/jamainternalmedicine/articlepdf/2530902/ioi160037.pdf.

55 MOZAFFARIAN, D.; MICHA, R.; WALLACE, S. Effects on Coronary Heart Disease of Increasing Polyunsaturated Fat in Place of Saturated Fat: A Systematic Review and Meta-Analysis of Randomized Controlled Trials. **PLoS Medicine**, v. 7, n. 3, p. e1000252, 2010. DOI 10.1371/journal.pmed.1000252. Disponível em: https://www.ncbi.nlm.nih.gov/pmc/articles/PMC2843598/#!po=17.1875.

56 LI, Y. *et al*. Saturated Fats Compared With Unsaturated Fats and Sources of Carbohydrates in Relation to Risk of Coronary Heart Disease: A Prospective Cohort Study. **Journal of the American College of Cardiology**, v. 66, n. 14, p. 1538-1548, 2015. DOI 10.1016/j.jacc.2015.07.055. Disponível em: https://www.ncbi.nlm.nih.gov/pubmed/26429077.

57 KRIS-ETHERTON, P. M.; HARRIS, W. S.; APPEL, L. J. Fish consumption, fish oil, omega-3 fatty acids, and cardiovascular disease. **Circulation**, v. 106, n. 21, p. 2747-2757, 2002. DOI 10.1161/01.cir.0000038493.65177.94. Disponível em: https://pubmed.ncbi.nlm.nih.gov/12438303/.

58 RAMSDEN, C. *et al*. n-6 Fatty acid-specific and mixed polyunsaturate dietary interventions have different effects on CHD risk: a meta-analysis of randomised controlled trials | British Journal of Nutrition | Cambridge Core. **British Journal of Nutrition**, v. 104, n. 11, p. 1586-1600, 2010. DOI 10.1017/S0007114510004010. Disponível em: https://www.cambridge.org/core/journals/british-journal-of-nutrition/article/n6-fatty-acidspecific-and-mixed-polyunsaturate-dietary-interventions-have-different-effects-on-chd-risk-a-metaanalysis-of-randomised-controlled-trials/938F3F74E18033ED061F7D8CEAB0A24A.

59 THIES, F. *et al*. Association of n-3 polyunsaturated fatty acids with stability of atherosclerotic plaques: a randomised controlled trial. **The Lancet**, v. 361, n. 9356, p. 477-485, 2003. DOI 10.1016/s0140-6736(03)12468-3. Disponível em: https://www.thelancet.com/journals/lancet/article/PIIS0140-6736(03)12468-3/fulltext.

60 SARAVANAN, P. *et al*. Cardiovascular effects of marine omega-3 fatty acids. **The Lancet**, v. 376, n. 9740, p. 540-550, 2010. DOI 10.1016/S0140-6736(10)60445-X. Disponível em: https://www.scopus.com/inward/record.uri?eid=2-s2.0-77956063072&doi=10.1016%2fS0140-6736%2810%2960445-X&partnerID=40&md5=eec8649c48b1187c28f54f09a35ba22d.

[61] FEINGOLD, K. *et. al*. **Triglyceride Lowering Drugs**. In: Feingold KR, *et al*., (Ed.). Endotext. South Dartmouth (MA): MDText.com, Inc.; 2000. 126 p.

[62] ESLICK, G. D. *et al*. Benefits of fish oil supplementation in hyperlipidemia: a systematic review and meta-analysis. **International Journal of Cardiology**, v. 136, n. 1, p. 4-16, 2009. DOI 10.1016/j.ijcard.2008.03.092. Disponível em: http://dx.doi.org/10.1016/j.ijcard.2008.03.092.

[63] RIZOS, E. C. *et al*. Association Between Omega-3 Fatty Acid Supplementation and Risk of Major Cardiovascular Disease Events: A Systematic Review and Meta-analysis. **JAMA**, v. 308, n. 10, p. 1024-1033, 2018. DOI 10.1001/2012.jama.11374. Disponível em: https://jamanetwork.com/journals/jama/articlepdf/1357266/jrv120006_1024_1033.pdf.

[64] BOSCH, J. *et al*. n-3 fatty acids and cardiovascular outcomes in patients with dysglycemia. The **New England Journal of Medicine**, v. 367, n. 4, p. 309-318, 2012. DOI 10.1056/NEJMoa1203859. Disponível em: http://dx.doi.org/10.1056/NEJMoa1203859.

[65] GALAN, P. *et al*. Effects of B vitamins and omega 3 fatty acids on cardiovascular diseases: a randomised placebo controlled trial. **BMJ**, v. 341, p. 1-9, 2010. DOI 10.1136/bmj.c6273. Disponível em: https://www.bmj.com/content/341/bmj.c6273.

[66] MERKEL, M. *et al*. Compared with saturated fatty acids, dietary monounsaturated fatty acids and carbohydrates increase atherosclerosis and VLDL cholesterol levels in LDL receptor-deficient, but not apolipoprotein E-deficient, mice. **Proceedings of the National Academy of Science of the United States of America**, v. 98, n. 23, p. 13294-13299, 2001. DOI 10.1073/pnas.231490498. Disponível em: https://www.ncbi.nlm.nih.gov/pubmed/11606787.

[67] KENNEDY, A. J. *et al*. Mouse models of the metabolic syndrome. **Disease Models & Mechanisms**, v. 3, n. 3-4, 2010. p.156-166. DOI 10.1242/dmm.003467. Disponível em: https://pubmed.ncbi.nlm.nih.gov/20212084/.

[68] GETZ, G. S.; REARDON, C. A. Animal models of atherosclerosis. **Arterioscler Thrombosis and Vascular Biology**, v. 32, n. 5, p. 1104-1115, 2012. DOI 10.1161/atvbaha.111.237693. Disponível em: https://www.ahajournals.org/doi/10.1161/ATVBAHA.111.237693.

[69] ISHIBASHI, S. *et al*. Hypercholesterolemia in low density lipoprotein receptor knockout mice and its reversal by adenovirus-mediated gene delivery. **The Journal of Clinical Investigation**, v. 92, n. 2, p. 883-893, 1993. DOI 10.1172/jci116663. Disponível em: https://www.ncbi.nlm.nih.gov/pmc/articles/PMC294927/.

[70] WU, L. *et al*. Addition of dietary fat to cholesterol in the diets of LDL receptor knockout mice: effects on plasma insulin, lipoproteins, and atherosclerosis. **Journal of Lipid Research**, v. 47, n. 10, p. 2215-2222, 2006. DOI 10.1194/jlr.M600146-JLR200. Disponível em: http://www.jlr.org/content/47/10/2215.full.

[71] O'REILLY, M. *et al*. High-Density Lipoprotein Proteomic Composition, and not Efflux Capacity, Reflects Differential Modulation of Reverse Cholesterol Transport by Saturated and Monounsaturated Fat Diets. **Circulation**, v. 133, n. 19, p. 1838-1850, 2016. DOI 10.1161/CIRCULATIONAHA.115.020278. Disponível em: https://www.ncbi.nlm.nih.gov/pubmed/27081117.

[72] PATTERSON, S. D.; AEBERSOLD, R. H. Proteomics: the first decade and beyond. **Nature Genetics**, v. 33, p. 311-323, 2003. DOI 10.1038/ng1106. Disponível em: https://www.ncbi.nlm.nih.gov/pubmed/12610541.

[73] CHAIT, B. T. Chemistry. Mass spectrometry: bottom-up or top-down? **Science**, v. 314, n. 5796, p. 65-66, 2006. DOI 10.1126/science.1133987. Disponível em: https://www.ncbi.nlm.nih.gov/pubmed/17023639.

[74] DAU, T.; BARTOLOMUCCI, G.; RAPPSILBER, J. Proteomics Using Protease Alternatives to Trypsin Benefits from Sequential Digestion with Trypsin. **Analytical Chemistry**, v. 92, n. 14, p. 9523-9527, 2020. DOI 10.1021/acs.analchem.0c00478. Disponível em: https://www.ncbi.nlm.nih.gov/pubmed/32628831.

[75] UZOZIE, A. C.; AEBERSOLD, R. Advancing translational research and precision medicine with targeted proteomics. **Journal of Proteomics**, v. 189, p. 1-10, 2018. DOI 10.1016/j.jprot.2018.02.021. Disponível em: http://www.sciencedirect.com/science/article/pii/S1874391918300769.

[76] MEISSNER, F.; MANN, M. Quantitative shotgun proteomics: considerations for a high-quality workflow in immunology. **Nature Immunology**, v. 15, n. 2, p. 112-117, 2014. DOI 10.1038/ni.2781. Disponível em: https://www.ncbi.nlm.nih.gov/pubmed/24448568.

[77] GILLET, L. C.; LEITNER, A.; AEBERSOLD, R. Mass Spectrometry Applied to Bottom-Up Proteomics: Entering the High-Throughput Era for Hypothesis Testing. **Annual Review of Analytical Chemistry**, v. 9, n. 1, p. 449-472, 2016. DOI 10.1146/annurev-anchem-071015-041535. Disponível em: https://www.annualreviews.org/doi/10.1146/annurev-anchem-071015-041535?url_ver=Z39.88-2003&rfr_id=ori%3Arid%3Acrossref.org&rfr_dat=cr_pub++0pubmed.

[78] COX, J.; MANN, M. MaxQuant enables high peptide identification rates, individualized p.p.b.-range mass accuracies and proteome-wide protein quantification. **Nature Biotechnology**, v. 26, n. 12, p. 1367-1372, 2008. DOI 10.1038/nbt.1511. Disponível em: https://www.nature.com/articles/nbt.1511.

[79] SINGH, S. A.; AIKAWA, M. Unbiased and targeted mass spectrometry for the HDL proteome. **Current Opinion in Lipidology**, v. 28, n. 1, p. 68-77, 2017. DOI 10.1097/MOL.0000000000000374. Disponível em: https://journals.lww.com/co-lipidology/Abstract/2017/02000/Unbiased_and_targeted_mass_spectrometry_for_the.11.aspx.

[80] LIU, H.; SADYGOV, R. G.; YATES, J. R. A model for random sampling and estimation of relative protein abundance in shotgun proteomics. **Analytical Chemistry**, v. 76, n. 14, p. 4193-4201, 2004. DOI 10.1021/ac0498563. Disponível em: https://pubs.acs.org/doi/10.1021/ac0498563.

[81] VIDOVA, V.; SPACIL, Z. A review on mass spectrometry-based quantitative proteomics: Targeted and data independent acquisition. **Analytica Chimica Acta**, v. 964, p. 7-23, 2017. DOI doi.org/10.1016/j.aca.2017.01.059. Disponível em: http://www.sciencedirect.com/science/article/pii/S0003267017301502.

[82] PICOTTI, P.; AEBERSOLD, R. Selected reaction monitoring-based proteomics: workflows, potential, pitfalls and future directions. **Nature Methods**, v. 9, n. 6, p. 555-566, 2012. DOI 10.1038/nmeth.2015. Disponível em:https://www.ncbi.nlm.nih.gov/pubmed/22669653.

[83] PETERSON, A. C. *et al*. Parallel Reaction Monitoring for High Resolution and High Mass Accuracy Quantitative, Targeted Proteomics. **Molecular & Cellular Proteomics**, v. 11, n. 11, p. 1475-1488, 2012. DOI 10.1074/mcp.O112.020131. Disponível em: http://www.mcponline.org/content/11/11/1475.abstract.

[84] LUDWIG, C. *et al*. Data-independent acquisition-based SWATH-MS for quantitative proteomics: a tutorial. **Molecular Systems Biology**, v. 14, n. 8, p. e8126, 2018. DOI 10.15252/msb.20178126. Disponível em: https://www.embopress.org/doi/full/10.15252/msb.20178126.

[85] AEBERSOLD, R. *et al*. Applications and Developments in Targeted Proteomics: From SRM to DIA/SWATH. **Proteomics**, v. 16, n. 15-16, p. 2065-2067, 2016. DOI 10.1002/pmic.201600203. Disponível em: https://www.ncbi.nlm.nih.gov/pubmed/27542680.

[86] AEBERSOLD, R. Editorial: From Data to Results. **Molecular & Cellular Proteomics**, v. 10, n. 11, p. E111.014787, 2011. DOI 10.1074/mcp.E111.014787. Disponível em: https://www.mcponline.org/article/S1535-9476(20)30091-8/fulltext.

CHAPTER 2 - Comparing Data-Independent Acquisition and Parallel Reaction Monitoring in Their Abilities to Differentiate High-Density Lipoprotein Subclasses

Journal of proteome research
Article
Cite This: J. Proteome Res. XXXX, XXX, XXX−XXX
pubs.acs.org/jpr

Comparing Data-Independent Acquisition and Parallel Reaction Monitoring in Their Abilities To Differentiate High-Density Lipoprotein Subclasses

Amanda R. M. Silva,[†] Marcos T. K. Toyoshima,[‡,§] Marisa Passarelli,[‡,∥] Paolo Di Mascio,[†] and Graziella E. Ronsein*[,†]

[†]Departamento de Bioquímica, Instituto de Química, Universidade de São Paulo, São Paulo 05513970, Brazil
[‡]Laboratório de Lípides (LIM-10), Hospital das Clínicas, Faculdade de Medicina da Universidade de São Paulo, São Paulo 01246903, Brazil
[§]Serviço de Onco-Endocrinologia, Instituto do Câncer do Estado de São Paulo Octávio Frias de Oliveira, Hospital das Clínicas, Faculdade de Medicina da Universidade de São Paulo, São Paulo 01246000, Brazil
[∥]Programa de Pós-Graduação da Universidade Nove de Julho, São Paulo 01504001, Brazil

Supporting Information

ABSTRACT: High-density lipoprotein (HDL) is a diverse group of particles with multiple cardioprotective functions. HDL proteome follows HDL particle complexity. Many proteins were described in HDL, but consistent quantification of HDL protein cargo is still a challenge. To address this issue, the aim of this work was to compare data-independent acquisition (DIA) and parallel reaction monitoring (PRM) methodologies in their abilities to differentiate HDL subclasses through their proteomes. To this end, we first evaluated the analytical performances of DIA and PRM using labeled peptides in pooled digested HDL as a biological matrix. Next, we compared the quantification capabilities of the two methodologies for 24 proteins found in HDL_2 and HDL_3 from 19 apparently healthy subjects. DIA and PRM exhibited comparable linearity, accuracy, and precision. Moreover, both methodologies worked equally well, differentiating HDL subclasses' proteomes with high precision. Our findings may help to understand HDL functional diversity.

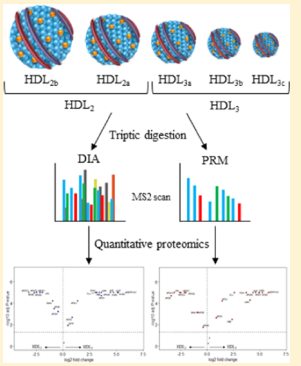

KEYWORDS: *HDL, DIA, PRM, targeted proteomics*

INTRODUCTION

High-density lipoprotein (HDL) has been linked to a variety of cardioprotective functions possibly due to its structural and compositional heterogeneity.[1] Depending on the detection method, more than 100 proteins were identified as belonging to HDL, although the two most abundant proteins, apolipoprotein A1 (APOA1) and apolipoprotein A2 (APOA2), make up around 90% of the HDL protein mass.[2] This finding strongly suggests that specific proteins are differentially localized in distinct HDL particles, which may explain the diverse biological functions of this lipoprotein.[3] Indeed, the notion that HDL is essentially a single entity with numerous interchanging protein components has been challenged by several studies.[1,3−6] HDL particles were first defined based on their flotation at a density range of 1.063−1.21 g/mL.[7] Since early studies, it became clear that HDL particles are diverse.[8−10] Based on density, HDL can be further separated into two distinct classes—a denser HDL_3 (1.125−1.21 g/mL) and a lighter HDL_2 (1.063−1.125 g/mL) class.[8,11]

Importantly, the vast majority of studies exploring HDL proteome used data-dependent acquisition (DDA, also termed shotgun proteomics) to detect and to quantify HDL.[1,3,12−14] Nevertheless, the stochastic nature of this untargeted method, along with the high rate of missing values, hampers accurate quantification of low abundance proteins.[15] Targeted strategies can overcome the limitations associated with DDA, achieving high sensitivity, accuracy, and reproducibility to quantify multiple peptides present in a complex biological sample.[16] The most widely used targeted strategy for quantitative proteomics is called selected reaction monitoring (SRM, also termed multiple reaction monitoring). Many studies have shown that SRM is precise and robust for multiplexed quantification.[17,18] This method is performed in triple quadrupole mass spectrometers and requires previous knowledge of peptides and their fragments. Generally, two to three peptides with two to three fragments each are monitored per protein.[19]

Another strategy employed for targeted proteomics is parallel reaction monitoring (PRM).[20,21] Typically, PRM experiments are performed in hybrid instruments, either quadrupole time-of-flight (Q-TOF) or quadrupole-Orbitrap mass spectrometers. In brief, predefined precursor ions are isolated in a quadrupole mass filter and transferred into the

Received: July 29, 2019

DOI: 10.1021/acs.jproteome.9b00511
J. Proteome Res. XXXX, XXX, XXX−XXX

collision cell, where they are fragmented. All resulting fragment ions are then simultaneously analyzed.[20−22] PRM has some potential advantages over SRM methodology. First, all fragment ions of a given peptide are obtained at the same time. Second, these fragments are obtained with high resolution, given the capabilities of these types of mass spectrometers. Previously, we have shown that PRM exhibits comparable analytical performance to that obtained with SRM to quantify multiple proteins in HDL.[23] Furthermore, PRM obtained equivalent results when compared to SRM to differentiate HDL abnormal composition in diabetic subjects with fenofibrate/rosiglitazone-induced hypoalphalipoproteinemia.[24] Despite their robustness and precision, SRM and PRM methods monitor a limited number of targets. Besides, both techniques are hypothesis-driven, and precursors must be known before starting the experiment.[25]

On the other hand, data-independent acquisition (DIA), a more recently introduced approach to mass spectrometry (MS)-based proteomics, alleviates the limitations in multiplexing by combining advantages of untargeted and targeted proteomics.[26] DIA is performed on the same hybrid instruments used for PRM, but in DIA, all precursor ions within a defined m/z window are deterministically fragmented.[27] Thus, a comprehensive data set is recorded through repeated cycling of consecutive isolation windows. The great advantage of DIA over SRM and PRM methodologies lies in the fact that samples need to be acquired only once and can be analyzed endlessly in silico, since all fragment ions are determined.[28] It is worth noting that when DIA methods are acquired using Q-TOF instruments, they are sometimes termed sequential window acquisition of all theoretical mass spectra (SWATH-MS).[29]

DIA showed good reproducibility in a multilaboratory assessment,[27] but analysis of DIA performance in translational studies is still missing. In this work, we compared the capabilities of DIA and PRM through quantification of proteins in distinct HDL subclasses. To this end, we first generated calibration curves for labeled peptides in pooled digested HDL as a biological matrix, and the analytical performances of DIA and PRM were systematically assessed. Next, using clinical samples, we compared the capabilities of DIA and PRM to quantify 24 proteins found in HDL subclasses. Our observations indicate that DIA and PRM work equally well, differentiating HDL_2 and HDL_3 proteomes. Moreover, our results confirm that HDL subclass proteome is distinct, strengthening the idea that subclasses of HDL may be associated with different biological functions.

EXPERIMENTAL SECTION

Sample Collection

Nineteen apparently healthy subjects, with age ranging from 23 to 68 years, were selected for the study. The criteria for recruitment excluded subjects with altered glycated hemoglobin and with continuous use of any medication. Venous blood was collected after overnight fasting in ethylenediaminetetraacetic acid-containing tubes, and plasma was isolated after centrifugation at 4 °C for 20 min. Preservatives were added (phenylmethylsulfonyl fluoride in dimethyl sulfoxide, 0.5% aprotinin, and 0.25% gentamicin/chloramphenicol) to the plasma, and samples were stored at −80 °C until HDL subclass isolation. All participants signed an informed written consent previously approved by the Hospital das Clínicas Ethical Committee.

HDL Isolation and Proteolytic Digestion

Plasma was quickly thawed at 37 °C, and HDL_2 (density 1.063−1.125 g/mL) and HDL_3 (density 1.125−1.21 g/mL) were isolated from plasma by discontinuous density ultracentrifugation (100 000g, 24 h, 4 °C, Sw40 rotor; Beckman ultracentrifuge)[30] and immediately placed at −80 °C until further analysis. Total protein concentration in each HDL subclass was measured using the Bradford assay (Bio-Rad, Hercules, CA) with albumin (ALB) as the standard. HDL (10 μg protein) was solubilized in 100 mM ammonium bicarbonate, reduced with dithiothreitol, alkylated with iodoacetamide, and digested with trypsin (1:40, w/w HDL; Promega, Madison, WI) for 4 h at 37 °C. A second aliquot of enzyme (1:50, w/w HDL) was added, and samples were incubated overnight at 37 °C.[23,31] After acidic hydrolysis with 2% trifluoroacetic acid, samples were desalted using the StageTip protocol.[32] Samples were dried and stored at −80 °C until MS analyses. Digested and desalted samples were resuspended in 0.1% formic acid (final protein concentration of 25 ng/μL) and submitted to MS analyses. Angiotensin (0.2 pmol/μL) was used as a global internal standard to control for MS variability, and iRT peptides (Pierce Biotechnology, Rockford, 0.1 pmol/μL) were used to normalize the retention time of all peptides. iRT peptides in pooled HDL were also employed to address linearity, recovery, and precision of methods (see below).

Preparation of HDL Pool for Quality Control (QC) Assessments

After digestion, an HDL pool was created using 16 randomly selected samples of HDL_2 or HDL_3. Pooled HDL was employed to evaluate the analytical performances of targeted methodologies and as MS quality control.

Data-Dependent Acquisition (DDA)

An Easy-nLC 1200 UHPLC (Thermo Scientific, Bremen, Germany) was used for peptide separation with a linear gradient of solvent A (0.1% formic acid) and solvent B (0.1% formic acid in 80% acetonitrile). Twelve digested HDL samples (50 ng, four HDL_2 samples and eight HDL_3 samples) were randomly selected for shotgun analysis. Each sample was loaded onto a trap column (nanoViper C18, 3 μm, 75 μm × 2 cm, Thermo Scientific) with 12 μL of solvent A at 980 bar. After this period, the trapped peptides were eluted onto a C18 column (nanoViper C18, 2 μm, 75 μm × 15 cm, Thermo Scientific) at a flow rate of 300 nL/min. Peptides were eluted from the column using a linear gradient of 5−28% B for 25 min followed by a linear gradient of 28−40% B for 5 min. Finally, the percentage of solvent B was increased to 95% in 2 min and the column was washed for 10 min with this solvent proportion. Re-equilibration of the system with 100% A was performed before each injection. Acquisition of the data was performed using an Orbitrap Fusion Lumos mass spectrometer (Thermo Scientific, Bremen, Germany) with a nanospray Flex NG ion source (Thermo Scientific, Bremen, Germany). A full MS scan was followed by data-dependent MS2 scans in a 3 s cycle time. Precursor ions selected for MS2 were excluded for subsequent MS2 scans for 20 s. The resolution for the full scan mode was set as 120 000 (at m/z 200) and the automatic gain control (AGC) target at 4×10^5. The m/z range 400−1600 was monitored. Each full scan was followed by a data-dependent MS2 acquisition with a resolution of 30 000 (at m/z 200), maximum fill time of 54 ms, isolation window of 1.2 m/z, and normalized collision energy of 30.

DOI: 10.1021/acs.jproteome.9b00511
J. Proteome Res. XXXX, XXX, XXX−XXX

Protein Identification

Tandem mass spectrometry (MS/MS) spectra were searched against the reviewed UniProt human database (August 2018, version 109, 20 404 entries), using the MaxQuant search engine (version 1.6.3.3)[33] with fixed Cys carbamidomethylation, variable Met oxidation, and *N*-terminal acetylation. MaxQuant default mass tolerance was used for precursor and product ions. Trypsin was selected as the enzyme, and two missed cleavages were allowed. The results were processed by label-free quantification.

Liquid Chromatography (LC) Conditions for Targeted MS Analyses

The same trap and analytical columns used for DDA experiments were employed for targeted analyses. Digested HDL (50 ng) was injected onto the trap column and washed with 12 μL of solvent A at 980 bar. Next, the valve was switched and the peptides were eluted from the trap column onto the analytical column at a flow rate of 350 nL/min, using a linear gradient of 5−28% B for 15 min followed by 28−40% B for 2 min. Solvent B concentration was increased in 2 min, and the column was washed for 10 min at 95% B. Then, 12 and 6 μL of solvent A were respectively used to re-equilibrate trap and analytical columns before each run. The maximum pressure set for the re-equilibration period was 980 bar. Identical chromatographic conditions were employed to allow direct comparison of the two targeted methods.

DIA and PRM Analyses

Experiments were performed using an Orbitrap Fusion Lumos mass spectrometer (Thermo Scientific, Bremen, Germany) equipped with a nanospray Flex NG ion source (Thermo Scientific, Bremen, Germany). For both methods, the resolution was set at 15 000 (at m/z 200), the AGC target at 5×10^4 and maximum fill time 22 ms. For DIA, normalized collision energy of 30 was employed for fragmentation and isolation window of 15 m/z was selected. For PRM methodology, normalized collision energy was set at 27 and isolation window of 1.6 m/z was employed. MS proteomics data have been deposited to the Mass Spectrometry Interactive Virtual Environment with access via ftp://MSV000084151@massive.ucsd.edu and doi:10.25345/C5DS9K.

Linearity of iRT Peptides in Pooled HDL

Increasing concentrations of iRT peptides were added into pooled digested HDL spanning a 250-fold concentration range. Triplicate injections of each concentration were performed using DIA and PRM methodologies. A linear regression using a $1/x$ weighting for determining the best fit of all calibration curves was employed because the standard deviation (SD) increased with analyte concentration for all peptides analyzed.[34,35] A scheduled (3 min window) transition list was generated in Skyline software[36] for PRM analyses. This list contained m/z of precursor peptides of interest along with the collision energy and retention time (see Supplemental Table 1). For DIA analysis, the precursor peptides and product ions selected using the spectral library are given in Supplemental Table 2. For both methods, at least four different transitions for each peptide were monitored, and the sum of peak areas obtained for each transition was used for quantification. Skyline software[36] was employed for integration, and any product ion signal showing interferences was excluded. We excluded ions that did not match the retention time of the other monitored ions or that give intense signals in other regions of the chromatogram.

Recovery and Precision

The recovery of iRT peptides was estimated by the ratio of the experimentally determined concentration of each iRT peptide in the HDL matrix and its theoretical concentration. The precision of targeted methods was determined by the coefficient of variation (CV) obtained among replicates (n = 3) of each individual concentration of all iRT peptides (n = 12) used for constructing calibration curves in pooled HDL.

Lower Limit of Quantification (LLOQ) Determination

For each targeted method, the LLOQ was defined as the lowest concentration at which the CV of triplicate injections of iRT peptides in pooled HDL was less than 20% and had an average recovery within 75−125%.[37]

Selection of Peptides for Targeted Quantification of HDL Subclasses

Spectral libraries built from shotgun proteomic analyses were employed to assemble DIA and PRM methodologies. In total, 93 proteins were identified, but we reduced this number to 75 proteins eliminating keratin proteins (generally accepted as contaminants) and imunoglobulins (IgG). Proteins with <2 unique peptides and proteins present in only one HDL subclass were also excluded. Thirty-eight proteins remained after our exclusion criteria. A list of proteins identified by shotgun proteomics and the exclusion criteria employed are shown in Supplemental Table 3. Proteins are abbreviated by their gene name. To facilitate quantitative comparison, only proteins with at least two peptides detected satisfactorily by both DIA and PRM methods were included. Thus, 24 proteins present in widely different amounts (ranging from <1% to ∼70% of total protein) in HDL were selected and can be accessed in Supplemental Table 4.

Analysis of HDL Subclasses by DIA and PRM

HDL_2 (density 1.063−1.125 g/mL) and HDL_3 (density 1.125−1.21 g/mL) from each apparently healthy volunteer were analyzed using DIA and PRM methodologies. Overall, 24 common proteins to both methods were quantified, using at least two surrogate peptides per protein (69 common peptides in total). A list with proteins, peptides, and retention times employed is available in Supplemental Table 4.

Quality Controls (QCs)

The robustness of DIA and PRM methodologies was evaluated using the angiotensin peptide (DRVYIHPFHL) as a global internal standard. For this purpose, angiotensin (0.2 pmol/μL) was spiked in each sample and the variability in its integrated area was monitored across all injections (total of 79 for each method). Besides, overall variance (for all peptides quantified in HDL) was assessed injecting a pooled HDL sample every five samples. This QC was called MS QC, and for each method, a total of 21 replicates were obtained.

Data Processing and Statistical Analyses

Skyline (version 4.2), an open source software tool application for quantitative proteomic data processing, was employed for data analyses.[36] All integrated peaks were manually inspected to ensure correct peak detection and integration.

For each quantified peptide, comparison between the areas obtained by PRM and DIA methods was performed using Pearson's correlation and the Bland−Altman (B&A) plot. Proteins present in HDL subclasses were statistically differ-

DOI: 10.1021/acs.jproteome.9b00511
J. Proteome Res. XXXX, XXX, XXX−XXX

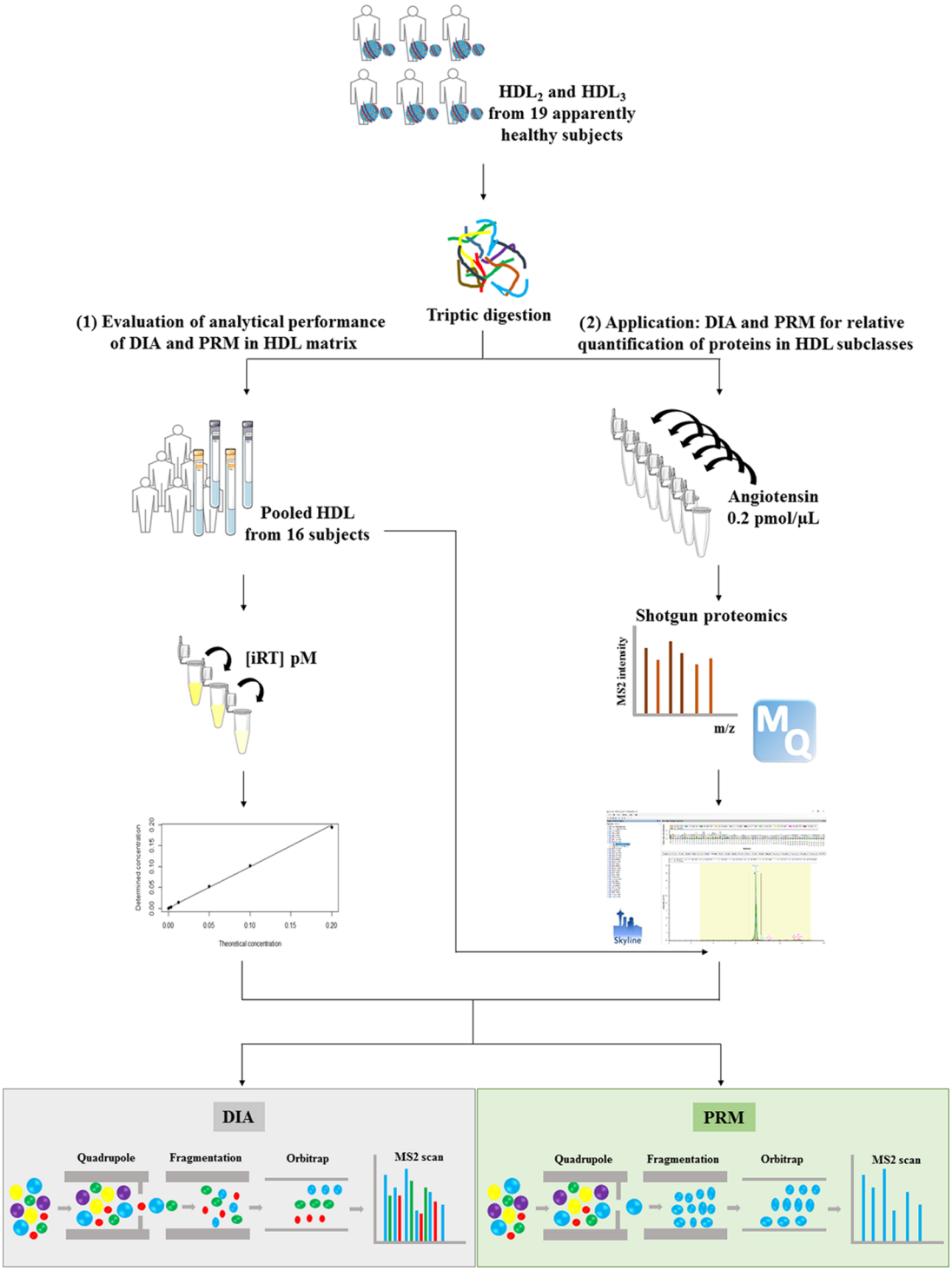

Figure 1. Schematic representation of the experimental design.

entiated by the paired Wilcoxon test. *P* values obtained from the statistical test were corrected using the method of Benjamini and Hochberg.[38−40] This step-up method is a false discovery rate-controlling procedure that assumes a non-negative correlation. For each protein, an adjusted *P* value was calculated, and only proteins with corrected *P* values <0.05 were considered significantly different.[39,40] The *P* values obtained for the 24 proteins analyzed are shown in Supplemental Table 5. Statistical analyses and plots were performed using R Studio software version 1.1.463 (RStudio, Inc.).

RESULTS AND DISCUSSION

Experimental Design

According to the workflow shown in Figure 1, our studies were conducted in two steps. First, we evaluated the performance of DIA and PRM methodologies through important analytical metrics, such as recovery, linearity, precision, and LLOQ. To this end, we generated calibration curves for 12 iRT peptides in

DOI: 10.1021/acs.jproteome.9b00511
J. Proteome Res. XXXX, XXX, XXX−XXX

Table 1. Reproducibility, Linear Response, and Recovery of iRT Peptides in the HDL Matrix As Determined by DIA and PRM

	DIA					PRM				
peptide sequence	CV[a] (%)	slope	y-intercept	r^2	recovery[a] (%)	CV[a] (%)	slope	y-intercept	r^2	recovery[a] (%)
SSAAPPPPPR	0.9	0.997	2.0×10^{-4}	0.998	102.4	1.6	0.974	2.0×10^{-3}	0.995	102.4
GISNEGQNASIK	5.4	0.999	-2.0×10^{-7}	0.998	102.8	2.2	0.990	8.0×10^{-4}	0.999	101.2
HVLTSIGEK	6.5	1.000	-1.7×10^{-8}	0.998	103.2	3.5	1.000	-1.7×10^{-7}	0.998	101.1
DIPVPKPK	4.4	1.000	3.0×10^{-10}	0.999	102.7	1.2	0.999	-1.0×10^{-7}	0.997	100.2
IGDYAGIK	4.4	1.000	-3.0×10^{-8}	0.999	102.7	2.2	0.995	3.0×10^{-4}	0.994	103.6
TASEFDSAIAQDK	5.4	0.999	8.1×10^{-8}	0.996	103.2	6.0	1.000	-4.0×10^{-8}	0.995	103.3
SAAGAFGPELSR	1.7	1.000	-3.0×10^{-8}	0.999	103.9	2.2	1.000	5.0×10^{-7}	0.999	101.3
ELGQSGVDTYLQTK	5.9	0.991	1.0×10^{-3}	0.998	96.2	3.3	1.017	-2.0×10^{-3}	0.997	94.4
SFANQPLEVVYSK	1.7	1.017	-2.0×10^{-3}	0.998	96.6	2.6	1.000	5.0×10^{-10}	0.993	95.4
GLILVGGYGTR	1.3	1.000	-6.0×10^{-5}	0.999	101.0	2.8	0.999	3.0×10^{-6}	0.999	99.6
GILFVGSGVSGGEEGAR	3.0	1.000	7.0×10^{-10}	0.955	87.9	2.7	1.000	-7.0×10^{-10}	0.948	86.9
LTILEELR	1.6	1.183	-2.0×10^{-2}	0.952	81.1	1.7	1.000	-7.0×10^{-11}	0.958	83.3

[a]Coefficient of variation (CV) and recovery were calculated from technical replicates ($n = 3$) at an experimentally determined concentration of 0.1 pM.

pooled digested HDL as a biological matrix and analyzed the standard points by DIA and PRM.

Second, we evaluated DIA as a potential method to be employed in translational studies of HDL and compared the obtained results with those derived from the PRM approach. With this aim, proteins from 12 randomly selected HDL_2 and HDL_3 samples were analyzed by shotgun proteomics and used to create a spectral library in Skyline software. After that, HDL_2 and HDL_3 samples from 19 subjects were quantified by DIA and PRM approaches. In this step, we evaluated the variability of methodologies by monitoring the area of the peptide angiotensin added to all samples and by injecting a pooled HDL QC every five runs.

Analytical Performance of DIA and PRM Methods in HDL Matrix

To compare the analytical performances of DIA and PRM methodologies, we initially used calibration curves of iRT peptides in the presence of HDL matrix. We chose iRT peptides because they are a commercial mixture of synthetic, heavy isotope-labeled peptides available in known concentrations. These peptides have different polarities, spanning the entire chromatographic region. We monitored 14 iRT peptides (see Supplemental Table 6), but two of them did not present satisfactory results for both methods and were excluded from our analyses. Therefore, 12 iRT peptides spanning over 250-fold concentration range were used to evaluate recovery, linearity, precision, and LLOQ of DIA and PRM methods.

The metrics of recovery and linearity were evaluated by constructing calibration curves for iRT peptides in the HDL matrix and plotting the theoretical concentration (x axis) of each point of the standard curve against its experimentally determined concentration (y axis).[41] The linear response varied according to the iRT peptide, and only concentrations precisely determined (<20% CV in triplicate injections) were considered to build the standard curves. Due to the wide dynamic range, a $1/x$ weighted regression was used.[35]

Finding values of 1 and 0, respectively, for the standard curve slope and y-intercept indicates that the experimentally determined concentrations are in excellent agreement with the theoretical concentrations. On the other hand, slopes <1 indicate recovery lower than the theoretical concentration, whereas slopes >1 indicate recovery yields greater than 100%.[42] As shown in Table 1, for the majority of peptides, the determined standard curve slopes had values close or equal to 1, showing that DIA and PRM exhibit excellent recovery. It is worth noting that a slope of 1.18 was found by DIA methodology for the peptide LTILEELR, probably because this peptide has a late eluting time and therefore might be subjected to interferences. Likewise, for all peptides analyzed by either DIA or PRM, values close to 0 were determined for the y-intercept, showing absence of significant interferences. In agreement, for both methods, the estimated recovery for the 0.1 pM standard point was higher than 95% for all but two peptides. The last two iRT peptides to elute (GILFVGSGVSGGEEGAR and LTILEELR) presented lower recovery values (81−87%). Importantly, the same results were obtained by DIA and PRM, showing that low recovery was likely related to the lack of stability or poor chromatographic behavior of the two peptides and not due to the use of a specific methodology. The same conclusion was reached by analyzing linearity of methods through the coefficient of determination (r^2) obtained by the calibration curves of these two peptides. Regardless of the method employed, r^2 of 0.95 was determined, contrasting with a value of 0.99 for all other 12 peptides. Therefore, the majority of peptides exhibited excellent linear response and recovery when measured by DIA and PRM approaches. Recovery for other points of calibration curve is available in Supplemental Tables 7 and 8.

Precision was evaluated by determining the CVs of triplicate injection of each point of the calibration curve. For each peptide, the CV obtained for 0.1 pM is shown in Table 1, and all other CVs are available in Supplemental Tables 7 and 8. Thus, DIA obtained CVs between 0.9 and 6.5%, and similar values were found by PRM (1.2−6.0%). Figure 2A provides the distribution of CVs for 12 iRT peptides analyzed at all concentrations employed for the standard curves. Both DIA and PRM methods obtained <20% CVs for all peptides and concentrations and median CVs <5%, in accordance with the limits established by the guide of best practices in proteomics.[43]

Differences between DIA and PRM emerged when evaluating the LLOQ. Defined as the lowest analyte concentration that can be accurately quantified,[42] frequently this measurement is considered as the value that provides a signal-to-noise ratio >10.[44] However, in MS/MS analyses such as DIA and PRM, background noise is extremely low. Therefore, we empirically determine the LLOQ as the lowest

DOI: 10.1021/acs.jproteome.9b00511
J. Proteome Res. XXXX, XXX, XXX−XXX

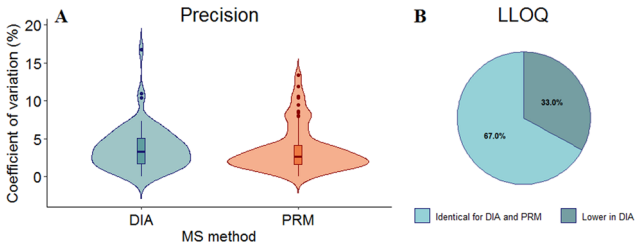

Figure 2. Comparison of the analytical performances of DIA and PRM methods for the quantification of iRT peptides in the HDL matrix. (A) Distribution of CV values obtained for DIA and PRM presented as a violin plot. The dark line in the center of each rectangular box is the median of the data, the upper and lower values of the rectangular box indicate the 75th and 25th percentiles, and the spikes are the range of the data. Outliers are represented by dots. The width of the plot outside the modified box plot is the density of values. (B) Comparison of the LLOQ values for DIA and PRM for each determined peptide. Twelve ions in a wide concentration range were monitored per quantification method.

analyte concentration with <20% CV[37] and an average recovery within 75−125%. Of the 12 peptides analyzed, 67% presented identical LLOQ for DIA and PRM, although for 33% of peptides, the DIA approach accurately determined a lower LLOQ value than PRM (Figure 2B). These findings are in contrast to 3- to 10-fold lower sensitivity of DIA when compared with PRM and SRM.[29,45,46] The reasons for such a discrepancy are unclear, but they may be related to the distinct criteria employed to determine the LLOQ. A detailed comparison of analytical responses, r^2, and LLOQ of the peptides analyzed is provided in Supplemental Table 9.

Taken together, the systematic comparison of the analytical performances extracted from calibration curves of 12 iRT peptides suggests that results obtained by DIA and PRM are quantitatively comparable. Our results corroborate the intrinsic features of targeted methods,[23,47,48] such as linearity, good recovery, high reproducibility, and sensitivity even in the presence of a complex biological matrix.

Targeted Method Development

The results described above demonstrated that DIA and PRM have similar analytical performance for the determination of 12 iRT peptides in the HDL matrix. Encouraged by these findings, we next evaluated the ability of both methods to quantify multiple proteins in HDL subclasses (HDL_2 and HDL_3) isolated from plasma of 19 healthy subjects. To this end, proteins and peptides were selected based on shotgun proteomic experiments and previous studies.[14,23] A spectral library composed of 38 proteins and 199 peptides was built in Skyline software. DIA yielded quantitative results for 30 proteins and 85 precursors in HDL_2 and HDL_3, while the same number of proteins and 91 precursors were determined by PRM (Supplemental Table 4). Peptides with high interfering signal and mass error >10 ppm were excluded. We also avoided peptides susceptible to ex vivo modification (e.g., methionine-containing peptides), and only peptides satisfactorily detected by both methods were included in the final analysis. To find the surrogate peptide for each protein of interest, we first determined the peptide pair with best Pearson's correlation coefficient. From these two peptides, we finally selected the peptide with the lowest CV in pooled HDL QC. The 24 surrogate peptides chosen for HDL proteins are highlighted in Supplemental Table 4.

Performance of External and Internal Quality Controls

We controlled variance in this study using two strategies. First, we generate a pooled HDL QC and injected this QC intercalating with samples over a 2 week period (21 times for each method). All peptides quantified in HDL_2 and HDL_3

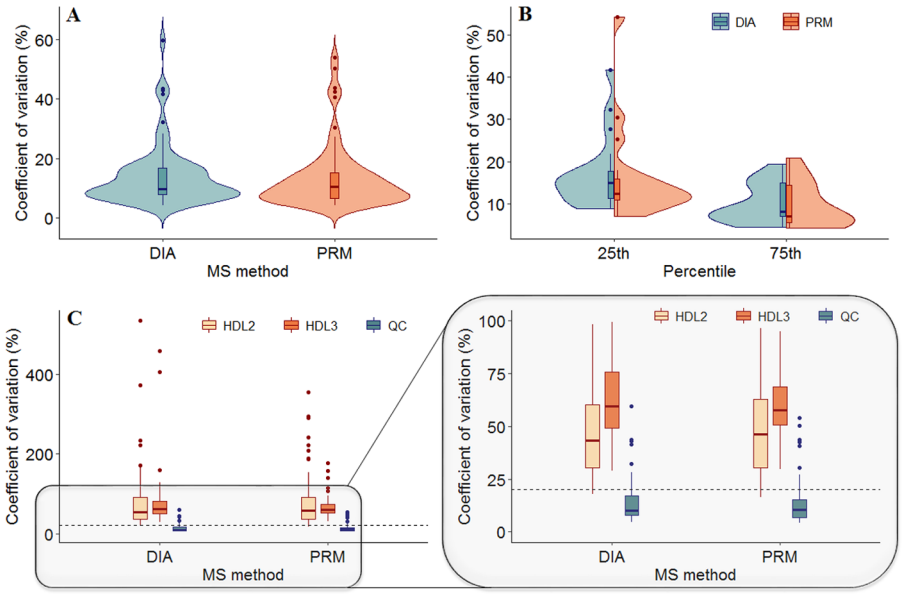

Figure 3. Reproducibility of DIA and PRM methods for quantification of HDL subclasses. Distribution of CV values obtained for (A) all proteins identified in pooled HDL (69 ions monitored per method), (B) bottom and top quartiles based on integrated areas (17 ions monitored per quartile, per method). The dark line in the center of each rectangular box is the median of the data, the upper and lower values of the rectangular box indicate the 75th and 25th percentiles, respectively, and the spikes are the range of the data. Outliers are represented by dots. The width of the plot outside the modified box plot is the density of values. (C) Comparison between QC variation (pooled HDL injected multiple times) and biological variability for HDL_2 and HDL_3 (69 ions monitored per method). The *Y* axis was amplified for clarity with a scale ranging from 0 to 100%. The dashed line indicates CV of 20%.

DOI: 10.1021/acs.jproteome.9b00511
J. Proteome Res. XXXX, XXX, XXX−XXX

were also analyzed in the QC sample and had their CV determined for DIA and PRM methods. Ideally, QC CVs should be low. As shown in Figure 3A, majority of CVs determined for QC peptides are below 20%, with median values of 9.9 and 10.5%, respectively, for DIA and PRM methods. To better investigate the variability of QC data, we divide peptides into quartiles, according to the values obtained by integrated areas. For both methods, median variation for peptides belonging to the 75th percentile regarding integrated areas was low (8.1 and 7.0%, respectively, for DIA and PRM, Figure 3B). As expected, peptides with lower integrated areas (25th percentile) presented higher CVs, although it is important to point out that the majority of these peptides had CVs < 20%, with medians of 14.9 and 12.3%, respectively, for DIA and PRM. Therefore, for presumably lower abundance peptides, PRM performs slightly better regarding reproducibility of the data.

We next compared the QC variation with biological variability for HDL_2 and HDL_3 using DIA and PRM methodologies (Figure 3C). QC variability is considerably lower than the biological variance obtained by comparing 19 healthy subjects, making these methods well suited for precise quantification of HDL proteome.

Besides using a sample QC, we also monitored the robustness of DIA and PRM methodologies employing angiotensin peptide DRVYIHPFHL spiked in all samples as a global internal standard. This is an effective strategy to monitor instrument performance. Thus, for each method, a total of 79 injections were performed spanning a 2 week period. Overall, low variances were obtained by DIA and PRM, with angiotensin CVs of 20.0 and 19.4%, respectively (see Supplemental Table 10).

Consistency between PRM and DIA Measurements

We compared the consistency of the measurements for each specific peptide by correlating the areas obtained by DIA and PRM (Pearson's correlation, Figure 4 and Supplemental Table 11). The methods yielded correlations ≥0.90 for 62% of the peptides in HDL_2 and for 92% of the peptides in HDL_3. It is worth noting that low correlation (r < 0.50) was found for hemoglobin subunit β (HBB), phosphatidylcholine-sterol acyltransferase (LCAT), and α-1B-glycoprotein (A1BG) surrogate peptides in HDL_2, likely due to the low abundance of these proteins in this HDL subclass. The same peptides displayed excellent agreement between DIA and PRM when measured in HDL_3 (r > 0.98). Likewise, the apolipoprotein B (APOB) surrogate peptide displayed poor correlation in HDL_3 (r = 0.62), where it was found in extremely low amounts but showed excellent correlation in HDL_2 (r = 0.99). Finally, the haptoglobin-related protein (HPR) peptide showed a poor correlation between DIA and PRM measurements, but in this population, HPR was present in very low amounts in both HDL subclasses. Representative results for correlations between DIA and PRM in HDL_2 (Figure 4B,D) and HDL_3 (Figure 4C,E) are shown for APOA2 (Figure 4B,C) and apolipoprotein L1 (APOL-1, Figure 4D,E). We choose APOA2 because it is the second most abundant protein in HDL and APOL-1, due to its low abundance in HDL, presenting peptide areas about 10-fold lower than the area found for the APOA2 peptide. In summary, for the vast majority of peptides measured, DIA and PRM measurements correlate well.

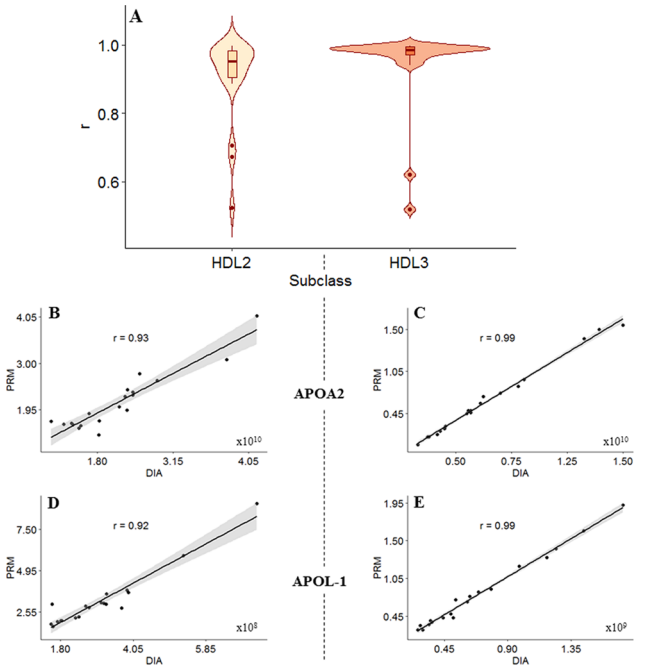

Figure 4. Relationship between DIA and PRM methods for peptides in HDL subclasses. (A) Pearson's correlation distribution with r > 0.5 obtained from peptides quantified by PRM and DIA in HDL_2 (20 ions monitored) and HDL_3 (24 ions monitored). The dark line in the center of each rectangular box is the median of the data, the box indicates the interquartile range, and the spikes of the rectangles are the range of the data. The width of the plot outside the modified box plot is the density of values. Comparison between DIA and PRM by areas obtained for the APOA2 surrogate peptide in HDL_2 (B) and in HDL_3 (C) and for the APOL-1 surrogate peptide in HDL_2 (D) and in HDL_3 (E). Pearson's correlation coefficient (r) is shown in the graph. The shaded area represents the 95% confidence interval of the measurements.

Another way to compare analytical methods is based on the agreement between them.[49] We evaluated the agreement between DIA and PRM approaches by constructing Bland–Altman (B&A) plots[50] for representative proteins present in different abundances in HDL[51] (Figure 5). A B&A plot is composed by the mean of the results obtained by the two methods in the x axis and by the absolute difference between the results obtained by the methods in the y axis, combined with 95% limits of agreement. When there is high variation in the data, it is recommended a logarithmic transformation.[52] Thus, our data were log 2 transformed according to the high variability found in our population (as can be seen in Figure 3C). Ideally, the measurements obtained by two methods must be exactly same, resulting in mean differences (represented in the plots as a dark blue dotted line) equal to zero. Following the same criteria adopted for Pearson correlations, we selected two proteins to show B&A plots: APOA2 and APOL-1 (Figure 5). The results show high agreement between DIA and PRM measurements, as corroborated by high Pearson's correlations obtained above. Means and critical differences (equals half the difference of lower and upper limits) were close to zero, and most of the data points were within 95% limits of agreement (represented in plots as a light blue dashed line).

DOI: 10.1021/acs.jproteome.9b00511
J. Proteome Res. XXXX, XXX, XXX−XXX

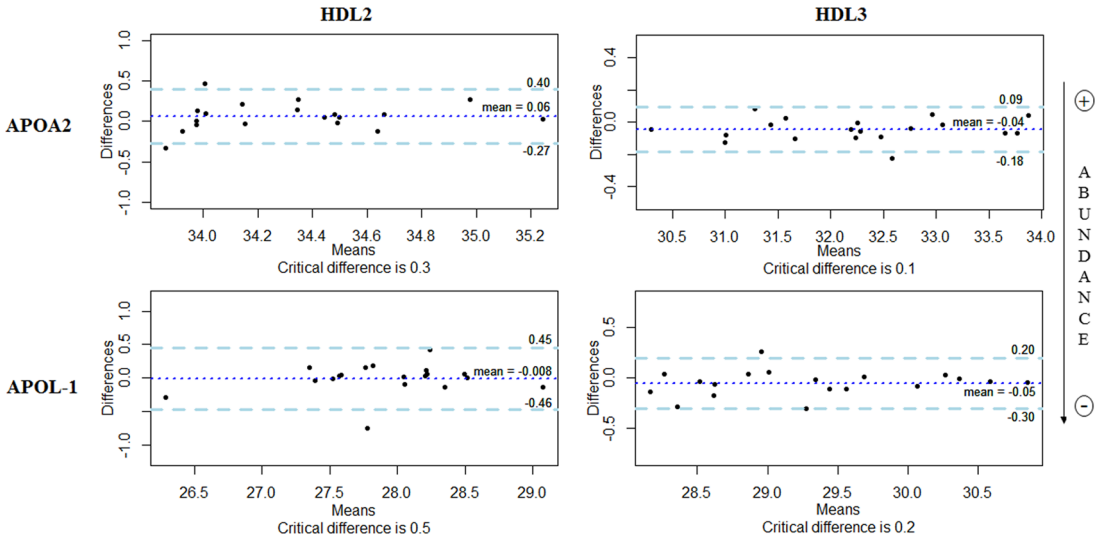

Figure 5. Bland–Altman plots for APOA2 and APOL-1 present in HDL_2 and HDL_3 isolated from plasma of 19 apparently healthy subjects. The *x* axis represents the mean of the results obtained by DIA and PRM, and the *y* axis, the absolute difference between the two methods. The mean difference is represented by a dark blue dotted line, and 95% limits of agreement [−1.96 to +1.96 standard deviation (SD)], by a light blue dashed line. The critical difference was calculated as half the difference of the lower limit and upper limit. Data were log 2 transformed.

DIA and PRM Methods Show that HDL_2 and HDL_3 Are Distinct Classes of Particles

After a careful evaluation of critical analytical metrics of DIA and PRM methodologies, we concluded that DIA and PRM presented comparable analytical performances, strong correlation, and high level of agreement. Therefore, DIA and PRM are suitable methods for precise quantification of HDL proteome. The vast majority of HDL proteome studies use DDA to address differentially expressed proteins in HDL. However, DDA quantification has several limitations,[31] even though efforts have been made toward improving its quantification ability. For instance, an acquisition mode that benefits signal detection of low abundance ions was recently reported,[53] in addition to data analysis strategies capable of increasing the number of identified peptides.[54] Nevertheless, the development of targeted methodologies for robust proteome quantification in translational studies is critical. SRM is the gold standard method for MS-based quantification.[17] The SRM assay correlated well with immunochemical measurements for six HDL proteins (apolipoproteins A-I, C-II, C-III, E, B, and J), in contrast to poor correlation obtained by shotgun proteomics.[31] We recently demonstrated that PRM is comparable to SRM in terms of sensitivity and precision to quantify HDL proteins. Moreover, PRM is more specific because many product ions can be used to confirm the identity of peptide.[23] On the other hand, DIA has some potential advantages over classical quantitative methods. First, the method development is straightforward even for an unknown proteome because DIA does not require a predefined list of peptides. Second, the presence and the amount of new peptides can be interrogated after acquisition, since all precursor ions within a user-defined m/z window are fragmented.[55] SWATH-MS, one of the DIA strategies, achieved comparable precision (mean CV of 14.9%) when compared to SRM for the quantification of *N*-linked glycoproteins in human plasma.[45] Excellent linear correlation ($r^2 \geq 0.95$) between SWATH-MS and SRM methods was also reported.[29] Moreover, Liu et al. quantified 342 unique plasma proteins in 232 samples collected from human twin population with low technical variability (mean CV of 7.2%).[56] A multilaboratory study conducted in 11 sites worldwide concluded that SWATH-MS measurements were reproducible to quantify >4000 proteins from embryonic kidney cells.[27]

However, to the best of our knowledge, DIA has not been used to provide robust and accurate quantification in the context of HDL and diseases. HDL proteome of patients with type 1 diabetes mellitus was quantified by DIA; however, reproducibility and robustness of the method were not evaluated.[57] We therefore compared the analytical performance of DIA with that of PRM to quantify HDL_2 and HDL_3 proteins. HDL is a clinically relevant target because low levels of HDL cholesterol are associated with the risk of developing cardiovascular diseases.[58] Moreover, HDL is a complex particle with multiple functions, and the clinical measurement of its cholesterol content does not capture HDL diversity.[51] Precise quantification of HDL proteome is a challenge due to the high content of lipids associated with proteins in the particle, but its composition is less complex than that of plasma proteome. Therefore, HDL is an attractive target to look for biomarkers of disease.[31]

Given HDL diversity, it is also reasonable to assume that distinct HDL particles may be associated with different biological functions. As discussed above, HDL particles can be separated into two distinct classes based on density.[11] We separated these particles in HDL_2 (1.063–1.125 g/mL) and HDL_3 (1.125–1.21 g/mL) and investigated the ability of DIA and PRM methodologies to differentiate their proteomes.

Almost equivalent results were obtained when comparing HDL_2 and HDL_3 subclasses by DIA and PRM (Figure 6), confirming the comparable quantification ability of the methods. HDL subclasses share all of the 24 proteins analyzed, but the amount of each specific protein differed significantly according to the subclass (Figure 6). Dense HDL_3 was significantly enriched with proteins related to antioxidant activity, such as paraoxonase (PON1) and APOL-1, and with proteins related to lipid metabolism and transport, such as apolipoprotein A-IV (APOA-IV), clusterin (also termed apolipoprotein J, APOJ), apolipoprotein D (APOD), LCAT,

DOI: 10.1021/acs.jproteome.9b00511
J. Proteome Res. XXXX, XXX, XXX–XXX

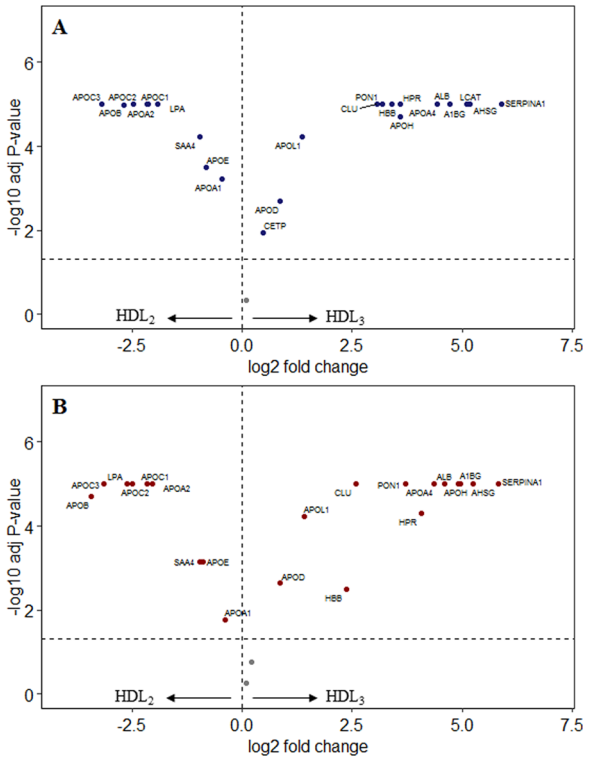

Figure 6. DIA (A) and PRM (B) analyses of proteins quantified in HDL_2 and HDL_3 isolated from plasma of 19 apparently healthy subjects. For each protein, the −log 10 of the adjusted *P* value from the paired Wilcoxon test is plotted against the log 2 fold change between HDL_3 and HDL_2. Proteins overexpressed in HDL_3 are displayed to the right of the value 0 on the *x* axis, while proteins enriched in HDL_2 are to the left.

and cholesteryl ester transfer protein (CETP). HPR, an acute-phase response protein; α-1-antitrypsin (SERPINA1), a protease inhibitor; apolipoprotein H (APOH), a protein related to hemostasis; and α-2-HS-glycoprotein (AHSG), an endopeptidase inhibitor were also more abundant in HDL_3. Importantly, other studies have confirmed these proteins as belonging to dense HDL_3.[3,14] Albumin (ALB) and hemoglobin subunit β (HBB) were also concentrated in HDL_3. These proteins are known as plasma contaminants. ALB is generally present in HDL isolated by UC or other HDL isolation methodologies.[3,59,60] A low level of HBB is also common, but high levels indicate significant hemolysis. Despite accepted as contaminants, we still found it useful to quantify these proteins in HDL to monitor the quality of each individual isolation technique. For instance, an isolation problem can be detected if a sample differs considerably in the ALB content from others.

Large HDL_2 was enriched with APOA2, apolipoprotein Cs (apoC-I, apoC-II, and apoC-III), apolipoprotein E (APOE), serum amyloid A-4 (SAA4), and apolipoprotein(a) (LPA), all proteins related to lipid metabolism.[14,51] The association of APOCs and APOE with HDL_2 is well established.[61−63] APOCs are involved in the metabolism of HDL and triglyceride-rich lipoproteins. Interestingly, APOC1 and APOC2 were found elevated in HDL of diabetic subjects that later developed hypoalphalipoproteinemia induced by fenofibrate/rosiglitazone treatment.[24] APOE-rich HDL_2 particles are efficient acceptors of cholesterol effluxed from macrophages via the ABCG1 transporter.[64] Also, APOE is produced by cholesterol-loaded macrophages[65] and may be important in the expansion of HDL particles, by enabling the incorporation of additional cholesteryl ester through LCAT activation.[66] SAA4 may be involved in the interaction between HDL and VLDL. Thus, adenoviral expression of SAA4 in mice increased the HDL size by 10% and VLDL (20-fold) and triglycerides levels (1.7-fold).[67] The presence of APOB and LPA in HDL_2 likely results from contamination during the isolation process since hydrated density of large HDL_2 is similar to the densities of LPA and LDL.

The specific roles of HDL subclasses in atheroprotection are still not fully understood. Larger and more buoyant HDL_2 and smaller and denser HDL_3 have been independently related to cardiovascular diseases.[68] However, a systematic review[69] concluded that the cholesterol content of HDL_2 and HDL_3 does not distinguish cardioprotective differences between HDL subclasses. A better characterization of HDL particles is needed to assess cardiovascular risk. In this way, precise quantification of proteins in HDL subclasses can add functional relevance to each specific particle.

This work has some potential limitations. First, our measurements did not provide absolute quantification of proteins in HDL subclasses. Second, HDL subclasses were isolated by UC, and the potential limitations of this methodology were not addressed. Although UC is considered the gold standard method for HDL isolation, gravitational forces and high ionic strength may cause loss of some HDL proteins.[70] Several studies have sought alternative methods for HDL isolation, such as gel filtration chromatography,[1,71] ionic exchange chromatography,[71] preparative isoelectric focusing,[71] and immunoaffinity column chromatography.[13] However, each distinct technique has its own limitations and the agreement among different isolation methodologies regarding proteins belonging to HDL is poor.[72] We recently compiled data from 37 proteomic studies on HDL that employed different isolation methodologies.[72] Of the 566 proteins reported as belonging to HDL, only APOA1 and APOL-1 were identified by all studies and only 21 proteins were found by ∼75% of studies.

CONCLUSIONS

HDL particles are diverse, and the clinical measurement of their cholesterol content does not fully capture HDL heterogeneity. More than 100 proteins were described in HDL; however, consistent quantification of HDL proteome has been a challenge in the field. Previously, we showed that SRM and PRM are comparable methodologies for precise quantification of HDL proteins.[23,24] In the current work, the analytical performances of DIA and PRM were compared in a study of HDL proteome. The methods worked equally well regarding precision, recovery, and linearity. Therefore, DIA and PRM are suitable methods for accurate quantification of HDL proteins. The remarkable concordance between DIA and PRM quantifications obtained in this work supports the proposal that DIA is a precise and robust quantitation strategy that can be applied in translational studies. Both methods revealed comparable ability in differentiating HDL_2 and HDL_3 proteomes. In this way, precise quantification of proteins in different HDL subclasses may help to understand the diverse functionality of these particles.

DOI: 10.1021/acs.jproteome.9b00511
J. Proteome Res. XXXX, XXX, XXX−XXX

■ ASSOCIATED CONTENT

Supporting Information

The Supporting Information is available free of charge on the ACS Publications website at DOI: 10.1021/acs.jproteome.9b00511.

Lists of proteins and peptides monitored by each method, along with analytical assessments of PRM and DIA methods (Suppl. Tables 1−11) (XLSX)

■ AUTHOR INFORMATION

Corresponding Author

*E-mail: ronsein@iq.usp.br. Tel: + 55 11 30911078.

ORCID

Amanda R. M. Silva: 0000-0002-9001-5999
Marcos T. K. Toyoshima: 0000-0002-9146-4606
Paolo Di Mascio: 0000-0003-4125-8350

Notes

The authors declare no competing financial interest.

■ ACKNOWLEDGMENTS

We thank Fundação de Amparo à Pesquisa do Estado de São Paulo (FAPESP), Grants 2017/07725-1, 2016/00696-3, and 2013/07937-8; Conselho Nacional de Desenvolvimento Científico e Tecnológico (CNPq), Grant 402683/2016-1; and Coordenação de Aperfeiçoamento de Pessoal de Nível Superior (CAPES) for financial support. A.R.M.S. is recipient of a FAPESP fellowship.

■ ABBREVIATIONS

HDL, high-density lipoprotein; MS, mass spectrometry; LC, liquid chromatography; LLOQ, lower limit of quantification; CV, coefficient of variation; r^2, coefficient of determination; SD, standard deviation

■ REFERENCES

(1) Swertfeger, D. K.; Li, H.; Rebholz, S.; Zhu, X.; Shah, A. S.; Davidson, W. S.; Lu, L. J. Mapping atheroprotective functions and related proteins/lipoproteins in size fractionated human plasma. *Mol. Cell. Proteomics* **2017**, *16*, 680−693.

(2) Davidson, W. S.; Thompson, T. B. The structure of apolipoprotein a-i in high density lipoproteins. *J. Biol. Chem.* **2007**, *282*, 22249−22253.

(3) Davidson, W. S.; Silva, R. A.; Chantepie, S.; Lagor, W. R.; Chapman, M. J.; Kontush, A. Proteomic analysis of defined HDL subpopulations reveals particle-specific protein clusters: relevance to antioxidative function. *Arterioscler., Thromb., Vasc. Biol.* **2009**, *29*, 870−876.

(4) Rosales, C.; Davidson, W. S.; Gillard, B. K.; Gotto, A. M., Jr.; Pownall, H. J. Speciated high-density lipoprotein biogenesis and functionality. *Curr. Atheroscler. Rep.* **2016**, *18*, 25−32.

(5) Li, H.; Gordon, S. M.; Zhu, X.; Deng, J.; Swertfeger, D. K.; Davidson, W. S.; Lu, L. J. Network-based analysis on orthogonal separation of human plasma uncovers distinct high density lipoprotein complexes. *J. Proteome Res.* **2015**, *14*, 3082−3094.

(6) Kontush, A.; Lindahl, M.; Lhomme, M.; Calabresi, L.; Chapman, M. J.; Davidson, W. S. Structure of HDL: particle subclasses and molecular components. In *High Density Lipoproteins*; von Eckardstein, A., Kardassis, D., Eds.; Handbook of Experimental Pharmacology; Springer: Cham, 2015; Vol. *224*, pp 3−51.

(7) Havel, R. J.; Eder, H. A.; Bragdon, J. H. The distribution and chemical composition of ultracentrifugally separated lipoproteins in human serum. *J. Clin. Invest.* **1955**, *34*, 1345−1353.

(8) Scanu, A. Studies on the conformation of human serum high-density lipoproteins HDL2 and HDL3. *Proc. Natl. Acad. Sci. U.S.A.* **1965**, *54*, 1699−1705.

(9) Kostner, G.; Alaupovic, P. Composition and structure of plasma lipoproteins. Separation and quantification of the lipoprotein families occurring in the high density lipoproteins of human plasma. *Biochemistry* **1972**, *11*, 3419−3428.

(10) Suenram, A.; McConathy, W. J.; Alaupovic, P. Evidence for the lipoprotein heterogeneity of human plasma high density lipoproteins isolated by three different procedures. *Lipids* **1979**, *14*, 505−510.

(11) Chapman, M. J.; Goldstein, S.; Lagrange, D.; Laplaud, P. M. A density gradient ultracentrifugal procedure for the isolation of the major lipoprotein classes from human serum. *J. Lipid Res.* **1981**, *22*, 339−358.

(12) Singh, S. A.; Aikawa, M. Unbiased and targeted mass spectrometry for the HDL proteome. *Curr. Opin. Lipidol.* **2017**, *28*, 68−77.

(13) Furtado, J. D.; Yamamoto, R.; Melchior, J. T.; Andraski, A. B.; Gamez-Guerrero, M.; Mulcahy, P.; He, Z.; Cai, T.; Davidson, W. S.; Sacks, F. M. Distinct proteomic signatures in 16 hdl (high-density lipoprotein) subspecies. *Arterioscler., Thromb., Vasc. Biol.* **2018**, *38*, 2827−2842.

(14) Vaisar, T.; Pennathur, S.; Green, P. S.; Gharib, S. A.; Hoofnagle, A. N.; Cheung, M. C.; Byun, J.; Vuletic, S.; Kassim, S.; Singh, P.; Chea, H.; Knopp, R. H.; Brunzell, J.; Geary, R.; Chait, A.; Zhao, X.-Q.; Elkon, K.; Marcovina, S.; Ridker, P.; Oram, J. F.; Heinecke, J. W. Shotgun proteomics implicates protease inhibition and complement activation in the antiinflammatory properties of HDL. *J. Clin. Invest.* **2007**, *117*, 746−756.

(15) Liu, H.; Sadygov, R. G.; Yates, J. R. A model for random sampling and estimation of relative protein abundance in shotgun proteomics. *Anal. Chem.* **2004**, *76*, 4193−4201.

(16) Vidova, V.; Spacil, Z. A review on mass spectrometry-based quantitative proteomics: Targeted and data independent acquisition. *Anal. Chim. Acta* **2017**, *964*, 7−23.

(17) Gillette, M. A.; Carr, S. A. Quantitative analysis of peptides and proteins in biomedicine by targeted mass spectrometry. *Nat. Methods* **2013**, *10*, 28−34.

(18) Addona, T. A.; Abbatiello, S. E.; Schilling, B.; Skates, S. J.; Mani, D. R.; Bunk, D. M.; Spiegelman, C. H.; Zimmerman, L. J.; Ham, A. J.; Keshishian, H.; Hall, S. C.; Allen, S.; Blackman, R. K.; Borchers, C. H.; Buck, C.; Cardasis, H. L.; Cusack, M. P.; Dodder, N. G.; Gibson, B. W.; Held, J. M.; Hiltke, T.; Jackson, A.; Johansen, E. B.; Kinsinger, C. R.; Li, J.; Mesri, M.; Neubert, T. A.; Niles, R. K.; Pulsipher, T. C.; Ransohoff, D.; Rodriguez, H.; Rudnick, P. A.; Smith, D.; Tabb, D. L.; Tegeler, T. J.; Variyath, A. M.; Vega-Montoto, L. J.; Wahlander, A.; Waldemarson, S.; Wang, M.; Whiteaker, J. R.; Zhao, L.; Anderson, N. L.; Fisher, S. J.; Liebler, D. C.; Paulovich, A. G.; Regnier, F. E.; Tempst, P.; Carr, S. A. Multi-site assessment of the precision and reproducibility of multiple reaction monitoring-based measurements of proteins in plasma. *Nat. Biotechnol.* **2009**, *27*, 633−641.

(19) Lange, V.; Picotti, P.; Domon, B.; Aebersold, R. Selected reaction monitoring for quantitative proteomics: a tutorial. *Mol. Syst. Biol.* **2008**, *4*, No. 222.

(20) Peterson, A. C.; Russell, J. D.; Bailey, D. J.; Westphall, M. S.; Coon, J. J. Parallel reaction monitoring for high resolution and high mass accuracy quantitative, targeted proteomics. *Mol. Cell. Proteomics* **2012**, *11*, 1475−1488.

(21) Gallien, S.; Duriez, E.; Crone, C.; Kellmann, M.; Moehring, T.; Domon, B. Targeted proteomic quantification on quadrupole-orbitrap mass spectrometer. *Mol. Cell. Proteomics* **2012**, *11*, 1709−1723.

(22) Bourmaud, A.; Gallien, S.; Domon, B. Parallel reaction monitoring using quadrupole-Orbitrap mass spectrometer: Principle and applications. *Proteomics* **2016**, *16*, 2146−2159.

(23) Ronsein, G. E.; Pamir, N.; von Haller, P. D.; Kim, D. S.; Oda, M. N.; Jarvik, G. P.; Vaisar, T.; Heinecke, J. W. Parallel reaction monitoring (PRM) and selected reaction monitoring (SRM) exhibit

comparable linearity, dynamic range and precision for targeted quantitative HDL proteomics. *J. Proteomics* **2015**, *113*, 388−399.
(24) Ronsein, G. E.; Reyes-Soffer, G.; He, Y.; Oda, M.; Ginsberg, H.; Heinecke, J. W. Targeted proteomics identifies paraoxonase/arylesterase 1 (pon1) and apolipoprotein cs as potential risk factors for hypoalphalipoproteinemia in diabetic subjects treated with fenofibrate and rosiglitazone. *Mol. Cell. Proteomics* **2016**, *15*, 1083−1093.
(25) Uzozie, A. C.; Aebersold, R. Advancing translational research and precision medicine with targeted proteomics. *J. Proteomics* **2018**, *189*, 1−10.
(26) Röst, H. L.; Aebersold, R.; Schubert, O. T. Automated SWATH data analysis using targeted extraction of ion chromatograms. *Methods Mol. Biol.* **2016**, 289.
(27) Collins, B. C.; Hunter, C. L.; Liu, Y.; Schilling, B.; Rosenberger, G.; Bader, S. L.; Chan, D. W.; Gibson, B. W.; Gingras, A. C.; Held, J. M.; Hirayama-Kurogi, M.; Hou, G.; Krisp, C.; Larsen, B.; Lin, L.; Liu, S.; Molloy, M. P.; Moritz, R. L.; Ohtsuki, S.; Schlapbach, R.; Selevsek, N.; Thomas, S. N.; Tzeng, S. C.; Zhang, H.; Aebersold, R. Multi-laboratory assessment of reproducibility, qualitative and quantitative performance of SWATH-mass spectrometry. *Nat. Commun.* **2017**, *8*, No. 291.
(28) Sajic, T.; Liu, Y.; Aebersold, R. Using data-independent, high-resolution mass spectrometry in protein biomarker research: perspectives and clinical applications. *Proteomics Clin. Appl.* **2015**, *9*, 307−321.
(29) Gillet, L. C.; Navarro, P.; Tate, S.; Röst, H.; Selevsek, N.; Reiter, L.; Bonner, R.; Aebersold, R. Targeted data extraction of the MS/MS spectra generated by data-independent acquisition: a new concept for consistent and accurate proteome analysis. *Mol. Cell. Proteomics* **2012**, *11*, No. O111.016717.
(30) Redgrave, T. G.; Roberts, D. C.; West, C. E. Separation of plasma lipoproteins by density-gradient ultracentrifugation. *Anal. Biochem.* **1975**, *65*, 42−49.
(31) Hoofnagle, A. N.; Becker, J. O.; Oda, M. N.; Cavigiolio, G.; Mayer, P.; Vaisar, T. Multiple-reaction monitoring−mass spectrometric assays can accurately measure the relative protein abundance in complex mixtures. *Clin. Chem.* **2012**, *58*, 777−781.
(32) Rappsilber, J.; Mann, M.; Ishihama, Y. Protocol for micro-purification, enrichment, pre-fractionation and storage of peptides for proteomics using StageTips. *Nat. Protoc.* **2007**, *2*, 1896−1906.
(33) Cox, J.; Mann, M. MaxQuant enables high peptide identification rates, individualized p.p.b.-range mass accuracies and proteome-wide protein quantification. *Nat. Biotechnol.* **2008**, *26*, 1367−1372.
(34) Johnson, E. L.; Reynolds, D. L.; Scott Wright, D.; Pachla, L. A. Biological sample preparation and data reduction concepts in pharmaceutical analysis. *J. Chromatogr. Sci.* **1988**, *26*, 372−379.
(35) Almeida, A. M.; Castel-Branco, M. M.; Falcão, A. C. Linear regression for calibration lines revisited: weighting schemes for bioanalytical methods. *J. Chromatogr. B* **2002**, *774*, 215−222.
(36) MacLean, B.; Tomazela, D. M.; Shulman, N.; Chambers, M.; Finney, G. L.; Frewen, B.; Kern, R.; Tabb, D. L.; Liebler, D. C.; MacCoss, M. J. Skyline: an open source document editor for creating and analyzing targeted proteomics experiments. *Bioinformatics* **2010**, *26*, 966−968.
(37) Green, J. M. A practical guide to analytical method validation. *Anal. Chem.* **1996**, *68*, 305A−309A.
(38) Simes, R. J. An improved Bonferroni procedure for multiple tests of significance. *Biometrika* **1986**, *73*, 751−754.
(39) Benjamini, Y.; Hochberg, Y. Controlling the false discovery rate: a practical and powerful approach to multiple testing. *J. R. Stat. Soc. B* **1995**, *57*, 289−300.
(40) Benjamini, Y.; Yekutieli, D. The control of the false discovery rate in multiple testing under dependency. *Ann. Stat.* **2001**, *29*, 1165−1188.
(41) Matuszewski, B. K.; Constanzer, M. L.; Chavez-Eng, C. M. Matrix effect in quantitative lc/ms/ms analyses of biological fluids: a method for determination of finasteride in human plasma at picogram per milliliter concentrations. *Anal. Chem.* **1998**, *70*, 882−889.
(42) Mani, D. R.; Abbatiello, S. E.; Carr, S. A. Statistical characterization of multiple-reaction monitoring mass spectrometry (MRM-MS) assays for quantitative proteomics. *BMC Bioinf.* **2012**, *13*, 1−18.
(43) Carr, S. A.; Abbatiello, S. E.; Ackermann, B. L.; Borchers, C.; Domon, B.; Deutsch, E. W.; Grant, R. P.; Hoofnagle, A. N.; Huttenhain, R.; Koomen, J. M.; Liebler, D. C.; Liu, T.; MacLean, B.; Mani, D. R.; Mansfield, E.; Neubert, H.; Paulovich, A. G.; Reiter, L.; Vitek, O.; Aebersold, R.; Anderson, L.; Bethem, R.; Blonder, J.; Boja, E.; Botelho, J.; Boyne, M.; Bradshaw, R. A.; Burlingame, A. L.; Chan, D.; Keshishian, H.; Kuhn, E.; Kinsinger, C.; Lee, J. S.; Lee, S. W.; Moritz, R.; Oses-Prieto, J.; Rifai, N.; Ritchie, J.; Rodriguez, H.; Srinivas, P. R.; Townsend, R. R.; Van Eyk, J.; Whiteley, G.; Wiita, A.; Weintraub, S. Targeted peptide measurements in biology and medicine: best practices for mass spectrometry-based assay development using a fit-for-purpose approach. *Mol. Cell. Proteomics* **2014**, *13*, 907−917.
(44) Lin, S.; Shaler, T. A.; Becker, C. H. Quantification of intermediate-abundance proteins in serum by multiple reaction monitoring mass spectrometry in a single-quadrupole ion trap. *Anal. Chem.* **2006**, *78*, 5762−5767.
(45) Liu, Y.; Huttenhain, R.; Surinova, S.; Gillet, L. C.; Mouritsen, J.; Brunner, R.; Navarro, P.; Aebersold, R. Quantitative measurements of N-linked glycoproteins in human plasma by SWATH-MS. *Proteomics* **2013**, *13*, 1247−1256.
(46) Schmidlin, T.; Garrigues, L.; Lane, C. S.; Mulder, T. C.; van Doorn, S.; Post, H.; de Graaf, E. L.; Lemeer, S.; Heck, A. J.; Altelaar, A. F. Assessment of SRM, MRM, and DIA for the targeted analysis of phosphorylation dynamics in non-small cell lung cancer. *Proteomics* **2016**, *16*, 2193−2205.
(47) Egertson, J. D.; Kuehn, A.; Merrihew, G. E.; Bateman, N. W.; MacLean, B. X.; Ting, Y. S.; Canterbury, J. D.; Marsh, D. M.; Kellmann, M.; Zabrouskov, V.; Wu, C. C.; MacCoss, M. J. Multiplexed MS/MS for improved data-independent acquisition. *Nat. Methods* **2013**, *10*, 744−746.
(48) Ludwig, C.; Gillet, L.; Rosenberger, G.; Amon, S.; Collins, B. C.; Aebersold, R. Data-independent acquisition-based SWATH-MS for quantitative proteomics: a tutorial. *Mol. Syst. Biol.* **2018**, *14*, 1−23.
(49) Giavarina, D. Understanding Bland Altman analysis. *Biochem. Med.* **2015**, *25*, 141−151.
(50) Bland, J. M.; Altman, D. G. Statistical methods for assessing agreement between two methods of clinical measurement. *Lancet* **1986**, *327*, 307−310.
(51) Shah, A. S.; Tan, L.; Long, J. L.; Davidson, W. S. Proteomic diversity of high density lipoproteins: our emerging understanding of its importance in lipid transport and beyond. *J. Lipid Res.* **2013**, *54*, 2575−2585.
(52) Dewitte, K.; Fierens, C.; Stöckl, D.; Thienpont, L. M. Application of the Bland−Altman Plot for interpretation of method-comparison studies: a critical investigation of its practice. *Clin. Chem.* **2002**, *48*, 799−801.
(53) Meier, F.; Geyer, P. E.; Winter, S. V.; Cox, J.; Mann, M. BoxCar acquisition method enables single-shot proteomics at a depth of 10,000 proteins in 100 minutes. *Nat. Methods* **2018**, *15*, 440−448.
(54) Bielow, C.; Mastrobuoni, G.; Kempa, S. Proteomics Quality Control: Quality Control Software for MaxQuant Results. *J. Proteome Res.* **2016**, *15*, 777−787.
(55) Aebersold, R.; Bensimon, A.; Collins, B. C.; Ludwig, C.; Sabido, E. Applications and developments in targeted proteomics: from SRM to DIA/SWATH. *Proteomics* **2016**, *16*, 2065−2067.
(56) Liu, Y.; Buil, A.; Collins, B. C.; Gillet, L. C.; Blum, L. C.; Cheng, L. Y.; Vitek, O.; Mouritsen, J.; Lachance, G.; Spector, T. D.; Dermitzakis, E. T.; Aebersold, R. Quantitative variability of 342 plasma proteins in a human twin population. *Mol. Syst. Biol.* **2015**, *11*, 786−803.
(57) Gourgari, E.; Ma, J.; Playford, M. P.; Mehta, N. N.; Goldman, R.; Remaley, A. T.; Gordon, S. M. Proteomic alterations of HDL in

DOI: 10.1021/acs.jproteome.9b00511
J. Proteome Res. XXXX, XXX, XXX−XXX

youth with type 1 diabetes and their associations with glycemic control: a case−control study. *Cardiovasc. Diabetol.* **2019**, *18*, 43−53.
(58) Toth, P. P. High-density lipoprotein and cardiovascular risk. *Circulation* **2004**, *109*, 1809−1812.
(59) Heller, M.; Stalder, D.; Schlappritzi, E.; Hayn, G.; Matter, U.; Haeberli, A. Mass spectrometry-based analytical tools for the molecular protein characterization of human plasma lipoproteins. *Proteomics* **2005**, *5*, 2619−2630.
(60) Gordon, S. M.; Deng, J.; Lu, L. J.; Davidson, W. S. Proteomic characterization of human plasma high density lipoprotein fractionated by gel filtration chromatography. *J. Proteome Res.* **2010**, *9*, 5239−5249.
(61) Yamashita, S.; Sprecher, D. L.; Sakai, N.; Matsuzawa, Y.; Tarui, S.; Hui, D. Y. Accumulation of apolipoprotein E-rich high density lipoproteins in hyperalphalipoproteinemic human subjects with plasma cholesteryl ester transfer protein deficiency. *J. Clin. Invest.* **1990**, *86*, 688−695.
(62) Schaefer, E. J.; Foster, D. M.; Jenkins, L. L.; Lindgren, F. T.; Berman, M.; Levy, R. I.; Brewer, H. B. The composition and metabolism of high density lipoprotein subfractions. *Lipids* **1979**, *14*, 511−522.
(63) Cheung, M. C.; Albers, J. J. Distribution of high density lipoprotein particles with different apoprotein composition: particles with A-I and A-II and particles with A-I but no A-II. *J. Lipid Res.* **1982**, *23*, 747−753.
(64) Pamir, N.; Hutchins, P.; Ronsein, G.; Vaisar, T.; Reardon, C. A.; Getz, G. S.; Lusis, A. J.; Heinecke, J. W. Proteomic analysis of HDL from inbred mouse strains implicates APOE associated with HDL in reduced cholesterol efflux capacity via the ABCA1 pathway. *J. Lipid Res.* **2016**, *57*, 246−257.
(65) Mazzone, T.; Gump, H.; Diller, P.; Getz, G. S. Macrophage free cholesterol content regulates apolipoprotein E synthesis. *J. Biol. Chem.* **1987**, *262*, 11657−11662.
(66) Matsuura, F.; Wang, N.; Chen, W.; Jiang, X.-C.; Tall, A. R. HDL from CETP-deficient subjects shows enhanced ability to promote cholesterol efflux from macrophages in an apoE- and ABCG1-dependent pathway. *J. Clin. Invest.* **2006**, *116*, 1435−1442.
(67) Kindy, M. S.; de Beer, M. C.; Yu, J.; de Beer, F. C. Expression of mouse acute-phase (SAA1.1) and constitutive (SAA4) serum amyloid A isotypes: influence on lipoprotein profiles. *Arterioscler., Thromb., Vasc. Biol.* **2000**, *20*, 1543−1550.
(68) Williams, P. T.; Feldman, D. E. Prospective study of coronary heart disease vs. HDL2, HDL3, and other lipoproteins in Gofman's Livermore Cohort. *Atherosclerosis* **2011**, *214*, 196−202.
(69) Superko, H. R.; Pendyala, L.; Williams, P. T.; Momary, K. M.; King, S. B.; Garrett, B. C. High-density lipoprotein subclasses and their relationship to cardiovascular disease. *J. Clin. Lipidol.* **2012**, *6*, 496−523.
(70) Munroe, W. H.; Phillips, M. L.; Schumaker, V. N. Excessive centrifugal fields damage high density lipoprotein[S]. *J. Lipid Res.* **2015**, *56*, 1172−1181.
(71) Gordon, S. M.; Deng, J.; Tomann, A. B.; Shah, A. S.; Lu, L. J.; Davidson, W. S. Multi-dimensional co-separation analysis reveals protein−protein interactions defining plasma lipoprotein subspecies. *Mol. Cell. Proteomics* **2013**, *12*, 3123−3134.
(72) Ronsein, G. E.; Vaisar, T. Deepening our understanding of HDL proteome. *Expert Rev. Proteomics* **2019**, *16*, 749−760.

DOI: 10.1021/acs.jproteome.9b00511
J. Proteome Res. XXXX, XXX, XXX−XXX

ACS Publications
Most Trusted. Most Cited. Most Read.

Comparing Data-Independent Acquisition and Parallel Reaction Monitoring in Their Abilities To Differentiate High-Density Lipoprotein Subclasses

Author: Amanda R. M. Silva, Marcos T. K. Toyoshima, Marisa Passarelli, et al
Publication: Journal of Proteome Research
Publisher: American Chemical Society
Date: Jan 1, 2020

PERMISSION/LICENSE IS GRANTED FOR YOUR ORDER AT NO CHARGE

This type of permission/license, instead of the standard Terms and Conditions, is sent to you because no fee is being charged for your order. Please note the following:

- Permission is granted for your request in both print and electronic formats, and translations.
- If figures and/or tables were requested, they may be adapted or used in part.
- Please print this page for your records and send a copy of it to your publisher/graduate school.
- Appropriate credit for the requested material should be given as follows: "Reprinted (adapted) with permission from {COMPLETE REFERENCE CITATION}. Copyright {YEAR} American Chemical Society." Insert appropriate information in place of the capitalized words.
- One-time permission is granted only for the use specified in your RightsLink request. No additional uses are granted (such as derivative works or other editions). For any uses, please submit a new request.

If credit is given to another source for the material you requested from RightsLink, permission must be obtained from that source.

BACK CLOSE WINDOW

CHAPTER 3 - Comparing Different DIA Quantification Strategies to Evaluate the Effects of Fish Oil Supplementation on the HDL Proteome of Mice Submitted to a High-Fat Diet

3.1. Introduction

Dietary guidelines recommend replacing saturated fatty acids by mono- (MUFA) and polyunsaturated fatty acids (PUFA)[1], to reduce the risk of developing cardiovascular diseases (CVD), the number one cause of morbidity and mortality worldwide[2; 3]. These guidelines were designed based on eating habits of some populations, as the Asians that typically eat a low-fat and high-carb diet and have less CVD than Westerners[4]. The same happen with Mediterranean countries which have diets enriched in MUFA[5]. Interest in the cardioprotective effects of dietary n-3 PUFAs also came from early observations of the native Eskimo who consume high-fat diets, but have low rate of CVD as consequence of high intake of fish[6]. Eicosapentaenoic acid (EPA; 20:5 n-3) and docosahexaenoic acid (DHA; 22:6 n-3) are n-3 PUFAs most commonly found in marine fish, such as tuna, salmon, mackerel, sardines and herring[7]. Results from several epidemiological and clinical studies have demonstrated important role of omega-3 in significantly decreasing triglycerides (TG) levels[8]. However, the cardiovascular benefits of fish oil supplementation still have inconsistent results[9]. Importantly, in the REDUCE-IT trial, a markedly reduction in cardiovascular events was achieved when subjects with hypertriglyceridemia were treated with statins and 4g of purified EPA[10].

The inverse relationship between HDL-C levels and cardiovascular disease (CVD) is historically established[11]. However, the disappointing clinical data obtained from raising HDL-C levels in patients with coronary injury without any clinical benefit has highlighted the fact that the cholesterol content in HDL does not capture its complexity[12; 13]. HDL is a heterogeneous, protein-enriched particle, with functions going beyond lipid metabolism[14]. Proteins with anti-inflammatory and antioxidant properties, as well as related to immune

response have been associated to HDL, reflecting the function plurality of this lipoprotein[15]. Little is known about the effect of omega-3 on HDL proteome. A small study reported that HDL proteome from six smoking healthy men was remodeled to a cardioprotective profile after consuming 2g/day of omega-3 for 5 weeks[16]. Most recently, supplementation with EPA-rich fish oil in normolipidemic subjects down-regulated HDL proteins involved in inflammation[17]. Randomized clinical trials require blindly monitoring a large number of people for a long time, which creates problems with adherence, as well as increasing the cost of the study. In opposition, animal models are a promising alternative to test the effects of diet on atherosclerosis[18]. LDL receptor knockout mice ($LDLr^{-/-}$) is the most widely employed animal model to study lipoprotein metabolism and atherosclerosis. In this context, a previous study[19] reported the association between HDL proteome remodeling and reduction of atherosclerosis in $LDL^{-/-}$ mice submitted to the high-fat diet enriched with fish oil isomers.

The majority of studies employed to quantify HDL of mice and humans use data dependent acquisition methodology (shotgun)[20]. However, the stochastic nature of the untargeted method makes it less reproducible, negatively impacting the accurate detection of low-abundance proteins[21]. In the other hand, quantitative proteomics providing robust and sensitive protein quantification, alleviating the drawbacks of discovery proteomics[21; 22]. Data independent analysis (DIA) is a recently developed methodology that bridges discovery and targeted proteomics. In this approach, thousands of proteins may be detected without prior knowledge (like in shotgun methodology), and targeted data extraction can be performed at both MS (precursor ion) and MS/MS (product ion) levels providing quantitative abilities similar to selected (or multiple) reaction

monitoring (SRM or MRM) analysis[23]. The data acquisition involves cyclical recording of consecutive MS1 scan followed by MS2 scans for all precursor ions in pre-determined isolation windows[24]. One of the great advantages of DIA is the ability to reinterrogate the data without the need to repeat sample analysis. As a resulted, the accuracy of data may be improved through removal of interferences, or additional quantitative information may be obtained on proteins that were not previously identified. We recently found that DIA and PRM (parallel reaction monitoring, another targeted methodology), worked equally well to quantify HDL proteome[25]. Our previous results show DIA delivers quantitative analysis of HDL proteome without the extensive work needed to develop an SRM or PRM methodology. However, a bottleneck is still the data processing, and up to date, there is no consensus in how to process DIA-derived data. Software platforms such as Skyline[26] and MaxDia[27] are continually improved and updated, but there is an urgent need to standardize data analysis.

In this work, we examined the performance of different quantification strategies using Skyline and MaxDIA software platforms to compare HDL proteome from $LDL^{-/-}$ mice submitted to a high-fat diet supplemented or not with omega-3. After a careful evaluation of different quantification strategies, we propose a pipeline to robustly quantify HDL proteome. By using this pipeline, our results show that supplementation with omega-3 remodels HDL proteome, considerably attenuating the inflammatory profile seen in HDL of mice treated only with a high-fat diet.

3.2. Methods

3.2.1. Animals and Experimental Design

Eight-week old male LDLr$^{-/-}$ mice were randomly separated in two treatment groups (n=10/group). One group was fed on a high-fat diet (western group), and the other group was fed on a combination of saturated fatty acids and omega-3 polyunsaturated fatty acids in a ratio of 2.5:1 (fish oil group) for a period of 14 weeks. Both custom-made isocaloric diets (PragSoluções Biociências, SP, Brazil) contained 21% (w/w) of saturated fatty acids and 0.2% (w/w) of cholesterol. **Supplemental Tables 1** and **2** detail the composition of macronutrients and fatty acids of each diet, respectively. Body weight of mice was measured weekly. At the end of the feeding period, mice fasted for 5 hours were anesthetized, randomly sacrificed, and blood was collected via inferior vena cava with syringe containing EDTA 10% (pH 7.4), following ethical principles from Sociedade Brasileira de Ciências em Animais de Laboratórios (SBCAL). Plasma was separated from blood samples by centrifugation (2000 rpm at 20 min), and stored in aliquots at -80^{o}C for further use. All experimental procedures were approved by the Animal Care Committee from Institute of Chemistry of the University of São Paulo (Brazil).

3.2.2. Plasma Lipids and Lipoprotein Analysis

Fasting plasma was analyzed for total cholesterol (TC), triglycerides (TG), HDL-C, and LDL-C, using commercial enzymatic kits (LabTest Diagnóstica S.A., MG, Brazil). Plasma lipoprotein profile from pooled plasma (n=5) was obtained after separation by fast protein liquid chromatography (FPLC). Briefly, one hundred microliters of pooled plasma were applied directly to a Superose 6 column (10/300 GL, Amersham Biosciences), and

eluted at a constant flow rate of 200 μL/min with phosphate buffer containing EDTA 1 mM and NaCl 0.15 M. Fractions of 500 μL were collected, and total cholesterol was measured enzymatically by a commercial kit (LabTest Diagnóstica S.A., MG, Brazil)[28].

3.2.3. Fatty acids composition of diets

Fatty acids analyses were performed on a gas chromatograph (Thermo Fisher Scientific, USA) equipped with a flamed ionization detector (GC/FID) following the protocol established by Massod *et al*.[29].

3.2.4. HDL Isolation and Proteolytic Digestion

Plasma was quickly thawed at 37 ºC, and HDL was isolated and digested as described previously[30]. Briefly, HDL was isolated from plasma by sequential density ultracentrifugation (density 1.063 to 1.210 g/mL, 120.2 rotor; Beckman Coulter Optima™ Max-XP ultracentrifuge), and its proteins concentration was determined by the Bradford assay (Bio-Rad, Hercules, CA, USA). Ten micrograms of HDL protein were solubilized in the presence of 0.01% ProteaseMAX™ (Promega, Madison, WI, USA), reduced with dithiothreitol, alkylated with iodoacetamide, and digested with trypsin (Promega, Madison, WI, USA). Samples were desalted following the StageTip protocol[31], dried and stored at -80 ºC until MS analyses.

3.2.5. Preparation of a pooled quality control

An HDL pool was prepared to evaluate the performance of the quantification methods and to monitor the MS variability. This pooled HDL quality control (QC) was created by combining two microliters of isolated HDL from each mice (n=20).

3.2.6. Data-Dependent Acquisition (DDA)

First, digested HDL samples (25 ng) were analyzed by DDA, as described previously[25], to build a library of proteins and peptides for further investigation using targeted analysis by Data-Independent Acquisition (DIA). Briefly, an Easy-nLC 1200 UHPLC (Thermo Scientific, Bremen, Germany) was used for peptide separation with a linear gradient of solvent A (0.1% formic acid) and solvent B (0.1% formic acid in 80% acetonitrile). Samples was loaded onto a trap column (nanoViper C18, 3 µm, 75 µm × 2 cm, Thermo Scientific) with 12 µL of solvent A at 800 bar. Next, the trapped peptides were eluted onto a C18 column (nanoViper C18, 2 µm, 75 µm × 15 cm, Thermo Scientific) at a flow rate of 300 nL/min. Elution was performed using a linear gradient of 5-28% B for 25 min followed by a linear gradient of 28-40% B for 3 min. Finally, the percentage of solvent B was increased to 95% in 6 min and the column was washed for 16 min with this solvent proportion. Re-equilibration of the system with 100% A was performed before each injection. Acquisition of the data was performed using an Orbitrap Fusion Lumos mass spectrometer (Thermo Scientific, Bremen, Germany) with a nanospray Flex NG ion source. A full MS scan was followed by data-dependent MS2 scans in a 3 s cycle time. Precursor ions selected for MS2 were excluded for subsequent MS2 scans for 20 s. The resolution for the full scan mode was set as 60 000 (at *m/z* 200) and the automatic gain

control (AGC) target at 5×10^5. The *m/z* range 400-1600 was monitored. Each full scan was followed by a data dependent MS2 acquisition with a resolution of 30 000 (at *m/z* 200), maximum fill time of 54 ms, isolation window of 1.2 *m/z*, and normalized collision energy of 30.

3.2.7. Protein Identification

Tandem mass spectrometry (MS/MS) spectra were searched against the reviewed UniProt *mus musculus* database (March 2021, 17 544 entries), using the MaxQuant search engine (version 2.0.3.0)[32] with fixed Cys carbamidomethylation, variable Met oxidation, and *N*-terminal acetylation. MaxQuant default mass tolerance was used for precursor and product ions. Trypsin was selected as the enzyme, and two missed cleavages were allowed. The results were processed by label-free quantification (LFQ).

3.2.8. DIA analysis

The same trap and analytical columns, and equipment used for DDA experiments were employed for DIA analyses[25]. Digested HDL (25 ng) was injected onto the trap column and washed with 12 µL of solvent A at 800 bar. Next, the valve was switched and the peptides were eluted from the trap column onto the analytical column at a flow rate of 300 nL/min, using a linear gradient of 5-28% B for 15 min followed by 28-40% B for 2 min. Solvent B concentration was increased in 2 min, and the column was washed for 11 min at 95% B. Then, 12 and 6 µL of solvent A were respectively used to re-equilibrate trap and analytical columns before each run. The maximum pressure set for the re-equilibration period was 800 bar. DIA analysis were performed as described

previously[25]. Briefly, the resolution, the AGC target, and maximum fill time for MS1 and MS2 were set at 30 000 (at *m/z* 200) and 15 000 (at *m/z* 200), at 4×10^5 and 5×10^4, and 50 and 22 ms, respectively. Normalized collision energy of 30 was employed for fragmentation and isolation window of 15 *m/z* was selected.

3.2.9. Data Processing

Data from DIA analyses were processed using two different analysis tools: Skyline (version 21.2)[26] and MaxDIA, a software platform embedded into MaxQuant environmental (version 2.0.3.0)[27]. For Skyline data analyses, first a spectral library derived from DDA data was created. Peptides from the library were then populated with DIA data. All peaks were manually inspected to ensure correct peak detection and integration. Peptides susceptible to *ex vivo* modification (e.g. methionine containing peptides) were avoided. At least four transitions for each peptide were monitored, and the peptide area was obtained from the sum of peaks of each transition. For quantification, proteins with peptides presenting poor chromatographic peak shape were excluded, and only proteins with CV<35% in the pooled HDL QC were considered. MaxDIA[27] was operated in the classical library-based DIA mode with the default values assumed for all parameters. MaxQuant was chosen as the library type, and peptide, evidence, and Msms files were obtained from previous MaxQuant search results from DDA analysis. The results were processed by protein intensity, intensity-based absolute quantification (iBAQ) and label-free quantification (LFQ)[33]. Two steps of protein refinement were performed on the data obtained from MaxDIA software platform. Only proteins with quantification values present in at least 50% of samples of at least one group were considered. The remaining

proteins were excluded in the first step. Second, only proteins with CV<35% in the pooled HDL QC were considered. Detailed protein refinement can be accessed in **Supplemental Table 3**.

3.2.10. Quantification Methods for HDL proteins from mice

Five different methods were employed to quantify HDL proteins by DIA: two from data processed by Skyline, and three from data obtained from MaxDIA software. For data processed by Skyline software, data analysis summing up the areas of 2 to 4 most intense peptides for each protein was the first quantification strategy used, since previous works have shown that combining the results of multiple peptides improves robustness and accuracy[34; 35]. This quantification method was called sum of peptides. The second method consisted of finding the best peptide to represent each protein of interest. For that purpose, the peptide pair with the highest Pearson's correlation coefficient was determined, followed by the selection of the peptide with the lowest CV in pooled HDL QC. This quantification method was called surrogate peptides. HDL proteins and their peptides can be accessed in **Supplemental Table 4**. Only unique peptides were considered for HDL quantification by both quantification methods. Since serum amyloid A (SAA) 1 and 2 share significant homology, in Skyline software a common peptide (termed as SAA1/2) was monitored, but not quantified. In addition, two and one unique peptides to the proteins SAA1 and SAA2, respectively, were quantified by Skyline (these peptides are termed as SAA1 and SAA2, respectively, in **Supplemental Table 4**). In the same way, two peptides shared by murinoglobulin-1 and 2 were quantified by Skyline, and results are reported as MUG1/2. When data were processed by MaxDIA software, protein

intensity, intensity-based absolute quantification (iBAQ) and label-free quantification (LFQ) were used to quantify HDL proteins. When peptides of a given protein were a subset of the peptides used for identification of another protein(s), these proteins were merged into a single protein group[33]. This was the case of the protein groups called HIST3H2BA, HSP90AB1/AA1, MUG1/2, SERPINA1C/1A/1E/1B and TUBA4A/1B/8/1C/3A/1A (**Supplemental Table 3**). Proteins quantified by each one these methods are presented in **Supplemental Table 3**.

3.2.11. Statistical Analyses

The variability of the five quantification methods (sum of peptides, surrogate peptides, intensity, iBAQ and LFQ) was evaluated using the coefficients of variation (CVs) obtained by quantifying all proteins in pooled QC samples. Protein data were log2 transformed, and Pearson's correlation was employed to compare the measures obtained by different quantification methods. HDL proteome from mice in a western diet supplemented or nor with fish oil was analyzed by linear regression followed by Benjamini-Hochberg[36] correction of the P-values (**Supplemental Table 5**). Only proteins with corrected P-values<0.05 and log2 Fold Change>0.5 were considered as significantly different. The variability among samples was evaluated by Principal Component Analysis (PCA). Paired samples t-test was used to compare the body weight gain of the mice from western and fish oil groups, and unpaired two samples t-test was used to test plasma lipid and lipoprotein profiles of the groups. Statistical analyses and plots were performed using R Studio software version 4.1.2 (RStudio, Inc.).

3.3. Results

3.3.1. Experimental Design

Our study was designed to investigate the performance of different quantification strategies using Skyline and MaxDIA software platforms to compare HDL proteome from mice submitted to a high-fat diet supplemented or not with omega-3 (see **Figure 1** for workflow). LDLr$^{-/-}$ mice were fed on a high-fat diet (western group) or on a saturated fat and omega-3 combined diet (fish oil group) for 14 weeks. Plasma lipid levels and lipoprotein profiles of these animals were obtained and their HDL was isolated by ultracentrifugation, digested with trypsin, and analyzed by quantitative mass spectrometry. Data analysis was performed employing five quantification strategies. First, by using the MaxDIA software, proteins were quantified using the iBAQ, intensity and LFQ tools. The results obtained by MaxDIA quantification strategies were compared to those obtained using Skyline software. Using Skyline, protein quantification was obtained by two different methods: first, the areas of 2 to 4 most intense peptides for each protein were summed up (this method was called sum of peptide) and second, a representative peptide for each protein was chosen (called surrogate peptide). A careful monitoring of the variability of each quantification strategy was performed during data processing.

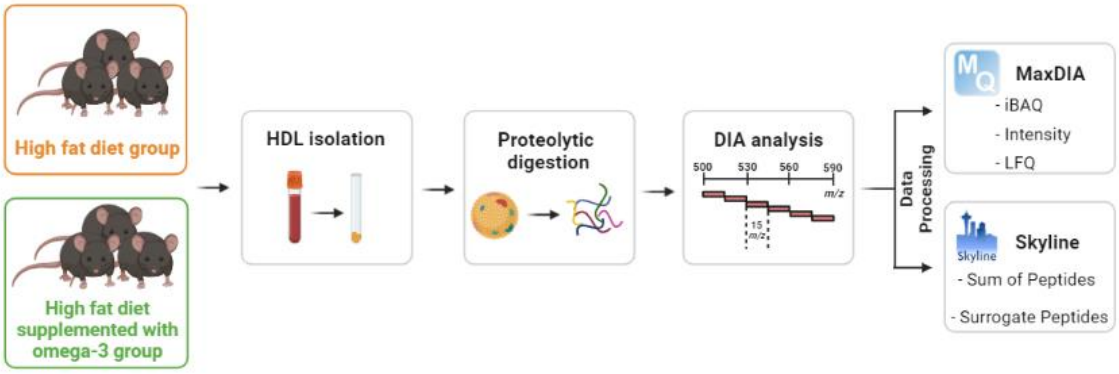

Figure 1. Workflow (figure created with BioRender.com).

3.3.2. Data Processing Improves the Precision of Different Quantification Methods

The performance of the analysis tools MaxDIA and Skyline was evaluated before and after data processing. In addition, the precision of the quantification methods (iBAQ, intensity, LFQ from MaxDIA, and sum of peptides and surrogate peptides from Skyline) was determined using a pooled HDL sample (Pooled QC) injected multiple times (n=8) intercalating with samples runs. Keratins, and protein groups flagged as “reverse”, “only identified by site” or “potential contaminant” by MaxDIA were removed from both MaxDIA and Skyline data sets before protein quantification. Initially, no data handling was performed. In the case of Skyline quantification, we assumed the integrated areas carried out by the software itself. Thus, both software platforms identified similar number of proteins in HDL of mice fed a high-fat diet supplemented or not with fish oil. MaxDIA identified 48 proteins (6 being exclusive), against 50 proteins determined by Skyline (8 exclusive proteins), with an overlap of 42 proteins between the two analysis tools (**Figure 2A** and **Supplemental Table 3**). For pooled HDL QC (n=8 injections), CVs of all proteins identified by MaxDIA (n=48) were obtained, as well as CVs of all peptides quantified in HDL using Skyline (n=304). Without data handling, iBAQ, intensity, and integrated areas by Skyline obtained median CVs >35% (43.5%, 42.5%, and 40.8%, respectively), in contrast to LFQ which showed low data variance (median CV of 9.3%, n=48), as can be seen in **Figure 2B**.

Then, we processed the data employing some exclusion criteria in order to analyze only reliably quantified proteins by both software. Two steps of refinement were performed with data obtained from MaxDIA. In the first refinement, only proteins with quantification values present in at least 50 % of samples of at least one group were considered. Second,

only proteins with CV<35% in pooled HDL QC were considered. For Skyline-derived data, proteins with CV>35% in pooled HDL QC were also eliminated. In addition, manual inspection of chromatographic peaks was performed, and proteins containing only peptides with poor chromatographic peak shape were excluded. Thus, using these refinement criteria, each quantification strategy yielded a distinct number of proteins classified as reliably detected in HDL of mice fed with a high-fat diet supplemented or not with fish oil. For MAxDia-derived results, 17 and 19 proteins remained in the analyses processed by iBAQ and intensity quantification strategies, respectively, while 30 proteins were kept after LFQ processing. Regarding Skyline processing strategies, 24 and 20 proteins were kept after processing the data using sum of peptides and surrogate peptides, respectively (**Figure 2C** and **Supplemental Table 3**). A substantial decrease in variance was found for all quantification strategies after data processing, pointing to the importance of data curating to improve the reliability of quantification. After curating the data, quantifications using LFQ, iBAQ, intensity, sum of peptides and surrogate peptides obtained median CVs of 8.7% (n=30 proteins), 20.3% (n=17), 23.3% (n=19), 21.4% (n=24), and 24.0% (n=20), respectively (**Figure 2D**). Refinement details are showed in **Supplemental Table 3**.

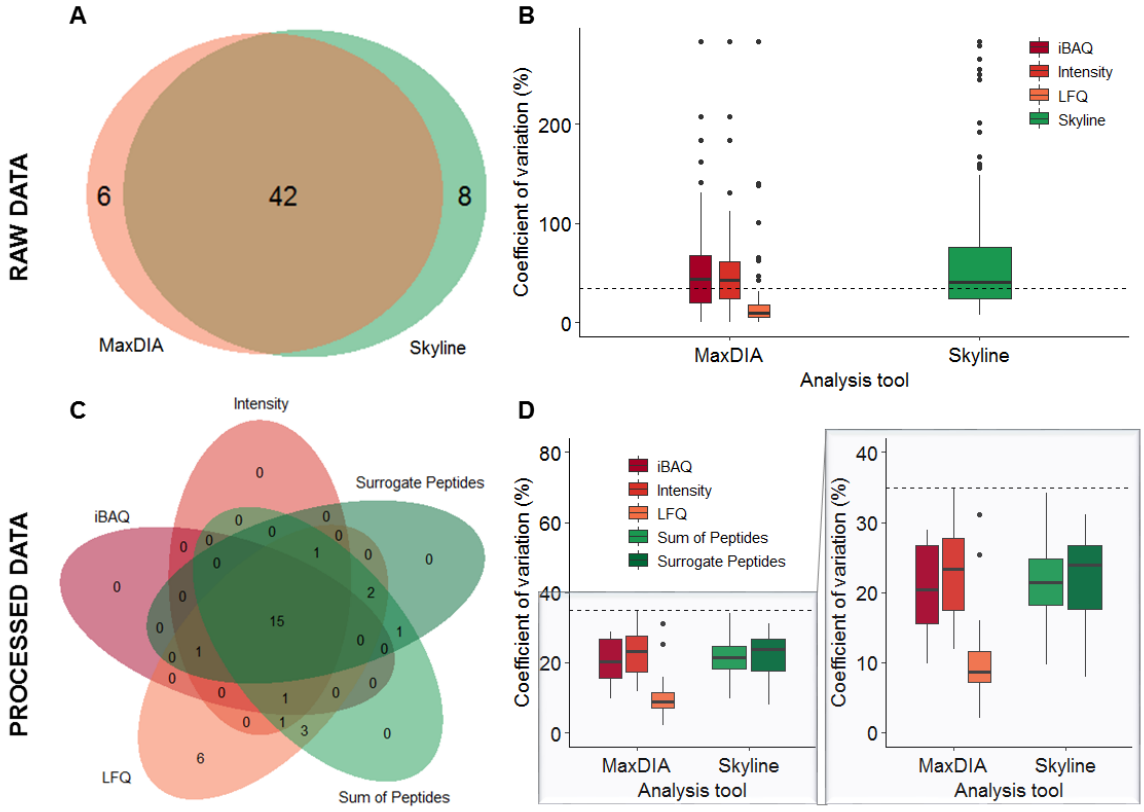

Figure 2. Number of proteins and precision in their quantification before and after data processing using MaxDIA and Skyline software platforms. Number of proteins identified with MaxDIA and Skyline before (**A**) and after data processing (**C**) in HDL of mice in a high-fat diet supplemented or not with fish oil. Variability of the quantification methods before (**B**) and after (**D**) data processing in the pooled HDL QC (n= 8 injections). Before data processing, iBAQ, intensity and LFQ were used as quantification tools in MaxDIA, and sum of integrated areas for all peptides was used as quantification strategy in Skyline (**B**). After data processing, data derived from Skyline software was processed using two quantification strategies, the first was called sum of peptides and the second named surrogate peptides (**D**) In **D**, the Y axis was amplified for clarity with a scale ranging from 0 to 40%. The dashed line indicates CV of 35%.

3.3.3. Technical Variability of the Quantification Methods is Lower than Biological variance

Next, we compared the technical variability obtained with pooled HDL QC with biological variation in HDL protein levels. For this purpose, the CVs obtained quantifying HDL proteins in pooled HDL QC (n=8) were compared with those obtained for each

separate diet group (western diet supplemented or not with fish oil, n=10, each). The results are displayed in **Figure 3** for the five different quantification strategies. As showed before, the LFQ quantification method showed the lowest technical variation (median CV of 8.7%). For comparison, using LFQ as the quantification strategy, the median CVs obtained for HDL proteins quantification were 23.0 and 19.6 %, respectively for western and fish oil diets. These results show that even though these are isogenic mice, the biological variability within the same diet is higher than the technical variance. For the other strategies of quantification used in this work, the technical variance was closer to the biological variability (this is true especially for Skyline quantification strategies). Importantly, this are isogenic mice, thus a high biological variance is not expected. Moreover, these results are not comparing the technical variability with the variation induced by the diet (treatment effect), since we are taking into account only variations within the same diet group.

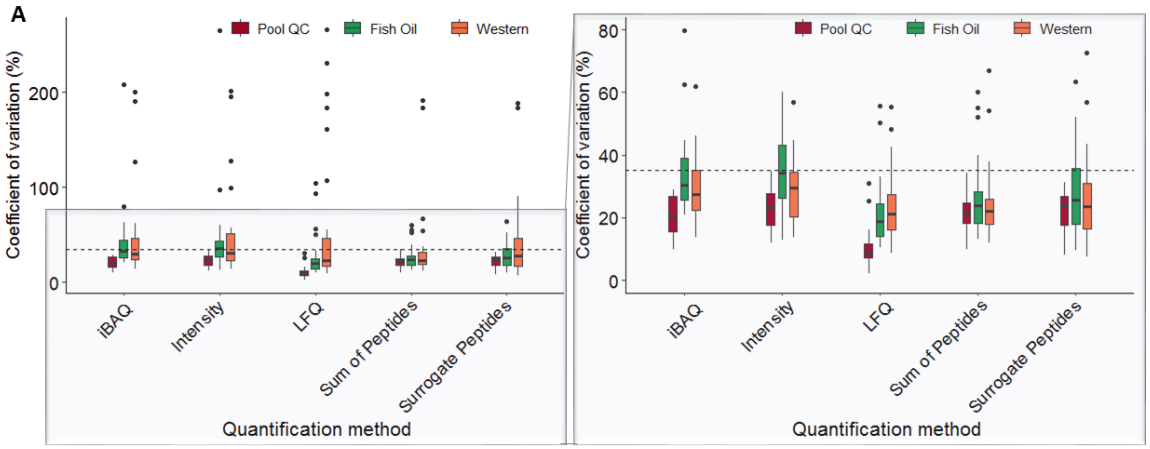

Figure 3. Comparison between QC variation (pooled HDL injected multiple times, n=8) and biological variability for HDL proteins from mice fed a diet enriched in saturated fatty acids supplemented or not with omega-3. iBAQ (n=17 proteins), intensity (n=19 proteins) and LFQ (n=30 proteins) measurements were used as quantification tools in MaxDIA, and sum of integrated areas of 2 to 4 most intense peptides (n=24 proteins) and surrogate peptides (n=20 proteins) were used as quantification strategies in Skyline. The Y axis was amplified for clarity with a scale ranging from 0 to 80%. The dashed line indicates CV of 35%.

3.3.4. Consistency of the Measurements among Different Quantification Strategies

Next, after having evaluated the precision of the five quantification strategies, we determined the consistency of their measurements. With that in mind, for each software platform, we chose the quantification strategy that achieved the greatest precision in our previous analyses (LFQ for MaxDia, and sum of peptides for Skyline), and correlated the results obtained by these two methods with those obtained by the other methods (iBAQ, intensity and surrogate peptides). Only proteins without missing values were correlated, and data were log2 transformed. The distribution of the Pearson's correlation coefficients is presented in **Figure 4** for HDL proteins from fish oil group (all correlations can be found in **Supplemental Table 6)**. Sum of peptides method correlates reasonably well with iBAQ, intensity and surrogate peptides (**Figure 4A**). Thus, values >0.8 were obtained for 78%,

56% and 84% of the proteins in HDL when sum of peptides was correlated with iBAQ, intensity and surrogate peptides, respectively. Surprisingly, LFQ correlated poorly (median r<0.5) with all quantification strategies, including with sum of peptide (**Figure 4B**).

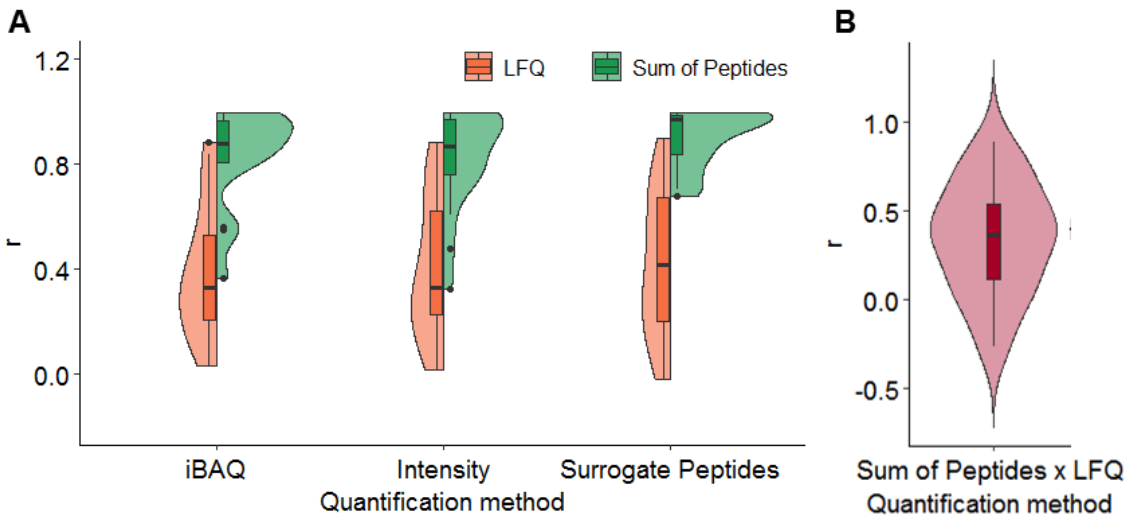

Figure 4. Relationship between pairs of quantification methods for HDL proteins from mice supplemented with omega-3 (fish oil group). (**A**) Pearson's correlation distribution obtained between HDL proteins quantified by LFQ (MaxDIA) or by summing up the areas of 2 to 4 most intense peptides (Skyline) and iBAQ (n=15 proteins for LFQ and n=14 proteins for sum of peptides), intensity (n=17 proteins for LFQ and n=16 proteins for sum of peptides) and surrogate peptides (n=17 proteins for LFQ and n=19 proteins for sum of peptides). (**B**) Pearson's correlation distribution obtained between HDL proteins quantified by LFQ (MaxDIA), and by summing up the areas of 2 to 4 most intense peptides (Skyline) (n=21). Only proteins without missing values were monitored. Data were log2 transformed. The dark line in the center of each rectangular box is the median of the data, the box indicates the interquartile range, and the spikes of the rectangles are the range of the data. The width of the plot outside the modified box plot is the density of values.

3.3.5. Body Weight Gain, and Plasma Lipid and Lipoprotein Profiles from LDLr$^{-/-}$ mice supplemented or not with omega-3

After a careful evaluation of some of the available quantification strategies for DIA data analyses, we proceed using LFQ for our investigation regarding the effects of consuming a diet enriched in saturated fats supplemented (or not) with omega-3 in a ratio

of 2.5:1 (saturated fatty acid:omega-3) in LDLr$^{-/-}$ mice (fish oil and western groups, respectively). Animals were fed for 14 weeks, and both groups gained weight similarly during the feeding period (P=0.054, **Figure 5A**). Plasma lipid profile was determined at the end of the treatment period (**Table 1**). Feeding LDLr$^{-/-}$ mice with saturated fatty acids resulted in marked hypercholesterolemia. Elevated plasma total cholesterol (TC), triglycerides (TG) and LDL-C levels were found when compared with omega-3 supplemented mice. Inclusion of EPA and DHA in diet triggered substantial reduction in plasma lipids levels, decreasing in 46% (P<0.0001), 60% (P=0.0001), and 77% (P=0.0013) the TC, TG, and LDL-C levels, respectively. Omega-3 also promoted a small decrease (16%) in HDL-C levels (P=0.0063). However, HDL-C levels are within normal limits established (>40 mg/dL).

Table 1. Plasma lipid profile in LDLr$^{-/-}$ mice supplemented or not with fish oil (fish oil and western groups, respectively).

Grupos	n	TC	TG	HDL-C	LDL-C
Western	10	544.4 ± 187.4	175.5 ± 57.4	58.7 ± 8.2	398.9 ± 213.3
Fish oil	10	294.7 ± 48.7	69.5 ± 21.7	49.4 ± 3.9	89.5 ± 10.9
P-value		<0.0001	0.0001	0.0063	0.0013

Data are given as mean ± SD in mg/dL, n = 10/group. P-value from unpaired two samples t-test. Statistical significance was set at P<0.05.

In addition, analysis of lipoproteins by FPLC also showed difference in the TC levels in VLDL, LDL and HDL fractions among the 2 treatment groups. (**Figure 5B**, and **Supplemental Table 7**). A considerable increase (about 3 times, P=0.0001) in TC levels was found in VLDL from mice fed only with saturated fatty acids when compared to

lipoprotein of the animals from fish oil group. Omega-3 supplementation promoted a slight increase of 11% (P=0.0216) in TC levels in LDL, and an increase of 30% (P=0.0027) in TC levels in HDL fraction when compared to mice from western group.

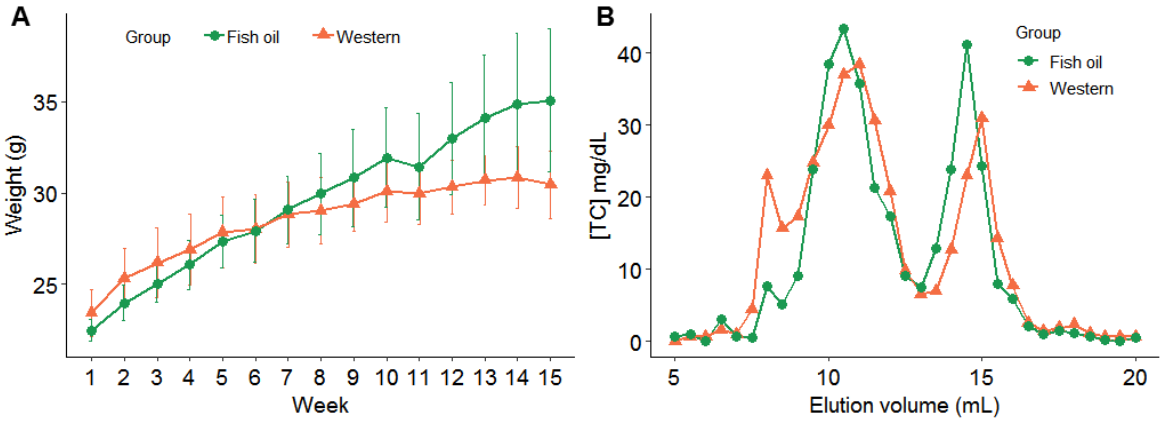

Figure 5. Effects of the high-fat diet supplemented (fish oil) or not (western) with omega-3 in (**A**) body weight gain, and in (**B**) plasma lipoprotein profile by FPLC of $LDLr^{-/-}$ mice.

3.3.6. Omega-3 reduces the inflammatory profile of HDL proteins in $LDLr^{-/-}$ mice fed with a high-fat diet

Finally, we explored the influence of omega-3 supplementation in a saturated fatty acids-enriched diet on the HDL proteome from $LDLr^{-/-}$ mice. As LFQ showed better precision in the QC measurements, we choose this method to quantify HDL proteins from mice fed with different diets. First, we evaluated the homogeneity of the two groups studied (western and fish oil groups) based upon similarities in their HDL proteome by Principal Component Analysis (PCA, **Figure 6A**). Only proteins without missing values were selected (n=25, **Supplemental Table 3**). Importantly, the first two dimensions on PCA were able to separate well fish oil and western diet-treated groups. With a combined variance of 55.4% the two first dimensions (Dim1 and Dim2), explained 41.1% and 14.3% of the HDL proteome variance, respectively.

Next, we tested if omega-3 supplementation in a saturated fatty acids-enriched diet would remodel the HDL proteome from LDLr$^{-/-}$ mice (**Figure 6B** and **Supplemental Table 5**). Samples with missing values were excluded, and can be accessed in **Supplemental Table 8**. Levels of 7 of 30 proteins were significantly increased in mice supplemented with omega-3 when comparing with mice fed only with saturated fats. HDL of mice from fish oil group had an increase of 1.5 times in the levels of complement C3 (C3, P=0.002), and of 2 times in the levels of apolipoprotein A-IV (APOA4, P<0.0001), phospholipid transfer protein (PLTP, P<0.0001), clusterin (CLU, P<0.0001), and insulin-like growth factor-binding protein complex acid labile subunit (IGFALS, P=0.04). Increased levels of Murinoglobulin-1/2 (MUG1/2, 4 times, P<0.0001) and phosphatidylinositol-glycan-specific phospholipase D (GPLD1, 5 times, P=0.001) were also found. Interestingly, the addition of fish oil in the high-fat diet lead to a reduction in the levels of the proteins of the serum amyloid A family (SAA). SAA1 and SAA2 were reduced by 90% (P=0.006 and P=0.042, respectively) in mice whose diet was supplemented with fish oil when compared with mice from the western group. Apolipoprotein C-II (APOC2, P<0.0001), apolipoprotein B-100 (APOB, P<0.0001), and H-2 class I histocompatibility antigen, Q10 alpha chain (H2-Q10, P=0.001) were also reduced, however with a smaller magnitude (reduction <2 times when compared to western diet group). All the reported P-values were adjusted for multiple comparisons. Distribution of the data for the most altered proteins in HDL (MUG1/2, CLU, PLTP, SAA2, SAA1 and APOC2) when comparing mice fed with a high-fat diet supplemented or not with fish oil is shown in **Figure 6C.**

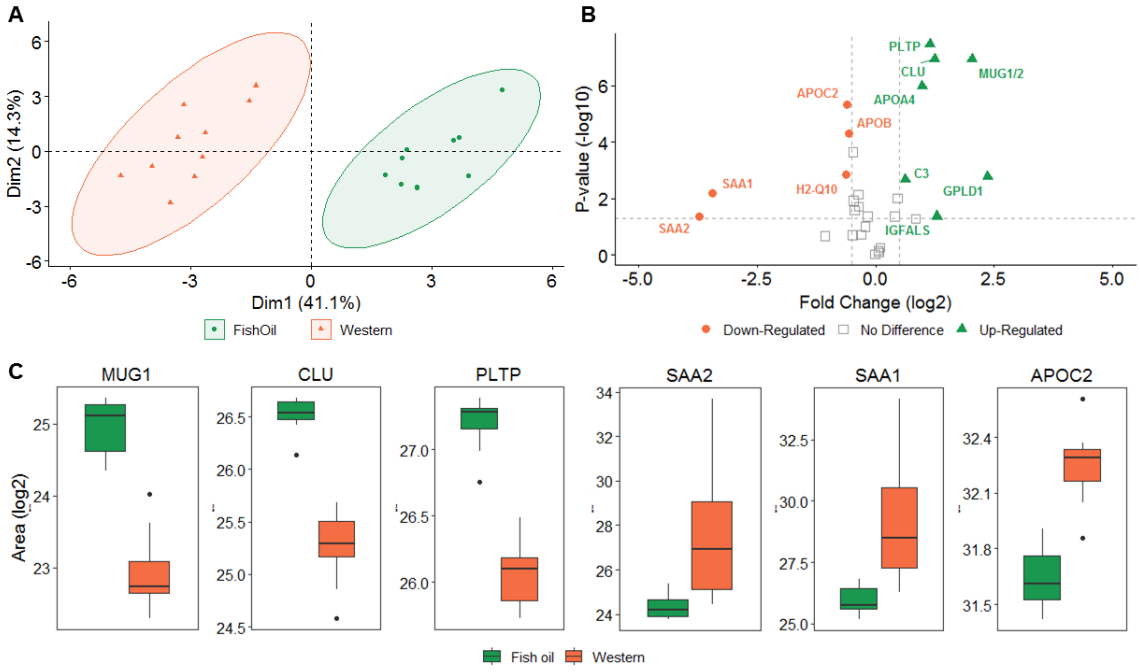

Figure 6. LFQ quantification of HDL proteome from LDLr$^{-/-}$ mice fed a high-fat diet supplemented (or not) with omega-3. (**A**) Principal Component Analysis (PCA). PCA plot representing 25 HDL proteins quantified by LFQ from MaxDIA analysis. Western group is represented as orange triangles and fish oil group is represented by green circles. (**B**) Significant altered HDL proteins obtained comparing mice supplemented or not with omega-3 (fish oil and western groups). For each protein, the –log 10 of the adjusted P-value from linear regression is plotted against the log2 fold change between fish oil and western groups. Proteins more abundant in HDL of mice not supplemented with omega-3 are displayed to the left of the value 0 on the x-axis, while proteins more abundant in HDL of omega-3 supplemented mice are to the right. (**C**) Distribution of the most altered proteins in both groups. The line in the center of each rectangular box is the median of the data, the upper and lower values of the rectangular box indicate the 75th and 25th percentiles, respectively, and the spikes are the range of the data.

3.4. Discussion

In this work, we have compared different quantification strategies for HDL proteome, through the data generated by two software platforms widely used in quantitative proteomics, MaxQuant and Skyline. iBAQ, intensity and LFQ were the tools employed to quantify MaxDIA-derived data, and sum of the areas of 2 to 4 most intense peptides for each protein and surrogate peptides were the strategies used for data processed by

Skyline. For all quantification methods, data refinement is key, resulting in a significant decrease in data variability. After a careful comparison among the five quantification strategies employed, our data showed that LFQ quantification using MaxDia software platform is the best tool to control technical variance in the data. This tool was therefore chosen to test the effects of omega-3 supplementation in LDLr$^{-/-}$ knockout mice fed a high-fat diet. The results show omega-3 reverts the inflammatory profile of HDL proteins caused by a high-fat diet.

MaxDIA is a recently launched tool integrated within MaxQuant software. This result in the sharing of many established MaxQuant concepts, such as iBAQ, intensity and LFQ quantification strategies[27]. To date, only three studies employed MaxDia to analyze data from DIA experiments. Thus, MaxDIA was applied to validate the proteome determined by DDA from patients with mitochondrial encephalomyopathy, lactic acidosis, stroke-like episodes, a neurodegenerative disease[37]. MaxDIA also was used as search engine to evaluate the efficiency of a database created with known biologically relevant proteolytic cleavages[38]. However, none of the studies described above explored the ability of the software to quantify proteins precisely. To date, a single study evaluated software performance more deeply. In agreement with our results, Sinitcyn *et al.*[27] found high quantification precision with MaxLFQ in MaxQuant when technical replicates of HepG2 cell lysate were analyzed. This study compared the performance of MaxDia with Spectronaut[39], another well-known quantification tool for DIA data. In our study, we choose to compare the performance of MaxDia with Skyline[26], a freely available software, pioneer in quantitative proteomics. Sinitcyn and collaborators found good agreement (r=0.87) between iBAQ protein intensities from MaxDIA and Spectronaut protein

intensities. In our study, we found good correlations (r>0.5) between all quantification strategies evaluated, except for LFQ (**Figure 4** and **Supplemental Table 6**). This probably happened because the LFQ measure is obtained from a normalized intensity profile according to the algorithms described in Cox *et al.*[40], whereas iBAQ and intensity do not normalize for the data. Peptide-feature intensities are taken at the peak maximum over the elution profile and include all isotopic peaks. iBAQ is distinguished from intensity as it is an approximation of protein copy number based on the sum of peptide-feature intensities of all peptides matching to a protein divided by the number of theoretically observable peptides[33]. In Skyline, the integrated peak area of one (surrogate) or more peptides (sum of peptides, up to 4 in this work) was considered for quantification.

In HDL context, the majority of studies still employ DDA strategies[20]. In recent years, there has been a growing use of quantitative tools in proteomics to deliver more robust and precise data, aiming to reduce the low reproducibility obtained using the discovery methodology. However, the performance of the targeted methodologies is still poorly evaluated, and a full description of the protein quantification strategies is lacking. Considering quantitative proteomics with label free quantification, only 9 studies used MRM/SRM, PRM and DIA to evaluate HDL proteome from 2014 to 2021. MRM[41; 42], PRM[43; 44], and DIA[30; 45] were used in two studies each. We carefully evaluated the analytical performance of these methodologies in two studies comparing SRM and PRM[46; 47], and in another one when PRM and DIA performances were compared[25]. From the 9 quantitative studies involving HDL proteome available, 7 used surrogate peptides for HDL proteins quantification, and 2 used sum of peptides. We have showed previously that DIA methodology using Skyline as a tool for HDL proteins quantification exhibits

comparable linearity and precision with PRM strategy. In the present work, we showed that using MaxDia, the technical variance of the data is considerably reduced. Another advantage is that the data processing time is significantly decreased when comparing with Skyline strategies of quantification. In this way, our study begins to open a new path of discussion towards data processing to quantify HDL proteins.

After a careful investigation of different quantification strategies, we applied MaxDIA approach with LFQ quantification to evaluate the effects of omega-3 supplementation in HDL proteome remodeling of LDLr$^{-/-}$ mice fed with a diet enriched in saturated fats. Omega-3 supplementation lead to an increase in the levels (2 times) of important HDL-resident proteins, such as PLTP, CLU, and APOA4. Clusterin was reported as having an important role in improving the functionality of plasma lipoproteins, preventing the increase in atherosclerotic lesion[48]. When LDLr$^{-/-}$ mice fed a high saturated fat diet were treated with a CLU mimetic peptide, atherosclerotic lesion was reduced by 43%, and antioxidant activity and cholesterol efflux capacity of HDL were improved. Furthermore, their LDL were more resistant to aggregation. Interesting, we recently found increased levels of these 3 proteins in HDL from subjects tested positive for SARS-CoV-2 with mild symptoms when compared with subjects in a severe stage of the disease[30].

Inflammation dramatically altered the HDL proteome in C57BL/6J mice, with substantial increases in SAA levels[49]. This inflamed HDL was less efficient in promoting cholesterol efflux from macrophages. In the same way, C57BL/6J mice fed a saturated fatty acids-enriched diet increased levels of SAA in HDL when compared with mice fed a low-fat diet or a diet rich in monounsaturated fatty acids[50]. In our work, supplementation

with omega-3 reduced SAA1 and SAA2 by 90% when comparing with the high-fat diet alone.

APOC2 also was more abundant in animals submitted to a high-fat diet. This apolipoprotein is an activator for lipase lipoprotein required for triglycerides-rich lipoproteins lipolysis[51]. Our high-fat diet fed mice had hypertriglyceridemia, and likely a dysfunctional intravascular lipolysis of triglycerides. Thus, mice fed on a high-fat diet had 60 % more triglycerides when compared with the group supplemented with fish oil. Moreover, we showed by FPLC that VLDL particles of mice fed on a high-fat diet have more cholesterol when comparing with fish oil supplementation. Importantly, a dynamic interaction between triglyceride-rich lipoproteins and HDL in the circulation leads to the remodeling of HDL particles[52]. Thus, elevations in APOC2 in HDL may be connected with the metabolism of triglycerides-rich lipoproteins. Interestingly, an increase in APOC2 was seen in diabetic subjects who later developed hypoalphalipoproteinemia (a striking reduction in HDL) on fenofibrate/rosiglitazone therapy[47].

Strengths of this work are the use of a robust animal model to investigate lipoprotein metabolism[53], and the use of a quantitative methodology that reduces technical variance to evaluate the effects of fish oil supplementation in HDL remodeling of mice submitted to high-fat diet. This work has also some potential limitations. We did not evaluate HDL functionality or atherosclerotic lesions from $LDLr^{-/-}$ mice, and further studies are needed to evaluate if the HDL remodeling seen with fish oil supplementation is connected with improved functionality.

In conclusion, this work showed that LFQ is able to quantify HDL proteins with low technical variance, with the advantage of requiring considerably less method development

than the current quantitative methodologies. These results should propel the field of HDL proteome quantification. The great majority of HDL proteome quantification studies relies mainly in shotgun proteomics, due to the amount of efforts needed to develop targeted quantification methodologies. However, shotgun proteomics lacks the precision needed for clinical and mechanistic studies in HDL field. Using MAxDIA software platform with LFQ as the quantification strategy, our results demonstrate that supplementing a diet with fish oil remodels HDL to a less inflammatory profile, even with the same amount of calories consumed, pointing towards the importance of the quality of a diet.

3.5. References

1 RAMSDEN, C. E.; DOMENICHIELLO, A. F. PURE study challenges the definition of a healthy diet: but key questions remain. **The Lancet**, v. 390, n. 10107, p. 2018-2019, 2017. DOI 10.1016/S0140-6736(17)32241-9. Disponível em: http://www.sciencedirect.com/science/article/pii/S0140673617322419.

2 ASTRUP, A. *et al*. Saturated Fats and Health: A Reassessment and Proposal for Food-Based Recommendations: JACC State-of-the-Art Review. **Journal of the American College of Cardiology,** v. 76, n. 7, p. 844-857, 2020. DOI 10.1016/j.jacc.2020.05.077. Disponível em: https://www.ncbi.nlm.nih.gov/pubmed/32562735.

3 GO, A. S. *et al*. Heart Disease and Stroke Statistics—2013 Update. **Circulation**, v. 127, n. 1, p. e6-e245, 2013. DOI 10.1161/CIR.0b013e31828124ad. Disponível em: https://www.ahajournals.org/doi/10.1161/CIR.0b013e31828124ad.

4 VIRANI, S. S. *et al*. Heart Disease and Stroke Statistics-2021 Update: A Report From the American Heart Association. **Circulation,** v. 143, n. 8, p. e254-e742, 2021. DOI 10.1161/CIR.0000000000000950. Disponível em: https://www.ncbi.nlm.nih.gov/pubmed/33501848.

5 KEYS, A.; ARAVANIS, C.; BLACKBURN, H. **Seven Countries: A Multi variate Analysis of Death and Coronary Heart Disease**. Cambridge, MA, and London, England: Harvard University Press Cambridge. 1980. p. 381.

6 BANG, H. O. *et al*. The composition of food consumed by Greenland Eskimos. **Acta medica Scandinavica,** v. 200, n. 1-2, p. 69-73, 1976. DOI 10.1111/j.0954-6820.1976.tb08198.x. Disponível em: https://www.ncbi.nlm.nih.gov/pubmed/961471.

[7] SURETTE, M. E. The science behind dietary omega-3 fatty acids. **Canadian Medical Association Journal**, v. 178, n. 2, p. 177-180, 2008. DOI 10.1503/cmaj.071356. Disponível em: https://www.ncbi.nlm.nih.gov/pubmed/18195292.

[8] LESLIE, M. A. *et al*. A review of the effect of omega-3 polyunsaturated fatty acids on blood triacylglycerol levels in normolipidemic and borderline hyperlipidemic individuals. **Lipids in Health and Disease**, v. 14, p. 53, 2015. DOI 10.1186/s12944-015-0049-7. Disponível em: https://www.ncbi.nlm.nih.gov/pubmed/26048287.

[9] AUNG, T. *et al*. Associations of Omega-3 Fatty Acid Supplement Use With Cardiovascular Disease Risks: Meta-analysis of 10 Trials Involving 77 917 Individuals. **JAMA Cardiology**, v. 3, n. 3, p. 225-234, 2018. DOI 10.1001/jamacardio.2017.5205. Disponível em: https://www.ncbi.nlm.nih.gov/pubmed/29387889.

[10] BHATT, D. L. *et al*. Cardiovascular Risk Reduction with Icosapent Ethyl for Hypertriglyceridemia. **The New England Journal of Medicine**, v. 380, n. 1, p. 11-22, 2019. DOI 10.1056/NEJMoa1812792. Disponível em: https://www.ncbi.nlm.nih.gov/pubmed/30415628.

[11] TOTH, P. P. High-density lipoprotein and cardiovascular risk. **Circulation,** v. 109, n. 15, p. 1809-1812, 2004. DOI 10.1161/01.CIR.0000126889.97626.B8. Disponível em: https://www.ncbi.nlm.nih.gov/pubmed/15096460.

[12] BODEN, W. E. *et al*. Niacin in patients with low HDL cholesterol levels receiving intensive statin therapy. **The New England Journal of Medicine**, v. 365, n. 24, p. 2255-2267, 2011. DOI 10.1056/NEJMoa1107579. Disponível em: https://www.ncbi.nlm.nih.gov/pubmed/22085343.

[13] RADER, D. J.; TALL, A. R. The not-so-simple HDL story: Is it time to revise the HDL cholesterol hypothesis? **Nature Medicine**, v. 18, n. 9, p. 1344-1346, 2012. DOI 10.1038/nm.2937. Disponível em: https://www.ncbi.nlm.nih.gov/pubmed/22961164.

[14] SHAH, A. S. *et al*. Proteomic diversity of high density lipoproteins: our emerging understanding of its importance in lipid transport and beyond. **Journal of Lipid Research**, v. 54, n. 10, p. 2575-2585, 2013. DOI 10.1194/jlr.R035725. Disponível em: https://www.ncbi.nlm.nih.gov/pmc/articles/PMC3770071/.

[15] VAISAR, T. *et al*. Shotgun proteomics implicates protease inhibition and complement activation in the antiinflammatory properties of HDL. **The Journal of Clinical Investigation**, v. 117, n. 3, p. 746-756, 2007. DOI 10.1172/JCI26206. Disponível em: https://www.jci.org/articles/view/26206/pdf.

[16] BURILLO, E. *et al*. Beneficial effects of omega-3 fatty acids in the proteome of high-density lipoprotein proteome. **Lipids in Health and Disease**, v. 11, p. 116, 2012. DOI 10.1186/1476-511X-11-116. Disponível em: https://www.ncbi.nlm.nih.gov/pubmed/22978374.

[17] YANG, Z. H. *et al*. Comparison of Omega-3 Eicosapentaenoic Acid Versus Docosahexaenoic Acid-Rich Fish Oil Supplementation on Plasma Lipids and Lipoproteins in Normolipidemic Adults. **Nutrients**, v. 12, n. 3, p. 749, 2020. DOI 10.3390/nu12030749. Disponível em: https://www.ncbi.nlm.nih.gov/pubmed/32178279.

[18] GETZ, G. S.; REARDON, C. A. Animal models of atherosclerosis. **Arterioscler Thrombosis and Vascular Biology**, v. 32, n. 5, p. 1104-1115, 2012. DOI 10.1161/atvbaha.111.237693. Disponível em: https://www.ahajournals.org/doi/10.1161/ATVBAHA.111.237693.

[19] YANG, Z.-H. *et al*. Dietary supplementation with long-chain monounsaturated fatty acid isomers decreases atherosclerosis and alters lipoprotein proteomes in LDLr−/− mice. **Atherosclerosis**, v. 262, p. 31-38, 2017. DOI 10.1016/j.atherosclerosis.2017.04.017. Disponível em: http://www.sciencedirect.com/science/article/pii/S0021915017301818.

[20] SINGH, S. A.; AIKAWA, M. Unbiased and targeted mass spectrometry for the HDL proteome. **Current Opinion in Lipidology**, v. 28, n. 1, p. 68-77, 2017. DOI 10.1097/MOL.0000000000000374. Disponível em: https://journals.lww.com/co-lipidology/Abstract/2017/02000/Unbiased_and_targeted_mass_spectrometry_for_the.11.aspx.

[21] LIU, H.; SADYGOV, R. G.; YATES, J. R. A model for random sampling and estimation of relative protein abundance in shotgun proteomics. **Analytical Chemistry**, v. 76, n. 14, p. 4193-4201, 2004. DOI 10.1021/ac0498563. Disponível em: https://pubs.acs.org/doi/10.1021/ac0498563.

[22] VIDOVA, V.; SPACIL, Z. A review on mass spectrometry-based quantitative proteomics: Targeted and data independent acquisition. **Analytica Chimica Acta**, v. 964, p. 7-23, 2017. DOI doi.org/10.1016/j.aca.2017.01.059. Disponível em: http://www.sciencedirect.com/science/article/pii/S0003267017301502.

[23] GILLET, L. C. *et al*. Targeted Data Extraction of the MS/MS Spectra Generated by Data-independent Acquisition: A New Concept for Consistent and Accurate Proteome Analysis. **Molecular & Cellular Proteomics**, v. 11, n. 6, p. O111.016717, 2012. DOI doi.org/10.1074/mcp.O111.016717. Disponível em: https://www.sciencedirect.com/science/article/pii/S1535947620304424

[24] LUDWIG, C. *et al*. Data-independent acquisition-based SWATH-MS for quantitative proteomics: a tutorial. **Molecular Systems Biology**, v. 14, n. 8, p. e8126, 2018. DOI 10.15252/msb.20178126. Disponível em: https://www.embopress.org/doi/full/10.15252/msb.20178126.

[25] SILVA, A. R. M. *et al*. Comparing Data-Independent Acquisition and Parallel Reaction Monitoring in Their Abilities To Differentiate High-Density Lipoprotein Subclasses. **Journal of Proteome Research**, v. 19, n. 1, p. 248-259, 2020. DOI 10.1021/acs.jproteome.9b00511. Disponível em: http://dx.doi.org/10.1021/acs.jproteome.9b00511.

[26] MACLEAN, B. *et al*. Skyline: an open source document editor for creating and analyzing targeted proteomics experiments. **Bioinformatics**, v. 26, n. 7, p. 966-968, 2019. DOI 10.1093/bioinformatics/btq054. Disponível em: https://academic.oup.com/bioinformatics/article-pdf/26/7/966/16897739/btq054.pdf.

[27] SINITCYN, P. et al. MaxDIA enables library-based and library-free data-independent acquisition proteomics. **Nature Biotechnology**, v. 39, n. 12, p. 1563-1573, 2021. DOI 10.1038/s41587-021-00968-7. Disponível em: https://www.ncbi.nlm.nih.gov/pubmed/34239088.

[28] PLUMP, A. S. *et al*. Severe hypercholesterolemia and atherosclerosis in apolipoprotein E-deficient mice created by homologous recombination in ES cells. **Cell**, v. 71, n. 2, p. 343-353, 1992. DOI 10.1016/0092-8674(92)90362-g. Disponível em: https://www.ncbi.nlm.nih.gov/pubmed/1423598.

[29] MASOOD, A.; STARK, K. D.; NORMAN SALEM, J. A simplified and efficient method for the analysis of fatty acid methyl esters suitable for large clinical studies. **Journal of Lipid Research**, v. 46, n. 10, p. 2299-2305, 2005. DOI 10.1194/jlr.D500022-JLR200. Disponível em: http://www.jlr.org/content/46/10/2299.full.

[30] JUNIOR, D. R. S. *et al*. HDL proteome remodeling associates with COVID-19 severity. **Journal of Clinical Lipidology**, v. 15, n. 6, p. 796-804, 2021. DOI 10.1016/j.jacl.2021.10.005. Disponível em: https://www.ncbi.nlm.nih.gov/pubmed/34802985.

[31] RAPPSILBER, J.; MANN, M.; ISHIHAMA, Y. Protocol for micro-purification, enrichment, pre-fractionation and storage of peptides for proteomics using StageTips. **Nature Protocols**, v. 2, n. 8, p. 1896-906, 2007. DOI 10.1038/nprot.2007.261. Disponível em: http://dx.doi.org/10.1038/nprot.2007.261.

[32] COX, J.; MANN, M. MaxQuant enables high peptide identification rates, individualized p.p.b.-range mass accuracies and proteome-wide protein quantification. **Nature Biotechnology**, v. 26, n. 12, p. 1367-1372, 2008. DOI 10.1038/nbt.1511. Disponível em: https://www.nature.com/articles/nbt.1511.

[33] TYANOVA, S. *et al*. The MaxQuant computational platform for mass spectrometry-based shotgun proteomics. **Nature Protocols**, v. 11, n. 12, p. 2301-2319, 2016. DOI 10.1038/nprot.2016.136. Disponível em: https://www.ncbi.nlm.nih.gov/pubmed/27809316.

[34] HENDERSON, C. M. *et al*. Measurement by a Novel LC-MS/MS Methodology Reveals Similar Serum Concentrations of Vitamin D-Binding Protein in Blacks and Whites. **Clinical Chemistry**, v. 62, n. 1, p. 179-187, 2016. DOI 10.1373/clinchem.2015.244541. Disponível em: https://www.ncbi.nlm.nih.gov/pubmed/26453697.

[35] TOTH, C. A. *et al*. On-column trypsin digestion coupled with LC-MS/MS for quantification of apolipoproteins. **Journal of Proteomics**, v. 150, p. 258-267, 2017. DOI 10.1016/j.jprot.2016.09.011. Disponível em: https://www.ncbi.nlm.nih.gov/pubmed/27667389.

[36] BENJAMINI, Y.; HOCHBERG, Y. Controlling the False Discovery Rate: A Practical and Powerful Approach to Multiple Testing. **Journal of the Royal Statistical Society. Series B (Methodological)**, v. 57, n. 1, p. 289-300, 1995. Disponível em: http://www.jstor.org/stable/2346101.

[37] LI, H. *et al*. Integrated proteomic and metabolomic analyses of the mitochondrial neurodegenerative disease MELAS. **Molecular Omics**, v. 18, n. 3, p. 196-205, 2022. DOI 10.1039/d1mo00416f. Disponível em: https://www.ncbi.nlm.nih.gov/pubmed/34982085.

[38] HARNEY, D. J.; LARANCE, M. Annotated Protein Database Using Known Cleavage Sites for Rapid Detection of Secreted Proteins. **Journal of Proteome Research**, v. 21, n. 4, p. 965-974,

2022. DOI 10.1021/acs.jproteome.1c00806. Disponível em: https://www.ncbi.nlm.nih.gov/pubmed/35156369.

[39] BRUDERER, R. *et al*. Extending the limits of quantitative proteome profiling with data-independent acquisition and application to acetaminophen-treated three-dimensional liver microtissues. **Molecular & Cellular Proteomics**, v. 14, n. 5, p. 1400-1410, 2015 May 2015. DOI 10.1074/mcp.M114.044305. Disponível em: https://www.ncbi.nlm.nih.gov/pubmed/25724911.

[40] COX, J. *et al*. Accurate proteome-wide label-free quantification by delayed normalization and maximal peptide ratio extraction, termed MaxLFQ. **Molecular & Cellular Proteomics**, v. 13, n. 9, p. 2513-2526, 2014. DOI 10.1074/mcp.M113.031591. Disponível em: https://www.ncbi.nlm.nih.gov/pubmed/24942700.

[41] YASSINE, H. N. *et al*. The application of multiple reaction monitoring and multi-analyte profiling to HDL proteins. **Lipids in Health and Disease**, v. 13, p. 8, 2014. DOI 10.1186/1476-511X-13-8. Disponível em: https://www.ncbi.nlm.nih.gov/pubmed/24397693.

[42] HENDERSON, C. M. *et al*. Isolating and Quantifying Plasma HDL Proteins by Sequential Density Gradient Ultracentrifugation and Targeted Proteomics. **Methods in Molecular Biology**, v. 1410, p. 105-120, 2016. DOI 10.1007/978-1-4939-3524-6_7. Disponível em: https://www.ncbi.nlm.nih.gov/pubmed/26867741.

[43] SANTANA, M. F. M. *et al*. Enrichment of apolipoprotein A-IV and apolipoprotein D in the HDL proteome is associated with HDL functions in diabetic kidney disease without dialysis. **Lipids in Health and Disease**, v. 19, n. 1, p. 1-14, 2020. DOI 10.1186/s12944-020-01381-w. Disponível em: https://lipidworld.biomedcentral.com/articles/10.1186/s12944-020-01381-w.

[44] RONSEIN, G. E. *et al*. Niacin Increases Atherogenic Proteins in High-Density Lipoprotein of Statin-Treated Subjects. **Arteriosclerosis, Thrombosis, and Vascular Biology**, v. 41, n. 8, p. 2330-2341, 2021. DOI 10.1161/ATVBAHA.121.316278. Disponível em: https://www.ncbi.nlm.nih.gov/pubmed/34134520.

[45] GOURGARI, E. *et al*. Proteomic alterations of HDL in youth with type 1 diabetes and their associations with glycemic control: a case–control study. **Cardiovascular Diabetology**, v. 18, n. 1, p. 43, 2019. DOI 10.1186/s12933-019-0846-9. Disponível em: https://cardiab.biomedcentral.com/articles/10.1186/s12933-019-0846-9.

[46] RONSEIN, G. E. *et al*. Parallel reaction monitoring (PRM) and selected reaction monitoring (SRM) exhibit comparable linearity, dynamic range and precision for targeted quantitative HDL proteomics. **Journal of Proteomics**, v. 113, p. 388-399, 2015. DOI 10.1016/j.jprot.2014.10.017. Disponível em: http://www.sciencedirect.com/science/article/pii/S1874391914004990.

[47] RONSEIN, G. E. *et al*. Targeted Proteomics Identifies Paraoxonase/Arylesterase 1 (PON1) and Apolipoprotein Cs as Potential Risk Factors for Hypoalphalipoproteinemia in Diabetic Subjects Treated with Fenofibrate and Rosiglitazone. **Molecular & Cellular Proteomcs**, v. 15, n. 3, p. 1083-1093, 2016. DOI 10.1074/mcp.M115.054528. Disponível em: http://www.mcponline.org/content/15/3/1083.full.

[48] URBINA, A. R. *et al*. Subcutaneous Administration of Apolipoprotein J-Derived Mimetic Peptide d-[113-122]apoJ Improves LDL and HDL Function and Prevents Atherosclerosis in LDLR-KO Mice. **Biomolecules**, v. 10, n. 6, p. 829, 2020. DOI 10.3390/biom10060829. Disponível em: https://www.ncbi.nlm.nih.gov/pubmed/32485898.

[49] VAISAR, T. *et al*. Inflammatory remodeling of the HDL proteome impairs cholesterol efflux capacity. **Journal of Lipid Research**, v. 56, n. 8, p. 1519-1530, 2015. DOI 10.1194/jlr.M059089. Disponível em: https://www.ncbi.nlm.nih.gov/pubmed/25995210.

[50] O'REILLY, M. *et al*. High-Density Lipoprotein Proteomic Composition, and not Efflux Capacity, Reflects Differential Modulation of Reverse Cholesterol Transport by Saturated and Monounsaturated Fat Diets. **Circulation**, v. 133, n. 19, p. 1838-1850, 2016. DOI 10.1161/CIRCULATIONAHA.115.020278. Disponível em: https://www.ncbi.nlm.nih.gov/pubmed/27081117.

[51] LAROSA, J. C. *et al*. A specific apoprotein activator for lipoprotein lipase. **Biochemical and Biophysical Research Communications**, v. 41, n. 1, p. 57-62, 1970. DOI 10.1016/0006-291x(70)90468-7. Disponível em: https://www.ncbi.nlm.nih.gov/pubmed/5459123.

[52] MC, CARR, M. C.; BRUNZELL, J.D. Abdominal obesity and dyslipidemia in the metabolic syndrome: importance of type 2 diabetes and familial combined hyperlipidemia in coronary artery disease risk. **The Journal of Clinical Endocrinology and Metabolism**, v. 89, n. 6, p. 2601-2607, 2004. DOI 10.1210/jc.2004-0432. Disponível em: https://www.ncbi.nlm.nih.gov/pubmed/15181030.

[53] GORDON, S. M. *et al*. A comparison of the mouse and human lipoproteome: suitability of the mouse model for studies of human lipoproteins. **Journal of Proteome Research**, v. 14, n. 6, p. 2686-2695, 2015. DOI 10.1021/acs.jproteome.5b00213. Disponível em: https://www.ncbi.nlm.nih.gov/pubmed/25894274.

4. Final Remarks

In this thesis, we shed light on two major bottlenecks that exist in the area of HDL proteomics: the almost complete absence of quantitative methodologies to precisely detect HDL proteins by mass spectrometry and the lack of standardization for data processing and analysis after mass spectrometry acquisition.

First, we evaluated the analytical performance of two targeted methodologies, DIA and PRM, using labeled peptides in pooled digested HDL as a biological matrix. In addition, we compared the quantification capabilities of both methodologies for 24 protein found in HDL subclasses from 19 apparently healthy subjects. DIA and PRM exhibited comparable linearity and precision, and worked equally well to differentiate HDL subclasses through their proteomes.

Next, we examined the performance of five different quantification strategies using Skyline and MaxDIA software platforms to quantify HDL proteins, proposing a pipeline to robustly quantify HDL proteome. This pipeline was employed to compare HDL proteome from $LDL^{-/-}$ mice submitted to a high-fat diet supplemented or not with omega-3. Even with the same amount of calories consumed, the supplementation with omega-3 remodels HDL proteome from mice, considerably attenuating the inflammatory profile seen in HDL of mice treated only with a high-fat diet.

Therefore, we were able to provide precise tools both at the level of protein detection by mass spectrometry and post data acquisition to deepen the understanding of HDL proteome.

5. Appendix 1: Supplemental Information - Chapter 3

Supplemental Table 1. Macronutrient composition of diets*.

Ingredients (g/kg)	Diets	
	Western	**Fish oil**
Casein	195.0	195.0
DL-Metionine	3.0	3.0
Maltodextrine	-	-
Sucrose	341.0	341.0
Corn starch	150.0	150.0
Cellulose	50.0	50.0
Cholesterol	1.5 (0.15%)**	1.5 (0.15%)**
Minerals mix	35.0	35.0
Calcium carbonate	4.0	4.0
Vitamins mix	10.0	10.0
Ethoxyquin	0.04	0.04
Milk fat (anhydrous)	187.2	93.6
Soybean oil	12.8	12.8
Fish oil	-	37.4
Nutritional values		
Energy, *Kcal/g*	4.5	4.5
Protein, *% of energy*	17.3	17.3
Carboydrate, *% of energy*	48.5	48.5
Fat, *% de energy*	21.2	21.2

*Diets were formulated according National Research Council requirements[1].

**Total of cholesterol: 0.2% (0.05% from milk fat and fish oil).

Supplemental Table 2. Fatty acids composition of diets.

% of total FA	Identification	Diets	
		Western	Fish oil
C10:0	capric acid	1.56	1.35
C12:0	lauric acid	2.40	1.35
C14:0	myristic acid	10.25	8.72
C15:0	pentadecyclin acid	1.07	0.89
C16:0	palmitic acid	35.55	28.93
C16:1n-7	palmitoleic acid	1.75	5.45
C17:0	margaric acid	0.83	0.86
C18:0	stearic acid	14.57	9.89
C18:1n-9	oleic acid	24.6	19.31
C18:2n-6	linoleic acid	5.60	5.60
C18:3n-3	α-linolenic acid	0.68	0.86
C20:1n-9	eicosenoic acid	–	0.99
C20:5n-3	eicosapentaenoic acid (EPA)	–	6.63
C22:1n-9	brassilic acid	–	1.15
C22:6n-3	docosahexaenoic acid (DHA)	–	4.24

Fatty acid composition was measured by GC/FID as described in Methods.

Supplemental Table 3. HDL proteins considered for DIA quantification before and after refinement. Samples were obtained from LDLR$^{-/-}$ mice fed on a high-fat diet with or without supplementation with omega-3.

Protein	Before refinament		After refinament				
	MaxDIA	Skyline	iBAQ	Intensity	LFQ	Sum of Peptides	Surrogate Peptides
ADGRE5		✓					
ALB	✓	✓	✓	✓	✓	✓	✓
AMBP		✓					
ANTXR2	✓	✓					
APOA1	✓	✓	✓	✓	✓		✓
APOA2	✓	✓			✓	✓	
APOA4	✓	✓	✓	✓	✓	✓	✓
APOB	✓	✓	✓	✓	✓	✓	✓
APOC1	✓	✓	✓	✓	✓	✓	✓
APOC2	✓	✓	✓	✓	✓	✓	✓
APOC3	✓	✓		✓	✓	✓	
APOC4	✓	✓	✓	✓	✓	✓	✓
APOD	✓	✓	✓	✓	✓	✓	✓
APOE	✓	✓	✓	✓	✓	✓	✓
APOM	✓	✓				✓	✓
B2M	✓	✓	✓	✓	✓	✓	✓
BPIFA2	✓	✓			✓		
C3	✓	✓			✓		
C4B	✓	✓			✓		
CAMP		✓					
CD97	✓						
CLU	✓	✓			✓	✓	
FGA	✓	✓					
GPLD1	✓	✓			✓		
H2-D1		✓					
H2-K1		✓					

H2-Q10	✓	✓	✓	✓	✓	✓	✓
H2-Q8		✓					
H4-C1		✓					
HBA	✓	✓			✓		
HIST1H4A	✓						
HIST3H2BA*	✓						
HSP90AB1/AA1*	✓	✓					
ICAM1	✓	✓					
IGFALS	✓	✓			✓		
IHH	✓						
LCAT	✓	✓					
MUG1/2*	✓	✓		✓	✓	✓	✓
NAPSA	✓	✓			✓	✓	✓
PCYOX1	✓	✓	✓	✓	✓	✓	
PKM		✓					
PLTP	✓	✓			✓	✓	
PON1	✓	✓	✓	✓	✓	✓	✓
PPIC	✓	✓					
PSAP	✓	✓	✓	✓	✓	✓	✓
SAA1	✓	✓	✓	✓	✓	✓	✓
SAA2	✓	✓	✓	✓	✓	✓	✓
SAA4	✓	✓	✓	✓	✓	✓	✓
SELL	✓	✓					
SERPINA1C/1A/1E/1B*	✓						
SFTPB	✓	✓					
TF	✓	✓					
TFPI	✓	✓					
TFRC	✓	✓			✓	✓	✓
TMEM247	✓	✓					
TUBA4A/1B/8/1C/3A/1A*	✓						

Proteins excluded for Principal Component Analysis (PCA), because they had missing values, are highlighted in red.

*Due to the high homology, the following proteins were merged in protein groups called HIST3H2BA (HIST3H2BA; HIST1H2BP; HIST1H2BK; HIST3H2BB; HIST1H2BC; HIST2H2BB; HIST2H2BE; HIST1H2BH; HIST1H2BB; HIST1H2BM; HIST1H2BF; HIST1H2BA), HSP90AB1/AA1 (HSP90AB1; HSP90AA1), MUG1/2 (MUG1; MUG2), SERPINA1C/1A/1E/1B (SERPINA1C; SERPINA1A; SERPINA1E; SERPINA1B), TUBA4A/1B/8/1C/3A/1A (TUBA4A; TUBA1B; TUBA8; TUBA1C; TUBA3A; TUBA1A).

Supplemental Table 4. Protein quantified in HDL from LDLr$^{-/-}$ mice supplemented or not with omega-3. Data processing in Skyline, by two quantification methods, sum of peptides and surrogate peptide (highlighted in blue).

Gene name	Protein name	Peptide sequence
ALB	Albumin	YNDLGEQHFK LVQEVTDFAK
APOA1	Apolipoprotein A-I	VQPYLDEFQK VAPLGAELQESAR SNPTLNEYHTR TQVQSVIDK
APOA2	Apolipoprotein A-II	TSEIQSQAK THEQLTPLVR
APOA4	Apolipoprotein A-IV	LGDASTYADGVHNK SLAPLTVGVQEK ALVQQLEQFR
APOB	Apolipoprotein B-100	LSISEQNAQR VPQTDVTFR EVQVPTFTIPK LSVDQFVR
APOC1	Apolipoprotein C-I	EFGNTLEDK AWFSEAFGK
APOC2	Apolipoprotein C-II	TYPISMDEK SSAAMSTYAGIFTDQLLTLLR
APOC3	Apolipoprotein C-III	TVQDALSSVQESDIAVVAR GWMDNHFR
APOC4	Apolipoprotein C-IV	VLEMVEPLVTR TQAWLQSSR
APOD	Apolipoprotein D	CPSPPVQENFDVK DILTSNGIDIEK
APOE	Apolipoprotein E	ELEEQLGPVAEETR LGPLVEQGR TANLGAGAAQPLR LQAEIFQAR
APOM	Apolipoprotein M	FLLYNR CVEEFQSLTSCLDFK
B2M	Beta-2-microglobulin	TPQIQVYSR VEMSDMSFSK
CLU	Clusterin	ASGIIDTLFQDR VSTVTTHSSDSEVPSR

H2-Q10	H-2 class I histocompatibility antigen, Q10 alpha chain	YFETSVSRPGLGEPR GYLQYAYDGR
MUG1/2	Murinoglobulin-1/2	HGIPFFVK HVAYAVYSLSK
NAPSA	Napsin-A	TSTSGGNPSFVPLSK FAIQYGTGR
PCYOX1	Prenylcystein oxidase	TGSETHSDFYDIVLVAAPLNR LFLSYDYAVR
PLTP	Phospholipid transfer protein	VTSAALDLVK AVEPQLEDDER
PON1	Serum paraoxonase/arylesterase 1	EVTPVELPNCNLVK YVYIAELLAHK IFFYDAENPPGSEVLR IQNILSEDPK
PSAP	Prosaposin	TVVTEAGNLLK TLVPATETIK
SAA1	Serum amyloid A-1 protein	EAFQEFFGR GHEDTIADQEANR
SAA1/2	Serum amyloid A-1/2 protein	GPGGVWAAEK
SAA2	Serum amyloid A-2 protein	ESFQEFFGR
SAA4	Serum amyloid A-4 protein	DNLEANYQNADQYFYAR NHGLETLQATQK NPNHFRPEGLPEK
TFRC	Transferrin receptor protein 1	ILNIFGVIK VEYHFLSPYVSPR

Supplemental Table 5. Adjusted P values obtained after linear regression comparing LDLr$^{-/-}$ mice omega-3 supplemented (fish oil group) or not (western group). P-values were corrected by Benjamini-Hochberg method.

Proteins	log2 FoldChange	Adjusted P-value
ALB	0.488	0.199
APOA1	0.363	0.007
APOA2	-0.460	0.010
APOA4	-0.982	0.000
APOB	0.572	0.000
APOC1	0.168	0.043
APOC2	0.613	0.000
APOC3	0.446	0.026
APOC4	0.357	0.020
APOD	0.216	0.100
APOE	0.013	0.941
B2M	0.471	0.012
BPIFA2	-0.843	0.052
C3	-0.628	0.002
C4B	-0.407	0.043
CLU	-1.245	0.000
GPLD1	-2.360	0.002
H2.Q10	0.617	0.001
HBA	1.068	0.216
IGFALS	-1.299	0.043
MUG1/2	-2.032	0.000
NAPSA	-0.098	0.553
PCYOX1	0.475	0.000
PLTP	-1.144	0.000
PON1	0.015	0.941
PSAP	-0.061	0.692
SAA1	3.440	0.006
SAA2	3.733	0.043
SAA4	-0.068	0.805
TFRC	0.306	0.188

Supplemental Table 6. Pearson's correlation coefficient obtained comparing areas of HDL proteins quantified by different quantification methods.

Protein	Sum of Peptides x Intensity		Sum of Peptides x iBAQ		Sum of Peptides x LFQ		Surrogate Peptide x Intensity		Surrogate Peptide x iBAQ		Surrogate Peptide x LFQ		Sum of Peptides x Surrogate Peptide		Intensity x iBAQ		Intensity x LFQ		iBAQ x LFQ	
	Western	FishOil	Western	FishOil	Western	FishOil	Western	FishOil	Western	FishOil	Western	FishOil	Western	FishOil	Western	FishOil	Western	FishOil	Western	FishOil
ALB	0.9125	0.7643	0.8983	0.8106	0.9261	0.6847	0.9641	0.9528	0.9777	0.9624	0.9271	0.8144	0.9570	0.8225	0.9796	0.9821	0.9254	0.8099	0.9209	0.8377
APOA1	-	-	-	-	-	-	0.4473	0.3640	0.1115	-0.1035	0.4701	-0.6061	-	-	0.9179	0.8562	-0.2603	-0.2118	-0.3381	0.0342
APOA2	-	-	-	-	0.8497	0.0636	-	-	-	-	-	-	-	-	-	-	-	-	-	-
APOA4	0.9441	0.9769	0.9367	0.9681	0.7446	0.6965	0.7440	0.9542	0.8139	0.9661	0.7942	0.6870	0.7411	0.9730	0.9846	0.9843	0.7425	0.6587	0.7872	0.7060
APOB	0.9242	0.7757	0.8819	0.8080	0.5376	0.0394	0.9120	0.9649	0.9332	0.9632	0.7382	0.1684	0.8534	0.7056	0.9694	0.9843	0.4739	0.1367	0.5562	0.1581
APOC1	0.9979	0.9968	0.9975	0.9966	0.3412	0.3639	0.7520	0.9826	0.7716	0.9807	0.2947	0.2848	0.7711	0.9802	0.9984	0.9998	0.3249	0.3325	0.3616	0.3273
APOC2	0.6516	0.7560	0.5574	0.3666	0.6048	-0.2661	0.6346	0.5993	0.5750	0.4228	0.4740	-0.4788	0.8577	0.7792	0.9506	0.8716	0.8379	0.0191	0.8590	0.1075
APOC3	0.8350	0.3259	-	-	0.6724	0.3585	-	-	-	-	-	-	-	-	-	-	0.6201	-0.3115	-	-
APOC4	0.9408	0.8692	0.9403	0.8680	0.7487	0.4786	0.8358	0.8283	0.8355	0.8273	0.8063	0.4368	0.8865	0.9583	1.0000	1.0000	0.6286	0.5855	0.6301	0.5870
APOD	0.9075	0.6047	0.8949	0.5621	0.8358	0.4861	0.8549	0.2239	0.8431	0.1840	0.7672	0.4155	0.9569	0.8755	0.9984	0.9969	0.7329	0.2032	0.7310	0.1514
APOE	0.9696	0.9968	0.9557	0.9958	0.6959	0.8928	0.9513	0.9944	0.9431	0.9925	0.7423	0.8991	0.9786	0.9978	0.9952	0.9992	0.6031	0.8864	0.6318	0.8827
APOM	-	-	-	-	-	-	-	-	-	-	-	-	0.9932	0.9986	-	-	-	-	-	-
B2M	0.8343	0.9520	0.8343	0.9520	0.3264	0.3709	0.8656	0.9656	0.8656	0.9656	0.1868	0.2932	0.9792	0.9871	1.0000	1.0000	0.0042	0.2518	0.0042	0.2518
CLU	-	-	-	-	0.6644	0.3515	-	-	-	-	-	-	-	-	-	-	-	-	-	-
H2-Q10	0.8175	0.9693	0.8271	0.9251	0.4078	0.5925	0.8119	0.9333	0.7172	0.9029	0.7718	0.6857	0.7497	0.9779	0.9337	0.9627	0.5482	0.4627	0.3490	0.4647
MUG1/2	0.7458	0.7616	-	-	0.6543	0.2572	0.6597	0.6660	-	-	0.4872	0.2303	0.8250	0.8781	-	-	0.8917	0.7704	-	-
NAPSA	-	-	-	-	0.4515	0.0183	-	-	-	-	0.4185	-0.0182	0.8446	0.9698	-	-	-	-	-	-
PCYOX1	0.6117	0.4802	0.5753	0.5492	0.5277	0.7309	0.6243	0.8212	0.8971	0.8747	0.7753	0.6627	0.6784	0.8523	0.7196	0.9879	0.4262	0.2653	0.6011	0.3552
PLTP	-	-	-	-	0.3647	0.4896	-	-	-	-	-	-	-	-	-	-	-	-	-	-
PON1	0.8727	0.9695	0.8901	0.9893	0.9135	0.1964	-	-	-	-	-	-	-	-	0.9945	0.9725	0.7362	0.2512	0.7786	0.2728
PSAP	0.8934	0.8700	0.9039	0.8939	0.8381	0.4207	-0.2792	0.7155	-0.2635	0.7543	-0.2221	0.5262	-0.1454	0.6780	0.9854	0.9862	0.7384	0.4187	0.7770	0.4784
SAA1	-	-	-	-	-	-	-	-	-	-	-	-	0.9997	0.9995	-	-	-	-	-	-
SAA2	-	-	-	-	-	-	-	-	-	-	-	-	0.9787	0.7113	-	-	-	-	-	-

SAA4	0.9842	0.9940	0.9218	0.8553	0.9333	-0.0121	0.9906	0.9856	0.9342	0.8637	0.9432	0.0260	0.9948	0.9915	0.9649	0.8823	0.9443	0.0418	0.8742	0.3297
TFR1	-	-	-	-	-0.5288	0.1611	-	-	-	-	-0.4646	0.1598	0.9875	0.9945	-	-	-	-	-	-
Median	*0.9005*	*0.8696*	*0.8966*	*0.8810*	*0.6644*	*0.3639*	*0.8119*	*0.9333*	*0.8393*	*0.8888*	*0.7382*	*0.2932*	*0.8865*	*0.9698*	*0.9846*	*0.9843*	*0.6286*	*0.2653*	*0.6318*	*0.3297*
N	*16*	*16*	*14*	*14*	*21*	*21*	*15*	*15*	*14*	*14*	*17*	*17*	*19*	*19*	*15*	*15*	*17*	*17*	*15*	*15*

r<0.5 are highlighted in red

Supplemental Table 7. Total cholesterol content of the lipoproteins in pooled plasma samples from LDLr$^{-/-}$ mice supplemented with omega-3 or not (fish oil and western groups, respectively).

Lipid (mg/dL)	Western	Fish Oil	P-value
VLDL	22.5 ± 0.7	7.7 ± 1.6	0.0001
LDL	38.4 ± 1.4	43.3 ± 1.8	0.0216
HDL	28.9 ± 0.5	41.2 ± 1.0	0.0027

Data are expressed as mean ± SD (n = 5). Total cholesterol measurement was performed in triplicate. P-value from unpaired two samples t-test. Statistical significance was set at $P<0.05$.

Supplemental Table 8. Number of missing values obtained when HDL proteins were quantified by LFQ.

Protein	Number of missing value	Group
BPIFA2	1	Western
GPLD1	2	Western
HBA	6	Western
	1	Fish oil
HBB.B2	3	Western
IGFALS	1	Western
LCAT	4	Western
	1	Fish oil
SAA1	1	Fish oil
SAA2	1	Western
	4	Fish oil

REFERENCES

1. Nutrition NRCUSoLA. **Nutrient Requirements of Laboratory Animals**. 4. ed. 1995. Washington (DC): National Academies Press (US); 1995. ISBN-10: 0-309-05126-6.

SÚMULA CURRICULAR

1.DADOS PESSOAIS

Nome: Amanda Ribeiro Martins da Silva
Local e data de nascimento: Piracicaba, 28/12/1988

2.EDUCAÇÃO

Colégio Liceu Terras do Engenho, Piracicaba, 2005.

Universidade Estadual “Júlio de Mesquita Filho” (UNESP), Rio Claro, 2013.
Graduação (Ciências Biológicas - Bacharelado).

Centro de Energia Nuclear na Agricultura (CENA/USP), Piracicaba, 2016.
Mestrado em Ciências com Atribuições em Química.

3.FORMAÇÃO COMPLEMENTAR

May Institute: Computation and statistics for mass spectrometry and proteome, Northeastern Universit (USA), 2019

Targeted Proteomics Course, Centro Nacional de Pesquisa em Energia e Materiais (CNPEM, Campinas), 2018.

VII Proteomics Workshop, Centro Nacional de Pesquisa em Energia e Materiais (CNPEM, Campinas), 2016.

4.OCUPAÇÃO

Bolsista de Doutorado, FAPESP, Jan/2022.

5.PUBLICAÇÕES (Artigos Completos e Resumos em Congressos)

ARTIGOS:

SOUZA JUNIOR, DOUGLAS RICARDO ; SILVA, AMANDA RIBEIRO MARTINS ; ROSA-FERNANDES, LIVIA ; REIS, LORENNA ROCHA ; ALEXANDRIA, GABRIELLY ; BHOSALE, SANTOSH D. ; GHILARDI, FABIO DE ROSE ; DALÇÓQUIO, TALIA FALCÃO ; BERTOLIN, ADRIADNE JUSTI ; NICOLAU, JOSÉ CARLOS ; MARINHO, CLAUDIO R.F. ; WRENGER, CARSTEN ; LARSEN, MARTIN R. ; SICILIANO, RINALDO FOCACCIA ; DI MASCIO, PAOLO ; PALMISANO, GIUSEPPE ; RONSEIN, GRAZIELLA ELIZA . HDL proteome remodeling associates with COVID-19 severity. Journal of Clinical Lipidology, v. 15, p. 796-804, 2021.

SILVA, AMANDA R. M.; TOYOSHIMA, MARCOS T. K. ; PASSARELLI, MARISA ; DI MASCIO, PAOLO ; RONSEIN, GRAZIELLA E. Comparing Data-Independent Acquisition and Parallel Reaction Monitoring in Their Abilities To Differentiate High-Density Lipoprotein Subclasses. JOURNAL OF PROTEOME RESEARCH, v. 19, p. 248-259, 2020.

SANTANA, MONIQUE F. M. ; LIRA, AÉCIO L. A. ; PINTO, RAPHAEL S. ; MINANNI, CARLOS A. ; SILVA, AMANDA R. M. ; SAWADA, MARIA I. B. A. C. ; NAKANDAKARE, EDNA R. ; CORREA-GIANNELLA, MARIA L. C. ; QUEIROZ, MARCIA S. ; RONSEIN, GRAZIELLA E. ; PASSARELLI, MARISA . Enrichment of apolipoprotein A-IV and apolipoprotein D in the HDL proteome is associated with HDL functions in diabetic kidney disease without dialysis. Lipids in Health and Disease JCR, v. 19, p. 205-219, 2020.
RODRIGUEZ, ANNABELLE TRIGATTI, BERNARDO L. MINEO, CHIEKO KNAACK, DARCY WILKINS, JOHN T. SAHOO, DAISY ASZTALOS, BELA F. MORA, SAMIA CUCHEL, MARINA POWNALL, HENRY J. ROSALES, CORINA BERNATCHEZ, PASCAL RIBEIRO MARTINS DA SILVA, AMANDA GETZ, GODFREY S. BARBER, JACOB L. SHEARER, GREGORY C. ZIVKOVIC, ANGELA M. TIETGE, UWE J.F. SACKS, FRANK M. CONNELLY, MARGERY A. ODA, MICHAEL N. DAVIDSON, W. SEAN SORCI-THOMAS, MARY G. VAISAR, TOMAS RUOTOLO, GIACOMO , et al. ; Proceedings of the Ninth HDL (High-Density Lipoprotein) Workshop. ARTERIOSCLEROSIS THROMBOSIS AND VASCULAR BIOLOGY, v. 39, p. 2457-2467, 2019.

SILVA, AMANDA R.M.; KAMOGAWA, MARCOS Y. ; MELCHERT, WANESSA R. . A versatile and greener multicommuted flow-based system for exploiting relatively slow chemical reactions. Microchemical Journal (Print), v. 133, p. 121-125, 2017.

RESUMOS:

SILVA, A. R. M.; TOYOSHIMA, M. T. K. ; PASSARELI, M. ; MASCIO, P. ; RONSEIN, G. E. . High-density Lipoprotein Subclasses Mapping by Targeted Quantitative Proteomics. In: Vascular Discovery From Genes to Medicine 2019 Scientific Sessions, 2019, Boston. Vascular Discovery From Genes to Medicine 2019 Scientific Sessions, 2019.

SILVA, A. R. M.; TOYOSHIMA, M. T. K. ; PASSARELI, M. ; MASCIO, P. ; RONSEIN, G. E. . High-density Lipoprotein Subclasses Mapping by Targeted Quantitative Proteomics. In: 2019 HDL Workshop, 2019, Boston. 2019 HDL Workshop, 2019.

SILVA, A. R. M.; RONSEIN, G. E. . Comparing analytical performance of DIA and PRM for quantitative HDL proteomics. In: VIII Proteomics Workshop Skyline, 2018, Campinas. VIII Proteomics Workshop Skyline, 2018.

SILVA, A. R. M.; MELCHERT, W. R. . Explorando reação lenta em sistema de análises em fluxo com multicomutação e determinação espectrofotométrica. In: 18o Encontro Nacional de Química Analítica, 2016, Florianópolis. 18o. Encontro Nacional de Química Analítica, 2016.

SILVA, A. R. M.; MELCHERT, W. R. . A multi-pumping flow-based procedure for iodate determination in waters. In: Flow Analysis XIII, 2015, Prague/Czech Republic. Flow Analysis XIII, 2015.

SILVA, A. R. M.; MELCHERT, W. R. . Sistema de análises em fluxo com multicomutação para determinação espectrofotométrica de iodato em águas naturais. In: VIII Simpósio Científico dos Pós-graduandos no CENA/USP, 2015, Piracicaba. VIII Simpósio Científico dos Pós-graduandos no CENA/USP, 2015.

SILVA, A. R. M.; ROCHA, D. L. ; MELCHERT, W. R. . Determinação de sulfonamidas totais em águas naturais empregando clean up online e microbombas solenoide. In: VII Simpósio Científico dos Pós-graduandos no CENA/USP, 2014, Piracicaba/SP. XII Simpósio Científico dos Pós-graduandos no CENA/USP, 2014.

SILVA, A. R. M.; ABREU, M. G. ; ROCHA, D. L. ; MELCHERT, W. R. . Determinação espectrofotométrica de sulfonamidas em sistema de análises em fluxo com microbombas solenoide. In: 37a. Reunião Anual da Sociedade Brasileira de Química, 2014, Natal/RN. 37a. Reunião Anual da Sociedade Brasileira de Química, 2014.